Chapter 5

Stratospheric Ozone Changes and Climate

Lead Authors
A.Yu. Karpechko
A.C. Maycock

Coauthors
M. Abalos
H. Akiyoshi
J.M. Arblaster
C.I. Garfinkel
K.H. Rosenlof
M. Sigmond

Contributors
V. Aquila
A. Banerjee
A. Chrysanthou
D. Ferreira
H. Garny
N. Gillett
P. Landschützer
E.-P. Lim
M.J. Mills
W.J. Randel
E. Ray
W. Seviour
S.-W. Son
N. Swart

Review Editors
C. Cagnazzo
L. Polvani

Cover photo: An image of a cyclone off the coast of Antarctica from the MODIS satellite instrument. Stratospheric ozone depletion has led to a poleward shift in summertime cyclone frequency over the Southern Ocean. Photo: NASA

Chapter 5

Stratospheric Ozone Changes and Climate

CONTENTS

Chapter 5

Stratospheric Ozone Changes and Climate

SCIENTIFIC SUMMARY

Since the 2014 Ozone Assessment, new research has better quantified the impact of stratospheric ozone changes on climate. Additional model and observational analyses are assessed, which examine the influence of stratospheric ozone changes on stratospheric temperatures and circulation, tropospheric circulation and composition, surface climate, the oceans, and sea ice. The new results support the main conclusions of the previous Assessment; the primary advances are summarized below.

STRATOSPHERIC TEMPERATURES

- **New estimates of satellite-observed stratospheric temperature changes show net global stratospheric cooling of around 1.5 K (at 25–35 km), 1.5 K (at 35–45 km), and 2.3 K (at 40–50 km) between 1979 and 2005, with differences between datasets of up to 0.6 K.**
    - There are now better estimates of observed stratospheric temperature trends than were available during the last Assessment. Two datasets from satellite measurements have been re-processed and now show greater consistency in long-term temperature trends in the middle and upper stratosphere.
    - Satellite temperature records show smaller stratospheric cooling rates over 1998–2015 compared to 1979–1997, consistent with the observed differences in stratospheric ozone trends during these periods.
    - Global average temperature in the lower stratosphere (13–22 km) cooled by about 1 K between 1979 and the late 1990s but has not changed significantly since then.
- **In the lower stratosphere (13–22 km), ozone trends were the major cause of the observed cooling between the late 1970s and the mid-1990s. In the middle and upper stratosphere, however, increases in long-lived greenhouse gases played a slightly larger role than ozone changes in cooling trends over this period.** Ozone recovery will continue to play an important role in future stratospheric temperature trends.
    - There is now improved understanding of the causes of stratospheric temperature trends and variability. For the upper stratosphere (40–50 km), new studies suggest that one-third of the observed cooling over 1979–2005 was due to ozone-depleting substances (ODSs) and associated ozone changes, while two-thirds was due to other well-mixed greenhouse gases.
    - Chemistry–climate models show that the magnitude of future stratospheric temperature trends is dependent on future greenhouse gas concentrations, with most greenhouse gas scenarios showing cooling in the middle and upper stratosphere over the 21st century. The projected increase in global stratospheric ozone during this period would offset part of the stratospheric cooling due to increasing greenhouse gases.

STRATOSPHERIC OVERTURNING CIRCULATION

- **There are indications that the overturning circulation in the lower stratosphere has accelerated over the past few decades.**

- Observations of the latitudinal profile of lower stratospheric temperature trends and changes in constituents show that tropical upwelling in the lower stratosphere has strengthened over the last ~30 years, in qualitative agreement with model simulations and reanalysis datasets.
- New studies using measurements provide evidence for structural changes in the stratospheric overturning circulation which is comprised of a strengthening in the lower stratosphere and a weakening in the middle and upper stratosphere.
- According to models, in addition to well-mixed greenhouse gases, changes in ODSs (and associated changes in ozone) are an important driver of past and future changes in the strength of the stratospheric overturning circulation, notably the increase in downwelling over the Antarctic over the late 20th century.
- Estimates of externally forced long-term changes in the stratospheric overturning circulation from observations remain uncertain, partially due to internal variability.
- Models project future increases in stratosphere–troposphere exchange of ozone as a consequence of a strengthening of the stratospheric overturning circulation and stratospheric ozone recovery.

IMPACTS ON THE TROPOSPHERE, OCEAN, AND SEA ICE

- **New research supports the findings of the 2014 Ozone Assessment that Antarctic ozone depletion was the dominant driver of the changes in Southern Hemisphere tropospheric circulation in austral summer during the late 20th century, with associated weather impacts.**
  - Over the period 1970 to 2000, tropospheric jets in the Southern Hemisphere shifted poleward and strengthened, the Southern Annular Mode (SAM) index increased, and the southern edge of the Hadley Cell expanded poleward. Since 2000, the SAM has remained in a positive phase.
  - For austral summer, most model simulations show a larger contribution to these trends from Antarctic ozone depletion compared to increases in well-mixed greenhouse gases during the last decades of the 20th century. During other seasons, the contribution of ozone depletion to circulation changes is comparable to that from well-mixed greenhouse gases.
  - Paleoclimate reconstructions of the SAM index suggest that the current period of prolonged positive summer SAM conditions is unprecedented in at least the past 600 years.
  - No robust link between stratospheric ozone depletion and long-term Northern Hemisphere surface climate has been established; there are indications that occurrences of extremely low springtime ozone amounts in the Arctic may have short-term effects on Northern Hemisphere regional surface climate.
- **Changes in tropospheric weather patterns driven by ozone depletion have played a role in recent temperature, salinity, and circulation trends in the Southern Ocean, but the impact on Antarctic sea ice remains unclear.**
  - Progress has been made since the last Assessment in understanding the physical processes involved in the Southern Ocean response to ozone depletion, which is now believed to entail a fast surface cooling followed by a slow long-term warming.
  - Modeling studies indicate that ozone depletion contributes to a decrease in Antarctic sea ice extent and hence cannot explain the observed sea ice increase between 1979 and 2015. This is in agreement with the conclusions of the previous Assessment. However, in general, climate models still cannot

reproduce the observed Antarctic sea ice trends since 1979, which limits the confidence in the modeled sea ice response to ozone depletion.

- **New observation-based analyses indicate that a causal link between the strength of the Southern Ocean carbon sink and ozone depletion cannot be established, in contrast to earlier suggestions.**
    - New observation-based analyses confirmed the previously reported slowdown of the carbon sink between the 1980s and early 2000s but also revealed a remarkable reinvigoration of the carbon sink since then. The new results indicate that atmospheric circulation changes (whether driven by ozone depletion or not) have not had a considerable impact on the net strength of the Southern Ocean carbon sink.

MONTREAL PROTOCOL CLIMATE IMPACTS

- **New studies since the 2014 Ozone Assessment have identified that future global sea level rise of at least several centimeters has been avoided as a result of the Montreal Protocol.** This would have arisen from thermal expansion of the oceans associated with additional global warming from unregulated ozone depleted substances emissions.

CHAPTER 5

STRATOSPHERIC OZONE CHANGES AND CLIMATE

5.1 INTRODUCTION AND SCOPE

The 2006 Ozone Assessment was the first to include a dedicated chapter on ozone–climate interactions (Baldwin and Dameris et al., 2007). The focus of that chapter was mostly on how anthropogenic climate change affects stratospheric ozone. Ozone–climate interactions were considered in a broader perspective in both the 2010 and 2014 Ozone Assessments. Chapter 4 of the 2014 Assessment (Arblaster and Gillett et al., 2014) addressed changes in stratospheric climate, their coupling with stratospheric ozone changes, and the impacts of stratospheric changes on tropospheric climate. This chapter is similar in scope and provides an assessment of the advances in scientific understanding of ozone–climate coupling since the last Assessment. To provide a basis for discussing these advances in the subsequent sections, the main conclusions from Chapter 4 of the 2014 Assessment are summarized here.

5.1.1 Summary of Findings from the Previous Ozone Assessment

The last Assessment concluded that the lower stratosphere (near 20 km) cooled in the global mean by approximately 1 K over the period 1979–1995, after which temperatures remained approximately constant. It also concluded that the middle (25–35 km) and upper (35–50 km) stratosphere have cooled in the global mean over this period; however, the available satellite datasets showed substantial differences in the estimated magnitude of cooling. In agreement with previous Ozone Assessments, it was concluded that stratospheric ozone changes were the primary cause of the observed lower-stratospheric cooling, while both ozone decreases and greenhouse gas (GHG) increases (primarily carbon dioxide, CO_2) made more comparable contributions to cooling in the middle and upper stratosphere.

The 2014 Ozone Assessment concluded from observations of composition and temperature that over the past several decades there has been an increase in tropical lower-stratospheric upwelling, consistent with a strengthening of the shallow branch of the stratospheric overturning circulation. At the same time, long-term changes in the deep branch of the overturning circulation were concluded to be uncertain. No long-term changes were found in stratospheric water vapor concentrations since 2000.

In agreement with the findings of earlier Assessments, the 2014 Assessment concluded that the ozone-induced springtime cooling of the Antarctic lower stratosphere has strongly affected the Southern Hemisphere (SH) tropospheric climate in austral summer. It was assessed that stratospheric temperature changes due to ozone depletion were likely the dominant driver of the observed summertime poleward shift of the mid-latitude tropospheric jet and have contributed to the poleward expansion of the SH Hadley Cell. It was noted that, in response to ozone depletion, some climate models simulate a poleward shift of subtropical precipitation patterns and that consistent changes are seen in observations. Changes in the Southern Ocean were discussed, and it was concluded that changes in surface wind stress, associated with the tropospheric circulation response to ozone depletion, likely caused the intensification of the subtropical ocean gyres, the meridional overturning circulation, and subsurface warming. Contrary to the findings of the 2010 Assessment, the 2014 Assessment concluded, though with low confidence, that stratospheric ozone depletion induces a decrease in Antarctic sea ice extent and therefore cannot explain the small observed increase in Antarctic sea ice extent over the past several decades. Possible impacts of ozone depletion-induced surface wind stress changes on carbon uptake in the Southern Ocean were also assessed to be uncertain. The 2014 Assessment did not find a robust link between ozone changes and tropospheric climate in the Northern Hemisphere.

The 2014 Assessment concluded that stratospheric ozone depletion contributed to a decrease in the flux of ozone into the troposphere but that coincident increases in emissions of ozone precursor species led to an

overall increase in the tropospheric ozone burden. The overall global radiative forcing (RF) between 1850 and 2011 due to the effect of long-lived ozone-depleting substances (ODSs) on both stratospheric and tropospheric ozone was estimated to be about −0.15 W m^{-2}.

For the future, the 2014 Assessment concluded that the impacts of ozone depletion on tropospheric climate will reverse as a result of ozone recovery and that this will offset part of the GHG-induced changes in SH tropospheric circulation in summer during the first half of this century. The projected strengthening of the stratospheric overturning circulation was assessed to have important implications for future stratospheric and tropospheric ozone abundances. The RF due to future stratospheric ozone changes was assessed to be uncertain even regarding its sign, due to uncertainty in model projections of tropical lower-stratospheric ozone trends.

5.1.2 Scope of the Chapter

Following Chapter 4 of the 2014 Ozone Assessment, this chapter begins with an assessment of changes in stratospheric constituents and external forcings (**Section 5.2**). Only a brief discussion of changes in ODSs and stratospheric ozone is given here, since these are assessed in detail in **Chapter 1** (ODS changes) and **Chapters 3 and 4** (ozone changes). **Section 5.3** assesses changes in stratospheric temperatures and circulation. That section includes an attribution of observed temperature and circulation changes to different drivers and also an analysis of projected changes. Stratosphere–troposphere exchange of ozone is also discussed, but since changes in tropospheric ozone have been recently assessed in detail in the Tropospheric Ozone Assessment Report (TOAR), led by the International Global Atmospheric Chemistry (IGAC) project (Young et al., 2018), the discussion of tropospheric chemistry is limited to assessing the effects of stratospheric ozone on the tropospheric ozone budget. **Section 5.4** discusses the effects of stratospheric ozone on tropospheric circulation, surface climate, the ocean, and sea ice, as well as the current scientific understanding of physical mechanisms for the downward dynamical coupling between the stratosphere and troposphere. Lastly, **Section 5.5** assesses the climate impacts that have been avoided as a result of the successful regulation of ODS emissions under the Montreal Protocol, as well as the future climate impacts that will be avoided if nations adhere to the phasedown of hydrofluorocarbons under the 2016 Kigali Amendment (see also **Chapter 2**).

5.2 OBSERVED CHANGES IN ATMOSPHERIC CONSTITUENTS AND EXTERNAL FORCINGS THAT RELATE TO CLIMATE

The species detailed in this section play a role in climate through their effects on radiative and chemical processes. Changes in these species can alter stratospheric ozone concentrations either through direct effects on ozone chemistry and/or via their effect on stratospheric temperatures and transport.

5.2.1 Long-Lived Greenhouse Gases and Ozone-Depleting Substances

Carbon dioxide (CO_2), methane (CH_4), and nitrous oxide (N_2O) are the three most important anthropogenically emitted GHGs in the atmosphere in terms of historical RF (Myhre and Shindell et al., 2013); however, it should be noted that ODSs and their replacement compounds are also significant GHGs. Such gases are more transparent to incoming (shortwave) radiation from the sun compared to outgoing infrared (longwave) radiation. Increases in the atmospheric concentrations of these gases lead to warming at the surface, producing a direct global climate response. These gases may also cause changes in stratospheric temperatures through effects on the local radiative balance; for example, increasing CO_2 cools the stratosphere (see **Box 5-1**). Ozone photochemistry responds to stratospheric temperature changes, as well as to changes in abundances of ODSs. Similarly, changes in ozone affect the stratospheric radiative balance; decreases in ozone will result in stratospheric cooling due to less absorption of solar ultraviolet radiation. Changes in the stratospheric overturning (Brewer–Dobson) circulation may be forced by changes in well-mixed GHGs and ozone concentrations (see **Section 5.3.2**); this may also impact the distributions of stratospheric and tropospheric ozone through transport changes (see **Section 5.3.3**).

Recent concentrations and growth rates for ODSs, including N_2O, are described in **Chapter 1** and for ODS replacement compounds in **Chapter 2**. Globally averaged annual average mole fraction values for 2017

were 405 ppm (parts per million) for CO_2 and 1,850 ppb (parts per billion) for CH_4. Global concentrations and growth rates for CO_2 and CH_4 are shown in **Figure 5-1**. These show that 2015 and 2016 had high CO_2 growth rates relative to the 1980–2016 average. This is likely related, at least in part, to the El Niño conditions that persisted from late 2014 through early 2016 (Le Quéré et al., 2018); the CO_2 growth rate is known to increase during El Niño conditions and decrease during La Niña conditions (Kim et al., 2016; Betts et al., 2016; Le Quéré et al., 2018). The CH_4 growth rate peaked in 2014 but remained positive and greater than 5 ppb yr^{-1} in 2015 and 2016. Multiple drivers have been suggested for the higher CH_4 growth rates since the 2000s and are discussed in **Section 1.5.2** (see also Saunois et al., 2016). These include changes in the atmospheric concentrations of the hydroxyl (OH) radical, increased emissions from oil and gas extraction, increased emissions from wetlands, and increased emissions from anthropogenic sources in East Asia.

5.2.2 Stratospheric Water Vapor

Stratospheric water vapor (SWV) modulates Earth's climate directly, mainly through longwave radiative processes, and indirectly through its influence on stratospheric ozone abundances. It impacts stratospheric ozone chemistry through its role as the major source of reactive hydrogen oxide molecules (HO_x) in the stratosphere and through the formation of polar stratospheric clouds (see **Chapter 4**). Changes to

Box 5-1. Why Does Increasing CO_2 Cool the Stratosphere?

Although carbon dioxide (CO_2) in the stratosphere plays only a small direct role in chemical processes, it is very important for the atmosphere's radiative balance. CO_2 emits and absorbs radiation mainly in the infrared part of the electromagnetic spectrum, with the strongest emission and absorption at wavelengths close to 15 μm. At these wavelengths, the absorption of infrared radiation by CO_2 is so efficient that most radiation emitted by Earth's surface is absorbed in the troposphere and does not reach the stratosphere. Radiation entering the stratosphere from below therefore comes from the relatively cold upper troposphere. At the same time, CO_2 in the stratosphere emits radiation to space, cooling the stratosphere. The largest cooling rates are in the upper stratosphere, where temperatures are highest due to absorption of incoming ultraviolet radiation by ozone. Since this local emission is not balanced by the absorption of upwelling radiation from below, CO_2 contributes a net cooling in the stratosphere. When the atmospheric CO_2 concentration increases, there is only a small increase in the absorption of radiation from the troposphere, which does not compensate for a relatively larger increase in local emission, leading to a greater loss of radiation to space. An increase in CO_2 therefore radiatively cools the stratosphere at all altitudes, with the largest cooling in the upper stratosphere.

Increases in other greenhouse gases (GHGs) that absorb and emit infrared radiation, such as methane, nitrous oxide, and chlorofluorocarbons (CFCs), also contribute to cooling in the upper stratosphere, because at stratospheric altitudes they emit more radiation to space than they absorb from below. However, when in the lower stratosphere, these gases, whose absorption bands lie at wavelengths between 7 and 12 μm, can absorb radiation from the warm lower troposphere and from Earth's surface. Therefore, an increase in these gases can contribute to warming of the lower stratosphere, although their contribution is usually small. Some non-CO_2 GHGs are also chemically reactive (such as methane, nitrous oxide, and CFCs) and thus have an indirect effect on stratospheric temperatures through changing ozone abundances (see **Chapters 3 and 4**). In some cases, this indirect effect on stratospheric temperatures via changes to ozone may be larger than the direct radiative effect of the gas itself.

In summary, increases in stratospheric CO_2 and other GHGs lead to stratospheric cooling, with the largest changes occurring in the upper stratosphere.

SWV also impact ozone indirectly by changing stratospheric temperatures, which in turn alter the rates of photochemical reactions.

Air enters the stratosphere with a water vapor concentration largely controlled by tropical tropopause temperatures. The primary source of SWV internal to the stratosphere is in situ oxidation of CH_4, yielding two water molecules for each CH_4 molecule oxidized. Convective overshooting of ice particles and transport across the extratropical tropopause are minor sources of SWV. The primary loss process internal to the stratosphere is dehydration through ice particle formation and sedimentation in polar regions (mostly in the Antarctic) during winter.

SWV has been measured by multiple in situ and remote sensing techniques, starting with World War II measurements aimed at understanding contrails using a manually operated aircraft-borne frost point hygrometer (FPH) (Brewer, 1946). The Boulder FPH record extends from 1980 to present day. A detailed analysis of time variations in the Boulder record using breakpoints revealed periods of both increases and decreases in SWV and variations in trends with altitude (Hurst et al., 2011). While the net source of SWV from CH_4 oxidation was found to vary with time, it is estimated to have caused about 25% of the increase in SWV in the altitude range 16–26 km between 1980 and 2010 (Hurst et al., 2011). Although the lack of continuous long-term measurements complicates SWV trend determination, several studies have shown an overall long-term increasing trend (Oltmans et al., 2000; Rosenlof et al., 2001; Hurst et al., 2014). In terms of the consistency between in situ and satellite measurements of SWV, a comparison of balloon FPH measurements with retrievals from the Aura Microwave Limb Sounder (MLS) satellite instrument for the period 2004–2012 revealed there was no statistically significant drift (Hurst et al., 2014). Subsequent analysis including more recent data (Hurst et al., 2016) shows a trend in the difference between the balloon FPH measurements and the Aura MLS measurements, the reasons for which are still under investigation.

Although it is known that tropical cold point temperatures and in situ production from CH_4 oxidation largely control SWV concentrations, there are still issues reproducing the absolute value of measured SWV using global temperature analyses. To produce accurate simulations (to within 0.5–1 ppmv [parts per million by volume]) of tropical stratospheric water vapor entry concentrations using trajectory models driven by global temperature analyses, proper representation of waves, convective influences, and microphysical processes are needed (Ueyama et al., 2014). There is also evidence (Avery et al., 2017) that injections of ice can at times impact SWV during extreme events.

Tropical Pacific sea surface temperature (SST) variability affects SWV entry through impacts on tropical tropopause temperatures; it has been suggested that SST changes contributed to the observed decrease in SWV in the lower stratosphere around the year 2000 (Rosenlof and Reid, 2008; Brinkop et al., 2016; Ding and Fu, 2017; Garfinkel et al., 2018). Variations of SWV are detailed in the State of the Climate reports published annually in the *Bulletin of the American Meteorological Society*; the most recent update (Blunden and Arndt, 2017) shows recent extreme variability of SWV in the tropical lower stratosphere, where water vapor enters the stratosphere, ranging from very high values to very low values between December 2015 and December 2016 (**Figure 5-2**); part of this change may be related to the transition from extreme El Niño conditions to weak La Niña conditions at the end of the period (Konopka et al., 2016; Garfinkel et al., 2018).

Trends in tropical tropopause temperature and atmospheric CH_4 concentrations are expected to be the major drivers of future SWV trends, but there are also suggestions from model simulations that trends in overshooting ice particles could contribute to trends in SWV (Dessler et al., 2016). Climate models predict that tropical lower-stratospheric humidity will increase in the future due to increased transport through the tropical tropopause layer (Smalley et al., 2017), though it should be noted that many climate models do not properly capture the processes that affect tropical tropopause temperatures (Kim et al., 2013). The magnitude of modeled increases in SWV over the 21st century, particularly in the middle and upper stratosphere, is strongly affected by future atmospheric CH_4 concentrations (Revell et al., 2016).

It has been suggested that convective injection of water vapor into the lower stratosphere could lead to enhanced heterogeneous destruction of ozone and

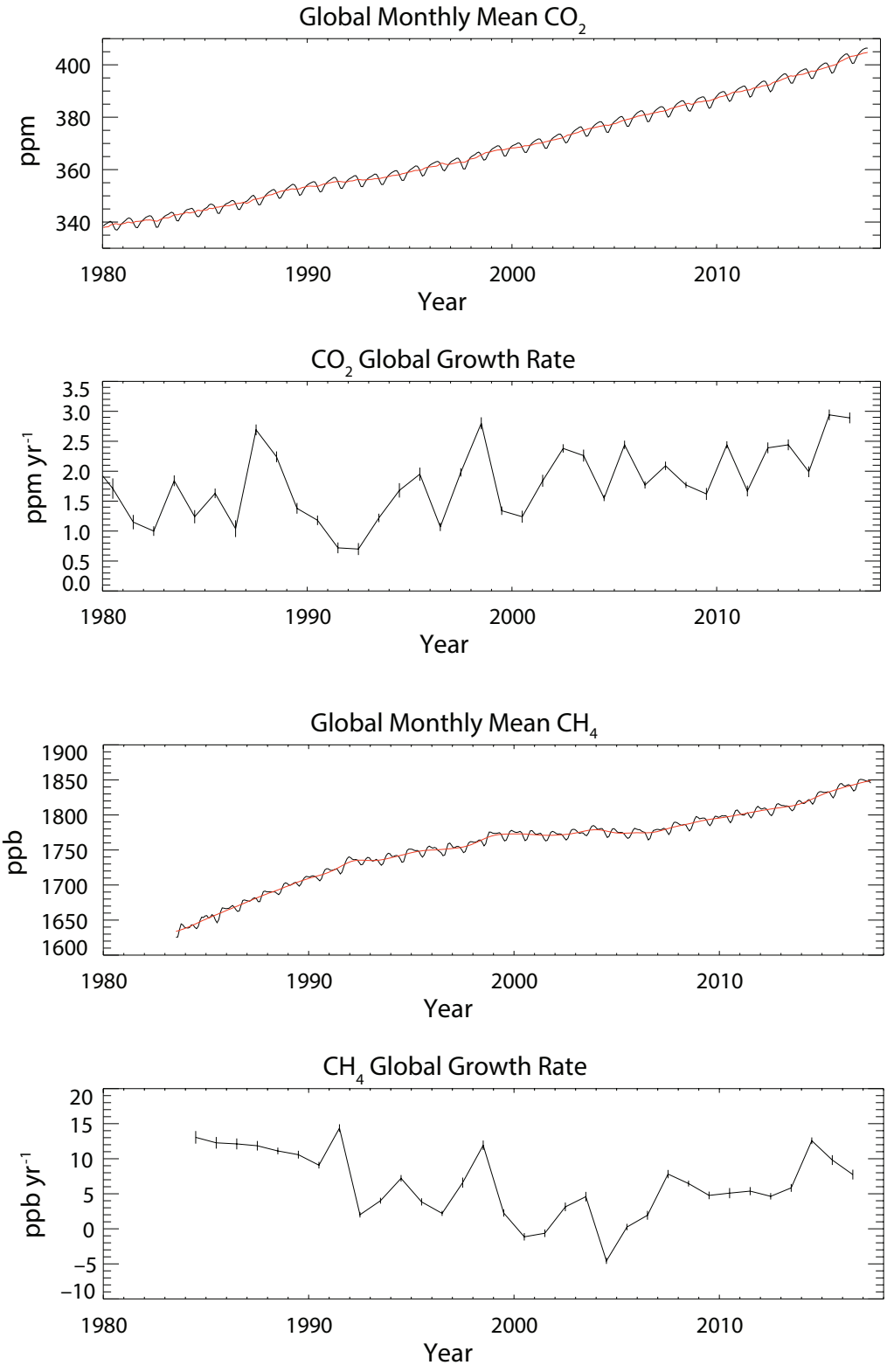

Figure 5-1. Time series of concentrations and growth rates for globally averaged CO_2 (*top two panels*) and CH_4 (*bottom two panels*). These time series were constructed with data provided by Ed Dlugokencky and Pieter Tans, NOAA/ESRL, and are available at www.esrl.noaa.gov/gmd/ccgg/trends/. See Masarie and Tans (1995) and Dlugokencky et al. (1994) for details of measurements.

reduced Northern Hemisphere (NH) mid-latitude column ozone amounts (Anderson et al., 2012, 2017; Anderson and Clapp, 2018). However, observational evidence that synoptic convective systems lead to enhanced catalytic ozone destruction in mid-latitudes is currently inconsistent (Schwartz et al., 2013; Solomon et al., 1997; Anderson et al., 2012, 2017). Though it has been posited that this mechanism may be enhanced in a warmer climate (Anderson and Clapp, 2018), the lack of evidence for any role for this mechanism in the current climate and the fact that in the future there will be lower atmospheric chlorine levels and hence reduced catalytic ozone destruction mean that there is low confidence in this proposed feedback.

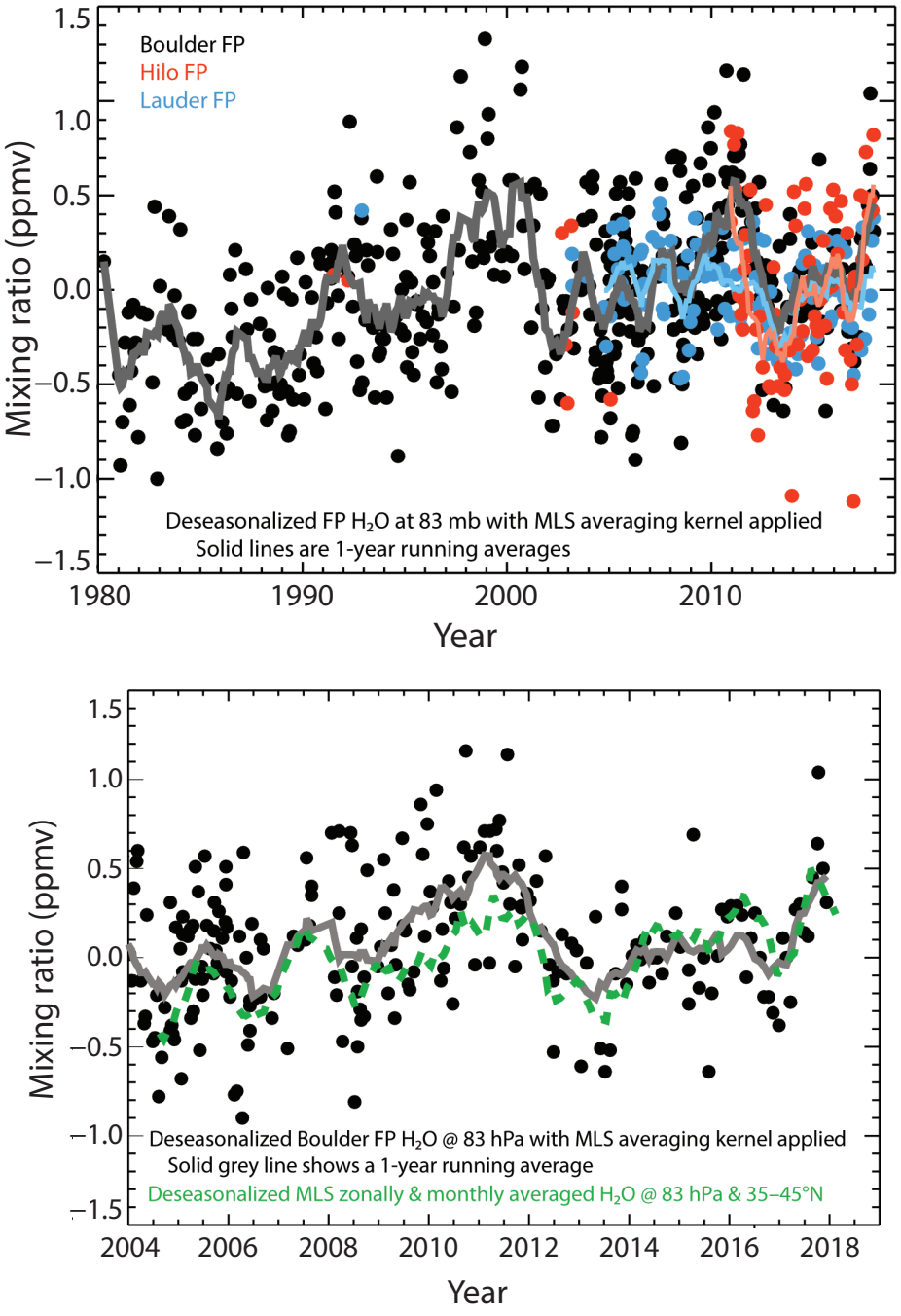

Figure 5-2. *Top panel:* Lower-stratospheric water vapor anomalies (black, red, and blue circles, plotted as difference from the monthly mean over the period 2004–2018) from balloon measurements taken between 1980 and 2018 at Boulder, Colorado (USA); Hilo, Hawaii (USA); and Lauder (New Zealand). *Bottom panel:* This graph is the same as the one above but shows only Boulder measurements (black circles) between 2004 and 2018, as well as zonally averaged water vapor anomalies (35–45°N) from the Aura Microwave Limb Sounder (MLS; green dashes). The frost point (FP) data extend the information plotted in Figure 2.55 of Blunden and Arndt (2017).

5.2.3 Stratospheric Aerosols

Stratospheric aerosols influence climate by scattering sunlight back to space, by modifying cloud microphysical processes, and by altering ozone chemistry. Trends and variability in stratospheric aerosols and their impact on ozone are discussed in detail in **Chapters 3** and **4** (see **Sections 3.2.1.4**, **4.2.3.1**, and **4.3.5.2**). Because they reflect sunlight, artificial enhancement of stratospheric aerosols has been proposed as a possible method for solar radiation management to cool the planet (see **Chapter 6**, **Section 6.2.5.2**). Stratospheric aerosols also warm the stratosphere by absorbing infrared radiation, and as such, they are important drivers of the observed stratospheric temperature variability (see **Section 5.3.1.2**). Major increases in stratospheric aerosols result from volcanic eruptions. The last major volcanic eruption that significantly perturbed stratospheric aerosols was Mount Pinatubo (in the Philippines) in 1991. What are believed to be background levels of stratospheric aerosols were reached in the late 1990s (Kremser et al., 2016), and since then, there have been moderate eruptions that have increased stratospheric aerosol loading (Neely et al., 2013). **Figure 5-3** (from Mills et al., 2016) shows the progression of the global aerosol burden from 1980 to 2015. Peak aerosol loading follows the Pinatubo eruption in 1991, with several shorter-lived increases following moderate eruptions during the early 21st century, the largest of which occurred in 2008. Sulfur-rich particles dominate stratospheric aerosols, but recent work has also highlighted the importance of organic aerosols (Murphy et al., 2014; Vernier et al., 2015; Yu et al., 2016) and has shown that they have likely increased significantly since the preindustrial period (Yu et al., 2016).

Increases in stratospheric aerosols in the presence of elevated stratospheric chlorine produce ozone loss. For example, the large October 2015 Antarctic ozone hole has been attributed to the presence of volcanic aerosols from the Calbuco eruption (in southern Chile) (Solomon et al., 2016). The potential for aerosols to enhance ozone loss is expected to decrease as chlorine loadings continue to decrease in the future (Klobas et al., 2017), but uncertainty in future levels of volcanic aerosol introduces uncertainty to determining when ozone recovery to 1980 levels is expected to occur (Naik et al., 2017).

Since the 2014 Ozone Assessment, there have been significant improvements in understanding of the existence of the Asian Tropopause Aerosol Layer (ATAL) (Vernier et al., 2011), which became evident only after aerosol concentrations returned to pre-Pinatubo concentrations. The ATAL is hypothesized to have a significant anthropogenic origin (Vernier et al., 2015) and, according to one study, likely contributes as much to the background aerosol in the Northern Hemisphere as small to moderate volcanic eruptions (Yu et al., 2017).

5.2.4 Ozone

Stratospheric ozone changes can impact climate by changing the large-scale atmospheric state, including impacts on the tropospheric circulation and ultimately surface weather (see **Section 5.4**), or by changing the amount of UV radiation that reaches the surface, both impacting surface temperatures and biogenic processes.

Since the late 1990s, concentrations of ODSs have declined in response to the implementation of the Montreal Protocol (see **Chapter 1**). **Chapter 3** reports that global (60°S–60°N) column ozone has been increasing by between 0.3% and 1.2% per decade since the late 1990s, but this increase is not statistically significant, owing to the comparatively large uncertainty of 1% per decade arising from dynamically forced interannual variability. Global column ozone is expected to increase with further reductions in the abundance of ODSs in the stratosphere. Current tropical column ozone is found to be unchanged compared to the period 1964–1980, consistent with the findings of the 2014 Assessment. Upper-stratospheric (35–45 km altitude) ozone in the tropics and mid-latitudes has increased by 1–3% per decade over the 2000–2016 period; these increases are statistically significant and are thought to be caused by a combination of reductions in ODSs and GHG-induced cooling. Climate models predict a decrease in tropical lower-stratospheric ozone due to a modeled increase in strength of the stratospheric overturning circulation. However, due to large internal variability, which is also seen in models, this decrease has not been detected in a statistically significant manner since 2000. As noted in **Chapter 4**, the characteristics of the Antarctic ozone hole in October during recent years are similar to those in the early 1990s; its size and duration are still

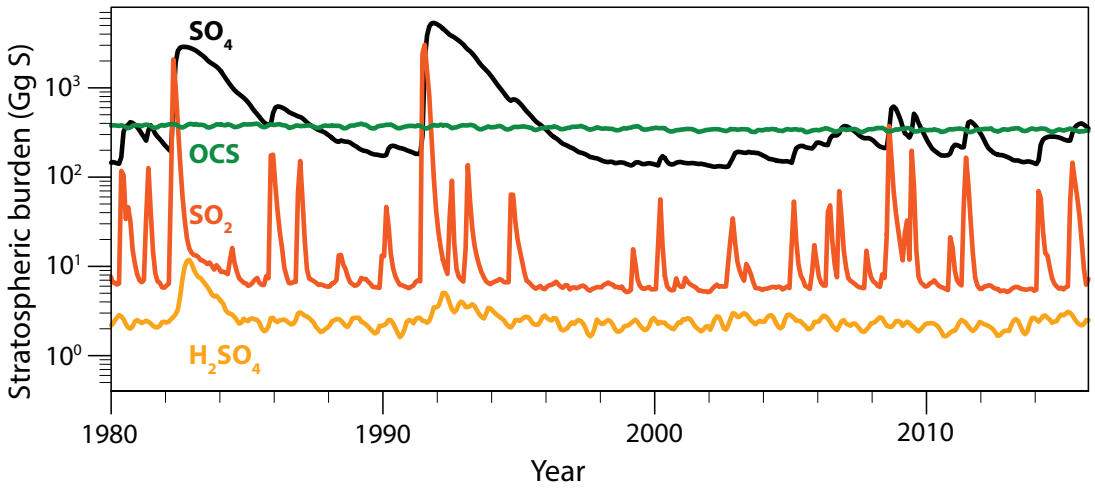

Figure 5-3. Calculated global mass burdens of major sulfur-bearing species from a specified dynamics (SD-) WACCM VOLC simulation above the tropopause, shown as a function of time from 1 January 1980 to 31 December 2015 (updated from Mills et al., 2016). The black line shows SO_4 (sulfate); the green line, OCS (carbonyl sulfide); the yellow line, H_2SO_4 (sulfuric acid); and the red line, SO_2 (sulfur dioxide). Mass burdens are shown in units of Gg (=10^9 g) of S. Note that the burden of dimethylsulfide in the stratosphere (10^{-3}–10^{-2} Gg S) is too small to be shown. The spikes in the SO_2 trace (red line) indicate where volcanic eruptions reached the stratosphere. The actual eruptions used are detailed in Mills et al. (2016). Note: there was an error in the originally published version due to an incorrect adjustment for molecular weights, so the burdens of the gases have shifted.

impacted in cases of high volcanic aerosol loading, such as from the Calbuco eruption in 2015 (Solomon et al., 2016). However, statistically significant positive trends in ozone have been observed in the Antarctic in September since 2000 (Solomon et al., 2016). Overall, there have been minimal long-term ozone changes found in the Arctic, where dynamically forced interannual variability in ozone in winter and spring is large compared to the long-term changes.

5.2.5 Solar Activity

Total solar irradiance (TSI), which measures the amount of solar radiation at the top of Earth's atmosphere, has been directly monitored by satellites since 1978. TSI varies on a wide range of timescales, the most relevant of which for understanding recent stratospheric climate and ozone changes is the approximately 11-year cycle during which TSI varies by about 1 W m^{-2} (<0.1%) between solar cycle maximum and minimum (Haigh, 2007). When solar activity is high, incoming solar UV radiation is enhanced, impacting ozone production in the stratosphere and mesosphere (Haigh, 2007). Changes in the absorption of UV radiation by ozone then impacts stratospheric temperature distributions and, consequently, circulation and climate (Gray et al., 2010). The impact of solar cycle variations on ozone depends on solar spectral irradiance (SSI) and, in particular, the fraction of variance in the UV spectral region. The peak of the current 24th 11-year solar cycle, which started in December 2008, was weaker than previous cycles (Hathaway, 2015). At present, the sun is approaching a minimum phase of the solar cycle.

5.3 OBSERVED AND SIMULATED CHANGES IN STRATOSPHERIC CLIMATE

Section 5.2 reviewed observed changes in some of the major constituents and external drivers of stratospheric climate. This section describes the current understanding from observations and model simulations of recent and future changes in stratospheric climate and their drivers.

5.3.1 Stratospheric Temperatures

Stratospheric temperature trends are a key marker for anthropogenic effects on the climate system (IPCC, 2013; USGCRP, 2017). Moreover, stratospheric temperature trends affect stratospheric ozone abundances through effects on the rates of photochemical reactions (see **Chapters 3** and **4**). The 2014 Assessment concluded that over the past several decades, increases in atmospheric GHGs and decreases in stratospheric ozone abundances have been the major radiative drivers of global mean cooling in the middle and upper stratosphere. In the lower stratosphere, observed global mean cooling was largely attributed to stratospheric ozone changes over the past few decades. The latitudinal structure of stratospheric temperature trends is strongly influenced by changes in the stratospheric overturning circulation (see **Section 5.3.2**), which may be externally forced and/or associated with internal variability. This section focuses on what has been learned about stratospheric temperature trends since the 2014 Ozone Assessment, notably, improved constraints on satellite-observed temperature trends and new efforts to attribute observed and model-simulated temperature variability and trends to natural and anthropogenic drivers.

5.3.1.1 Observed Temperature Changes

Observations of stratospheric temperatures come from operational radiosondes, operational polar orbiting satellites, GPS Radio Occultation satellite networks, and from research satellites and rocket sondes. Radiosonde observations span the longest time period (starting in the late 1950s), but there are discontinuities due to changes in instrumentation and location of stations, and they cover only the lower part of the stratosphere. Consequently, homogenized datasets based on radiosondes have been constructed to improve the accuracy of radiosonde temperature time series, e.g., IUK (Sherwood and Nishant, 2015); RATPAC (Lanzante et al., 2003); RAOBCORE and RICH (Haimberger et al., 2012); and HADAT2 (Thorne et al., 2005). Global temperature data for the stratosphere are available from the Microwave Sounding Unit (MSU) and Stratospheric Sounding Unit (SSU) satellite instruments that flew on operational polar orbiters and provided coverage from late 1978 to 2005. MSU and SSU measure stratospheric temperatures over four broad layers covering the lower stratosphere (MSU Channel 4 [MSU4], 13–22 km; and SSU Channel 1 [SSU1], 25–35 km), the middle stratosphere (SSU Channel 2 [SSU2], 35–45 km), and the upper stratosphere (SSU Channel 3 [SSU3], 40–50 km). These instruments were replaced by the Advanced Microwave Sounding Unit (AMSU), which started flying in 1998. Continuing the record has required merging the MSU/SSU data with AMSU data or with measurements from other recent satellite records (see below).

The 2014 Ozone Assessment highlighted a significant discrepancy in global long-term temperature trends in the middle stratosphere between the two independent analyses of the SSU record from the UK Met Office and the National Oceanographic and Atmospheric Administration (NOAA). The NOAA Center for Satellite Applications and Research (STAR) SSU v1.0 dataset (Wang et al., 2012) showed temperature trends over 1979–2006 of -1.24 ± 0.13, -0.93 ± 0.14, and -1.01 ± 0.19 K decade^{-1} in SSU1, SSU2, and SSU3, respectively (Wang et al., 2012). These could be compared with trends in the UK Met Office SSU dataset available at that time of -0.52 ± 0.23, -0.40 ± 0.23, and -1.27 ± 0.33 K decade^{-1} (Wang et al., 2012). The NOAA STAR dataset therefore showed substantially larger cooling trends in SSU1 and SSU2 and a weaker cooling trend in SSU3 compared to the UK Met Office dataset.

Since the 2014 Ozone Assessment, both groups have published revised versions of their SSU datasets (Nash and Saunders, 2015; Zou et al., 2014). The reprocessed SSU records show much greater consistency in the estimated global and annual mean temperature trends throughout the stratosphere than was reported in the 2014 Assessment (Seidel et al., 2016) (**Figure 5-4**). This reflects substantial progress in understanding the sources of differences in temperature trends between the two SSU datasets, but differences remain that are larger than the uncertainty estimates provided by each research team (Seidel et al., 2016). The satellite observations in **Figure 5-4** show global stratospheric cooling of about 1.5 K (25–35 km), 1.5 K (35–45 km), and 2.3 K (40–50 km) between 1979 and 2005. The largest outstanding discrepancies are in SSU2 and SSU3, where the NOAA dataset shows stronger cooling in SSU2 by about 0.6 K and weaker cooling in SSU3 by about 0.3 K than in the UK Met Office dataset. However, the reprocessed NOAA SSU dataset shows a vertical coherency in stratospheric temperatures that is more consistent with model simulations

than the UK Met Office dataset (Seidel et al., 2016), suggesting that the NOAA SSU dataset provides a more physically consistent representation of stratospheric temperatures.

Since the 2014 Assessment, there have been efforts to extend the SSU record, which ended in 2006, to near-present day using more recent satellite measurements, including AMSU-A (Zou et al., 2016; McLandress et al., 2015), SABER, and MLS (Randel et al., 2016). The signal weightings as a function of altitude of the more recent satellite instruments are different from those of the SSU instruments. Recent studies have focused on developing methods to map the current satellite retrievals onto the SSU weighting functions in order to produce a consistent merged record. Analysis of stratospheric temperature trends in satellite records covering the recent past has revealed weaker trends after around 1997 (Zou et al., 2016; McLandress et al., 2015; Randel et al., 2016; Khaykin et al., 2017) (**Figure 5-5**), which is consistent with current understanding of the timing of peak atmospheric chlorine loading (see **Chapter 1**), the coincident changes in stratospheric ozone trends (see **Chapters 3** and **4**), and associated effects on stratospheric temperatures (Ferraro et al., 2015; Randel et al., 2017).

In the lower stratosphere (13–22 km), the three MSU4 records, NOAA/STAR v4.0 (Zou et al., 2006), the Remote Sensing Systems (RSS) v3.3 (Mears et al., 2011), and the University of Alabama in Huntsville (UAH) v6.0 data sets (Christy et al., 2003), show a net cooling in the global mean between 1979 and 2016 of about 1 K. The majority of the observed global lower stratospheric cooling in the MSU4 record occurred before the mid-1990s (**Figure 5-4**). Since then there has been little overall global temperature change in the MSU4 record (Seidel et al., 2016; Polvani et al., 2017). The long-term cooling is interspersed by short-term global stratospheric warming for a few years following the two major tropical volcanic eruptions in the epoch (El Chichón in 1982 and Mt. Pinatubo in 1991). The stratospheric heating from volcanic aerosols peaks in the lower stratosphere (**Figure 5-4d**) but is also evident in the middle and upper stratosphere (**Figure 5.4a–5.4c**).

The University of Alabama in Huntsville (UAH) MSU4 dataset shows slightly stronger cooling over the record, by about 0.2 K, compared to the NOAA STAR and Remote Sensing Systems (RSS) MSU4 datasets (**Figure 5-4d**) (Seidel et al., 2016). The majority of the differences in temperature trends between the three MSU4 datasets are associated with temperature changes at high latitudes (Seidel et al., 2016). The three MSU4 records agree reasonably well, in the global mean, with the radiosonde datasets RAOBCORE and RICH (**Figure 5-4d**), but the comparison with the radiosonde data is problematic because the disagreement between the two radiosonde datasets is as large as the difference between either of them and the MSU4 datasets.

As reported in the last Assessment, long-term MSU4 temperature trends show considerable structure in latitude and by season. **Figure 5-6a** shows MSU4 temperature trends over 1979–1997. The trends show significant cooling throughout most of the year in the tropics and also in mid-latitudes, with enhanced cooling in the Antarctic in austral spring and summer. An enhanced cooling in the Arctic in mid-winter as well as a warming in SH high latitudes in August are also observed, but these are not reproduced by the chemistry–climate models (**Figure 5-6b**), suggesting this is likely a manifestation of the large internal variability in the polar stratosphere during winter affecting the calculated trends over a relatively short 19-year period (see **Section 5.3.1.3**). Over the period 1998–2016 (**Figure 5-6c**), the tropics is the only region where significant cooling has been observed in the MSU4 record in boreal late spring and early summer.

In addition to satellite and in situ stratospheric temperature measurements, there are numerous meteorological reanalysis datasets produced by the world's meteorological services. Reanalysis products are widely used in the literature for atmospheric process studies, but developers have cautioned against their use for climate trend studies, owing to potential discontinuities in the records that can be introduced by the integration of different satellite records into the model data assimilation system (Simmons et al., 2014). The WCRP SPARC Reanalysis Intercomparison Project (S-RIP) has recently assessed the representation of long-term stratospheric temperature changes in a number of current reanalysis systems (Long et al., 2017). These reanalysis products have been compared with the NOAA STAR MSU/AMSU v3.0 and SSU v2.0 SSU1 and SSU2 records by sampling the pressure level output fields with the satellite weighting functions

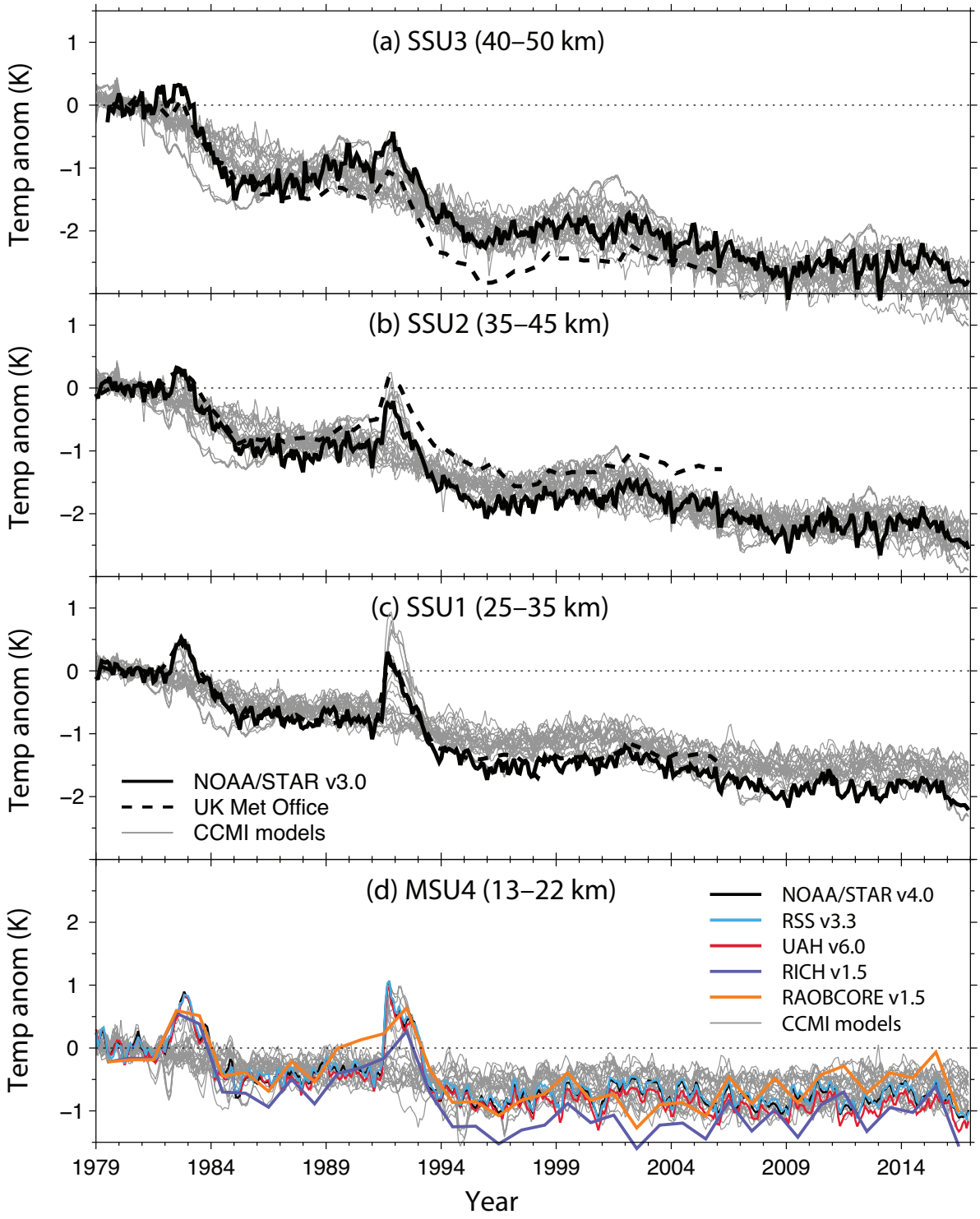

Figure 5-4. Time series of global mean stratospheric temperature anomalies from 1979 to 2016. Panels show SSU Channels 3, 2, 1 (SSU3, SSU2, SSU1; a, b, c) and MSU channel 4 (MSU4; d) for the altitude ranges, datasets, and model outputs indicated in the legends. Gray lines indicate results from a total of 23 ensemble members across 14 Chemistry-Climate Model Initiative (CCMI) models for the REF-C2 experiment, weighted by the appropriate satellite weighting function for comparison with observations. All data in panel d are shown as monthly averages except the UK Met Office dataset, which uses 6-month averages, and the two radiosonde datasets, which are annual means. The radiosonde data are as in Figure 2.8 of Blunden and Arndt (2017). Anomalies are shown relative to 1979–1981. Adapted from Maycock et al. (2018).

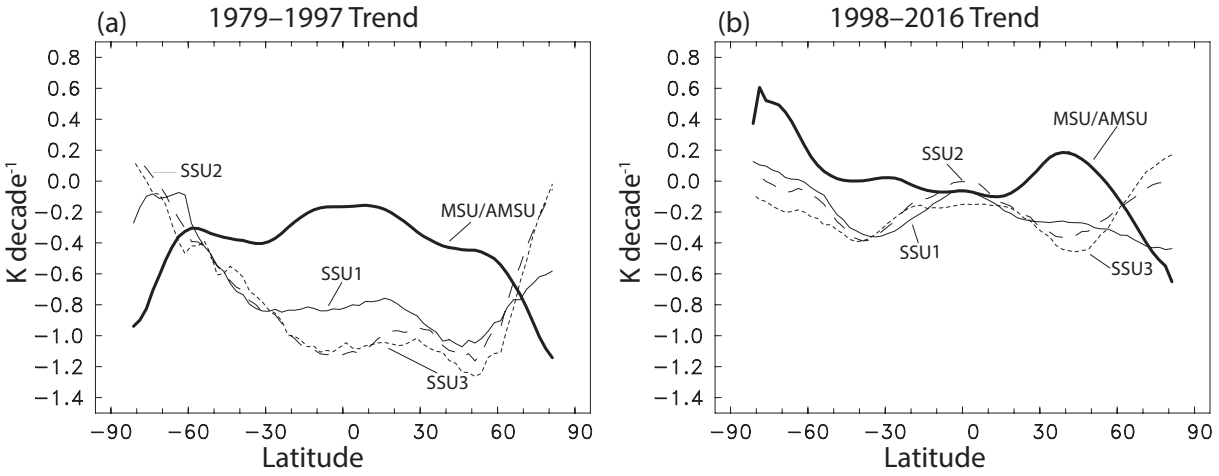

Figure 5-5. Observed annual mean stratospheric temperature trends in a merged satellite (SSU and MLS) record for the periods (a) 1979–1997 and (b) 1998–2016. Thick solid lines show MSU/AMSU, thin solid lines show SSU1, dashed lines show SSU2, and dotted lines show SSU3. Updated from Randel et al. (2016).

(Long et al., 2017). In the lower stratosphere, the reanalyses generally show weaker long-term cooling compared to MSU4, by up to ~0.5 K (~50%) over the period 1979–2015. There are larger differences in the temperature trends among the reanalyses in the middle and upper stratosphere, with the NCEP Climate Forecast System Reanalysis (CFSR) showing particularly large and unrealistic interannual and decadal variations, owing to its construction from multiple streams (Long et al., 2017). In other current reanalysis datasets, the differences in the long-term global mean temperature change in SSU1 and SSU2 compared to observations are typically <1 K over 1979–2015. In conclusion, current reanalyses show deficiencies in capturing both short- and long-term variations in stratospheric temperatures found in satellite measurements.

5.3.1.2 Simulation and Attribution of Past Global Stratospheric Temperature Changes

New studies published since the 2014 Assessment have quantified the contribution of different external factors, such as changing GHG concentrations and ozone (or ozone-depleting substance; ODS) concentrations, to observed stratospheric temperature changes over the satellite era.

According to one study, which applied a standard detection and attribution analysis to global stratospheric temperature records from the NOAA/STAR SSU v1.0 dataset, the effects of GHGs and ozone were not distinguishable separately in the middle to upper stratosphere (Mitchell, 2016), consistent with the conclusion of the 2014 Assessment. Another study, which analyzed chemistry–climate model experiments with incrementally added forcing agents and prescribed observed SSTs, found that ODSs contributed about 0.4 K (one-quarter) of the global mean cooling in SSU1 and about 0.7 K (one-third) of the cooling in SSU2 between 1979 and 1997, with virtually all cooling after 2000 being attributed to GHGs (Aquila et al., 2016) (see **Figure 5-7** for SSU2). In the upper stratosphere in SSU3, both a standard detection and attribution approach (Mitchell, 2016) and a chemistry–climate model study (Aquila et al., 2016) attribute about two-thirds of the long-term global average cooling between 1979 and 2005 to GHGs and one-third to ODSs. Chemistry–climate model experiments with incrementally added forcings further demonstrate that the relatively rapid decreases in global upper-stratospheric temperatures that occurred in the early 1980s and early 1990s were likely the result of a coincidence between a relative decrease in temperature following warming from major tropical volcanic eruptions and the declining phase of the 11-year solar cycle (Aquila et al., 2016). Stratospheric water vapor changes may have also contributed to cooling in the lower stratosphere over the last 30 years (Maycock et al., 2014); however,

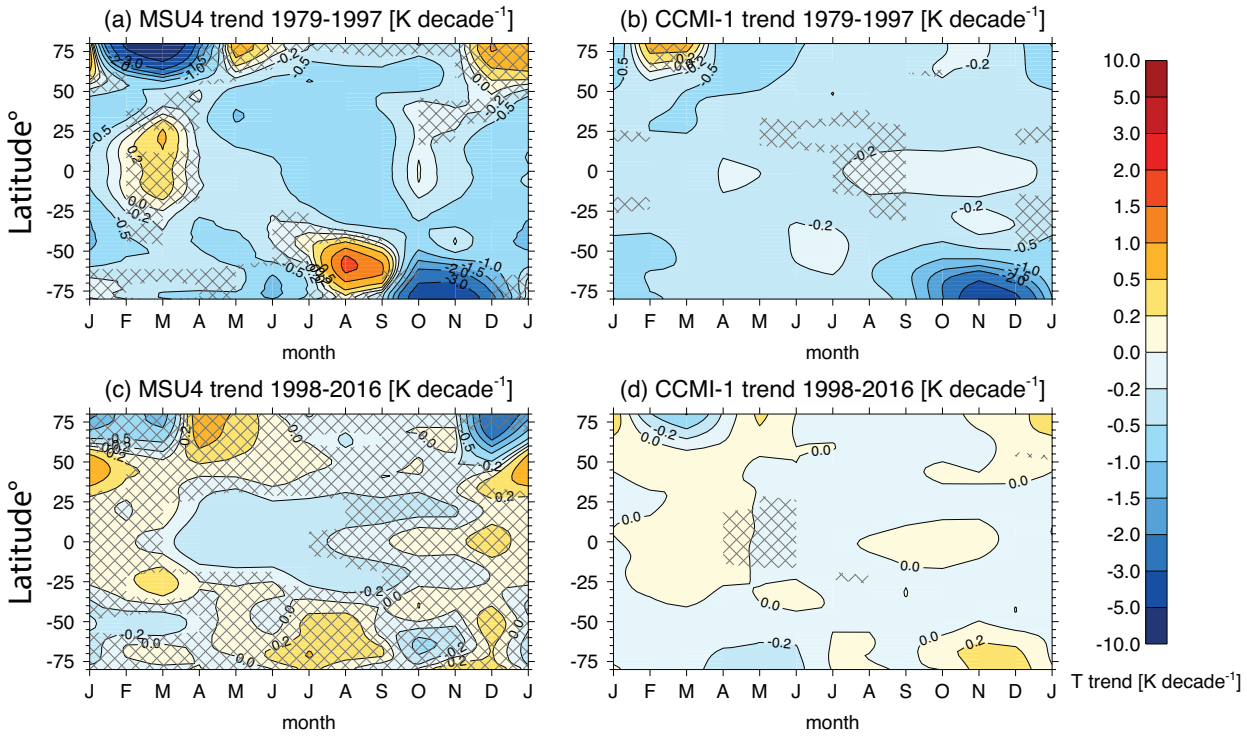

Figure 5-6. Lower-stratospheric temperature trends over the periods (a, b) 1979–1997 and (c, d) 1998–2016 in K per decade as a function of latitude and month from (a, c) satellite MSU/AMSU NOAA/STAR v4.0 (MSU4) and (b, d) multi-model mean MSU4 temperatures from 12 CCMI models for the REF-C2 simulation. The following years, which were influenced by volcanic eruptions, are treated as missing data in panels a and b: 1982, 1983, 1991, 1992, 1993. The hatching in panels a and c shows where the magnitude of the observed trend is within the 5–95% range of simulated internal variability, estimated from the spread in modeled trends, and is therefore estimated to be not statistically significant (at the 95% confidence level). Hatching in panels b and d shows where the observed MSU4 trends in panels a and c lie outside the 5–95% range of model trends, thus showing areas where the simulated and observed trends are inconsistent. Based on datasets described in Maycock et al. (2018).

the magnitude of this effect is not well constrained due to uncertainties in global long-term stratospheric water vapor trends (see **Section 5.2.2**).

In the last Assessment, simulations from climate models and chemistry–climate models were found to show weaker global average cooling than estimated from observations in the lower and upper stratosphere. In the middle stratosphere (35–45 km), the modeled trends were within the range of the observational uncertainty (Thompson et al., 2012). **Figure 5-4** shows simulated global average stratospheric temperature anomalies in the CCMI REF-C2 experiment (see **Chapter 3** and Morgenstern et al. (2017) for model details) alongside the satellite observation datasets described above (Maycock et al., 2018). The model pressure level output has been sampled according to the satellite weighting functions to facilitate the comparison with observations. The main new findings are that the model-simulated temperature changes are now in good agreement with the revised NOAA STAR SSU dataset in the upper stratosphere (40–50 km), whereas the revised UK Met Office record still shows stronger cooling than simulated in the chemistry–climate models, as was reported in the 2014 Assessment. In the lower stratosphere in the MSU4 (13–22 km) and SSU1 (25–35 km), the models show on average slightly weaker long-term cooling than observed, similar to the findings of the 2014 Assessment, though the observed trends lie within the range of individual model realizations (Maycock et al., 2018).

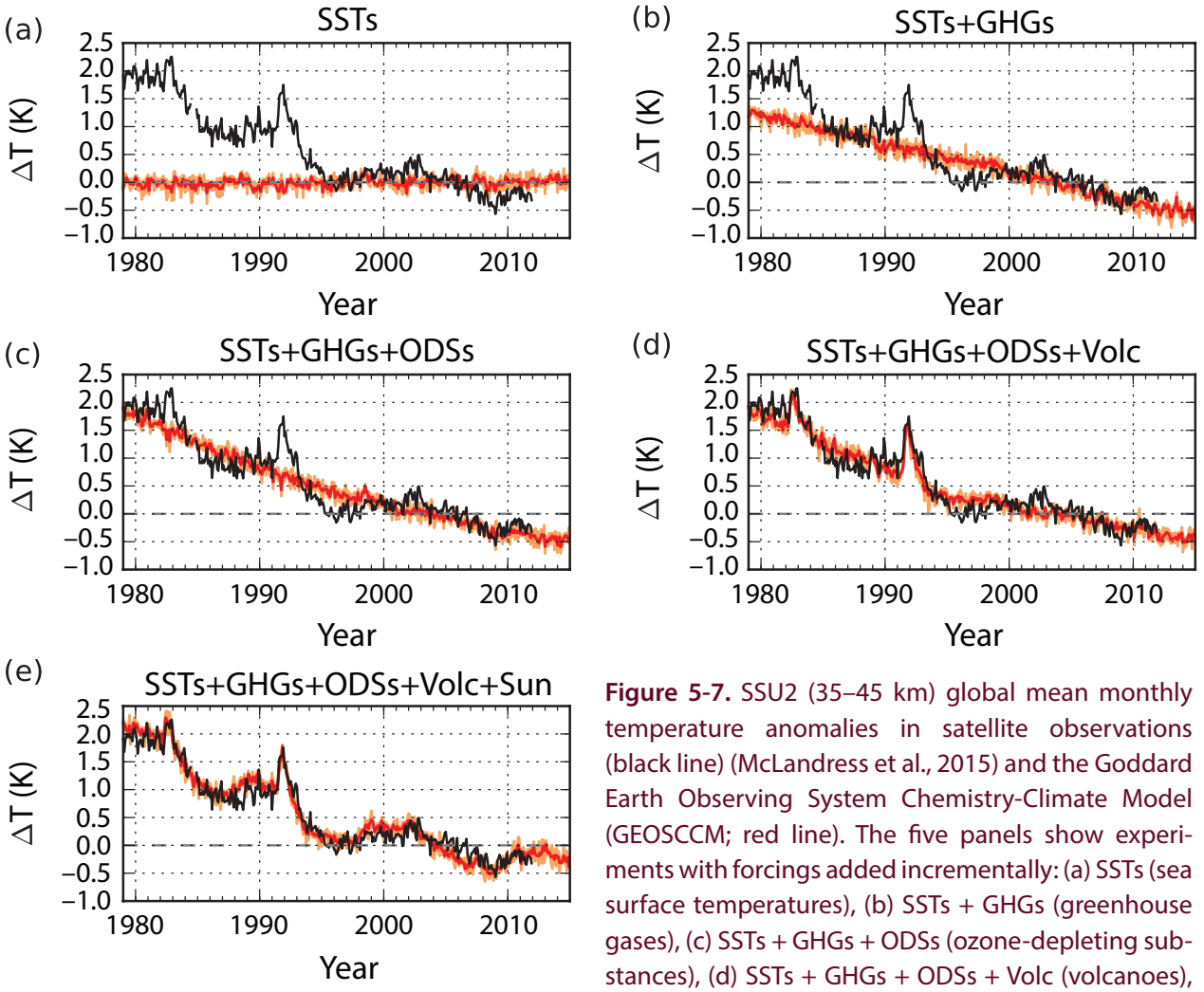

Figure 5-7. SSU2 (35–45 km) global mean monthly temperature anomalies in satellite observations (black line) (McLandress et al., 2015) and the Goddard Earth Observing System Chemistry-Climate Model (GEOSCCM; red line). The five panels show experiments with forcings added incrementally: (a) SSTs (sea surface temperatures), (b) SSTs + GHGs (greenhouse gases), (c) SSTs + GHGs + ODSs (ozone-depleting substances), (d) SSTs + GHGs + ODSs + Volc (volcanoes), (e) SSTs + GHGs + ODSs + Volc + Sun (solar). Time series are plotted as anomalies relative to the 1995–2011 average. The solid red lines show the model ensemble means, and the shaded areas show the spread across the three ensemble members. Adapted from Aquila et al. (2016).

The difference in global mean lower-stratospheric temperature trends is at least partly associated with the CCMI multi-model mean showing weaker cooling in the tropics than found in observations (**Figure 5-6b**). Note that many of the CCMI models did not include the radiative effects of volcanic aerosols in the REF-C2 experiment, following the interpretation of the experimental design by modeling groups, and hence most of the models do not capture stratospheric warming following the two major volcanic eruptions since 1979 (**Figure 5-4**). In conclusion, there is now greater consistency between observed and modeled global stratospheric temperature trends in all the SSU channels, and this is largely the result of the updates to the satellite records since the 2014 Assessment rather than any major changes in the modeled temperature trends (McLandress et al., 2015; Maycock et al., 2018).

5.3.1.3 Simulation and Attribution of Past Polar Stratospheric Temperature Trends

In addition to the attribution of global mean stratospheric temperature changes to different external factors, studies have separately analyzed the contribution of radiative and dynamical processes to seasonal polar stratospheric temperature trends. Dynamical contributions to temperature changes occur through adiabatic heating (cooling) associated with downwelling (upwelling) motion. In the Arctic, studies indicate an

important role for dynamical processes in determining the observed long-term lower-stratospheric cooling in boreal spring, though the precise magnitude of the dynamical contribution depends on the approach used to separate the radiative and dynamical contributions (Bohlinger et al., 2014; Ivy et al., 2016). In the Arctic in boreal summer, the observed stratospheric cooling at 50 hPa is smaller in magnitude and is, as expected, dominated by the radiative effects of increasing GHGs and ozone. In the Antarctic, changes in dynamics have acted to slightly enhance the radiative cooling from ozone loss in austral spring but have offset part of the radiative cooling in austral summer, resulting in weaker lower-stratospheric temperature trends than would arise from radiative effects alone (Keeley et al., 2007; Orr et al., 2013; Ivy et al., 2016). Thus, the observed long-term cooling trend in the Antarctic lower stratosphere in austral spring is slightly enhanced by the effect of dynamical feedbacks to the observed ozone trends (see **Chapter 4**). Since 2000, during the period when emergence of healing of the Antarctic ozone hole has been observed (Solomon et al., 2016), Antarctic lower-stratospheric temperature trends show a warming in austral spring, which can be partly attributed to radiative effects of ozone trends as well as to dynamical changes that may be associated with internal variability (Solomon et al., 2017).

Chemistry–climate model experiments show substantial differences in polar temperature trends, particularly in the lower stratosphere, between different ensemble members forced with identical observed SSTs, sea ice, and external forcing agents and initialized using a range of atmospheric initial conditions (Randel et al., 2017; Maycock et al., 2018) or with slight differences in the model parameterizations (Garfinkel et al., 2015a). In fact, the spread of simulated trends suggests that recent observed polar temperature trends (**Figure 5-6b**) are not inconsistent with internal variability, assuming that these models offer a realistic representation of the forced and unforced components of stratospheric temperature change. For example, although the CCMI REF-C2 multi-model mean does not capture the recent observed Arctic warming in boreal winter and cooling in boreal spring in the MSU4 (**Figure 5-6b**), the observed trends in the Arctic lie within the range of model simulations (Maycock et al., 2018). Observed SST changes have been estimated to account for about half of the recent Arctic stratospheric cooling trend in boreal spring (Garfinkel et al., 2015a), which is broadly in agreement with the estimated dynamical contribution to Arctic temperature trends discussed in **Section 5.3.1.2** (Bohlinger et al., 2014; Ivy et al., 2016). The models in **Figure 5-6b** either included a coupled ocean or used SST and sea ice boundary conditions from another model simulation, and thus the evolution of SSTs will likely differ from observations, though any forced component of SST change and its effect on polar temperature trends should be at least partly captured.

5.3.1.4 Simulated Future Stratospheric Temperature Changes

As described in the 2014 Ozone Assessment, future global stratospheric temperature trends will be determined by the relative rates of change in the major drivers of temperature in the stratosphere: CO_2, ozone, and, to a lesser extent, stratospheric water vapor. For a low GHG scenario, projected increases in ozone may result in a weak or even a small positive global temperature trend in the upper stratosphere (Maycock, 2016). For higher GHG scenarios, global cooling in the upper stratosphere due to projected CO_2 increases dominates over the warming effect from increasing ozone, and therefore temperatures are projected to decrease over the 21st century (Stolarski et al., 2010; Douglass et al., 2012; Maycock, 2016). One possible source of uncertainty in future temperature trends, particularly in the lower stratosphere, is the large spread in projected stratospheric water vapor concentrations (Smalley et al., 2017), though this effect has not yet been quantified.

The latitudinal and seasonal patterns of future temperature trends in the lower stratosphere also depend on the GHG scenario. **Figure 5-8** shows projected temperature trends at the altitude of the MSU4 channel from the CCMI REF-C2 experiment. The projected warming in the Antarctic in austral spring and summer is very prominent over the first half of this century as the ozone hole reduces in depth and extent (see **Chapter 4**). This warming is about a factor of two smaller for the medium-to-high GHG scenario (RCP-6.0; **Figure 5-8a**) than for the low GHG scenario (RCP-2.6; **Figure 5-8c**). Polar stratospheric temperature trends are also affected by changes in

the deep branch of the stratospheric overturning circulation (see **Section 4.3.4**). In the Arctic, the CCMI models simulate a mid-winter warming in the lower stratosphere over the first half of the century. Future Arctic lower-stratospheric temperature trends will be determined by a balance between changes in high-latitude wave driving and associated changes in downwelling over the pole as well as radiative effects from changes in ozone and GHGs (Oberländer et al., 2013; Rieder et al., 2014; Langematz et al., 2014; Bednarz et al., 2016). These findings are generally consistent with the 2014 Ozone Assessment. Over the second half of the 21st century, there is projected warming in the lower stratosphere across most of the tropics and subtropics in the low GHG scenario (**Figure 5-8d**), whereas the models project cooling in this region for the medium-to-high GHG scenario (**Figure 5-8b**). Thus, the sign of projected tropical lower-stratospheric temperature trends over the second half of the 21st century is dependent on the GHG scenario.

5.3.2 Brewer–Dobson Circulation

Changes in the strength of the stratospheric overturning circulation, or the Brewer–Dobson circulation (BDC), are key drivers of changes in stratospheric temperature (see **Section 5.3.1**), tracer concentrations (see **Chapter 3**, **Section 3.4.2**, and **Chapter 4**, **Section 4.3.4**), and stratosphere–troposphere exchange (**Section 5.3.3**). This section is dedicated to assessing the main advances in understanding of the BDC since the last Assessment, with special emphasis on the long-term trends.

5.3.2.1 Observations

The BDC is not directly measured and thus has to be derived indirectly from temperature observations, dynamical reanalysis fields, or tracer measurements. While a strengthening of the BDC is simulated in response to climate change, it has remained elusive in the observations. The 2014 Ozone Assessment

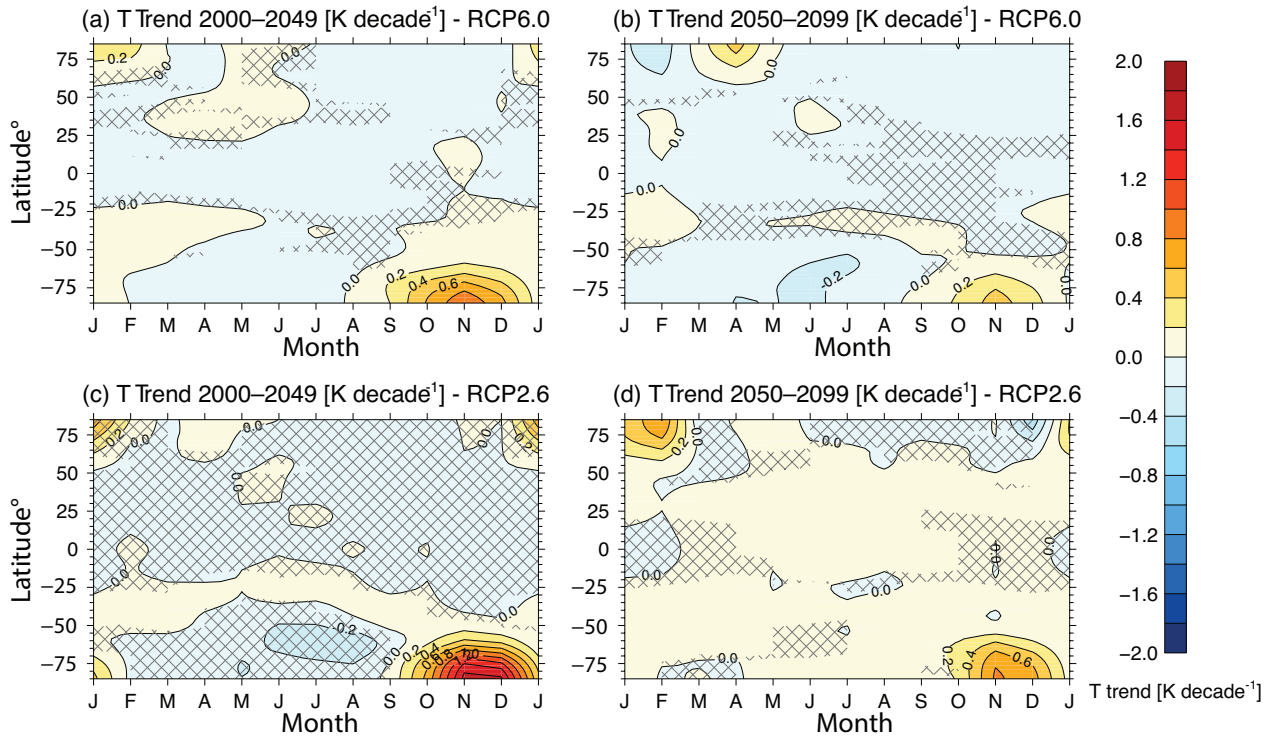

Figure 5-8. CCMI multi-model mean zonal-mean MSU4 channel (~13–22 km) temperature trends (K per decade) over the periods (a, c) 2000–2049 and (b, d) 2050–2099 under (a, b) the medium-to-high greenhouse gas (GHG) scenario (RCP-6.0; 12 models) and (c, d) the low GHG scenario (RCP-2.6; 4 models). Regions where less than two-thirds of the models agree on the sign of the trend are hatched. Based on model simulations described in Morgenstern et al. (2017) and Maycock et al. (2018).

examined a few studies that provided evidence of an acceleration in lower-stratospheric tropical upwelling in recent decades (Fu et al., 2010; Young et al., 2012), while no consistent trends in the BDC were found in the upper stratosphere. Since then, additional studies have inferred BDC trends from satellite and radiosonde temperature observations in the lower stratosphere (Ossó et al., 2015; Fu et al., 2015), obtaining an estimated acceleration of annual mean upwelling in the lower stratosphere of about 2% per decade, which is in quantitative agreement with climate model trends (e.g., Butchart, 2014). The 2014 Assessment highlighted inconclusive results on BDC trends inferred from reanalysis data; however, new studies have obtained estimates of an acceleration in lower-stratospheric tropical upwelling of 2–5% per decade in reanalyses (Fueglistaler et al., 2014; Abalos et al., 2015; Miyazaki et al., 2016), consistent with climate model trends. This advance is due to the combination of several reanalysis datasets and estimates to extract common signals among them. Nevertheless, these studies reveal a large spread in both the baseline magnitude and the long-term trends of the BDC among different reanalysis datasets and different methods for estimating the circulation. Moreover, in contrast with the broad agreement on acceleration in the lower-stratospheric BDC, the sign of the trends in the middle and upper stratosphere remains uncertain. This is because reanalyses are affected by major discontinuities above ~10 hPa, which hampers deriving trends at these levels (Simmons et al., 2014; Abalos et al., 2015). Note that in general, reanalyses are deemed to be unreliable for studying long-term stratospheric changes (see **Section 5.3.1.1**). While this undermines confidence in estimated BDC trends from reanalyses, reanalyses remain the only available observational-based source with global coverage; therefore, these estimates currently cannot be verified against independent data.

Long-lived tracer measurements in the stratosphere can be used to derive the age of air (AoA), a measure of the net tracer transport circulation strength that integrates effects of both the advection by the overturning circulation and mixing (see **Box 5-2**). Reconciling the observed and modeled AoA trends has been a major issue since an analysis of balloon measurements revealed a small aging of stratospheric air over the last decades (Engel et al., 2009), which was inconsistent with the negative AoA trends produced by climate models (Waugh, 2009). While the observed trends in AoA reported in one study (Engel et al., 2009) were not highly statistically significant, they have been recently supported with extended observations for 2015–2016 (Engel et al., 2017). In the 2014 Assessment, it was mentioned that spatiotemporal sparseness of the measurements could be a key issue for interpreting the disagreement between models and data (Garcia et al., 2011). To address this issue, long-term (>30 years) AoA trends have been obtained by combining observations with models of varying complexity (Ray et al., 2014; Hegglin et al., 2014). These combined data–model-derived AoA estimates show negative trends in the lower stratosphere and positive trends in the middle stratosphere (consistent with Engel et al., 2017). One such example is illustrated in **Figure 5-9**, which shows the AoA trends for the NH mid-latitudes as a function of altitude derived from tracer observations (Ray et al., 2014). AoA trends derived from the ERA-Interim reanalysis show a qualitatively similar structure (Diallo et al., 2012; Ploeger et al., 2015), although this result is likely to depend on the reanalysis dataset. The decrease in AoA in the NH mid-latitude lower stratosphere shown in **Figure 5-9** and in another study (Hegglin et al., 2014) is consistent with the estimated increase in the overturning circulation described above; however, as outlined in **Box 5-2**, AoA is strongly affected by mixing, and hence its local trends do not necessarily indicate changes in overturning circulation. Importantly, these new studies also demonstrate that the observed decrease in AoA in the lower stratosphere can be reconciled within uncertainties with the trends derived from chemistry–climate models, while the disagreement between observations and models remains at higher altitudes.

Global estimates of AoA from satellite tracer measurements are available only for about a decade after 2002. Over this recent period, the observations show trends of opposite sign in the two hemispheres, with AoA decreasing in the Southern Hemisphere and increasing in the Northern Hemisphere (Stiller et al., 2012; Haenel et al., 2015). This behavior is consistent with AoA trends over the same period independently derived from HCl measurements (Mahieu et al., 2014) and from the ERA-Interim reanalysis (Ploeger et al., 2015). The main difference between the decadal and the long-term trends in the reanalysis is that the

Box 5-2. What Is the Age of Stratospheric Air?

The Brewer–Dobson circulation (BDC) controls, to a large extent, the global distributions of tracers in the stratosphere, including ozone (see **Chapters 3** and **4**). Despite its relevance, there remain large uncertainties in the mean magnitude and the long-term trends of the BDC, as this planetary-scale circulation cannot be directly measured (Butchart, 2014). The mean age of stratospheric air (AoA) is an estimate of the time of residence of an air parcel in the stratosphere since it entered through the tropical tropopause (Hall and Plumb, 1994; Waugh and Hall, 2002). Mean AoA can be inferred from observations of long-lived tracers with near-linear tropospheric sources, such as SF_6 or CO_2, and thus constitutes a useful benchmark for the representation of stratospheric transport in models (Waugh and Hall, 2002). The annual mean climatology of AoA derived from the MIPAS satellite data is shown in **Box 5-2 Figure 1a**. There is broad agreement among independent observations showing ages of 4–6 years in the lower stratosphere mid-latitudes (~40–60°N, ~20–25 km) and less agreement at high and low latitudes and at higher levels (Haenel et al., 2015).

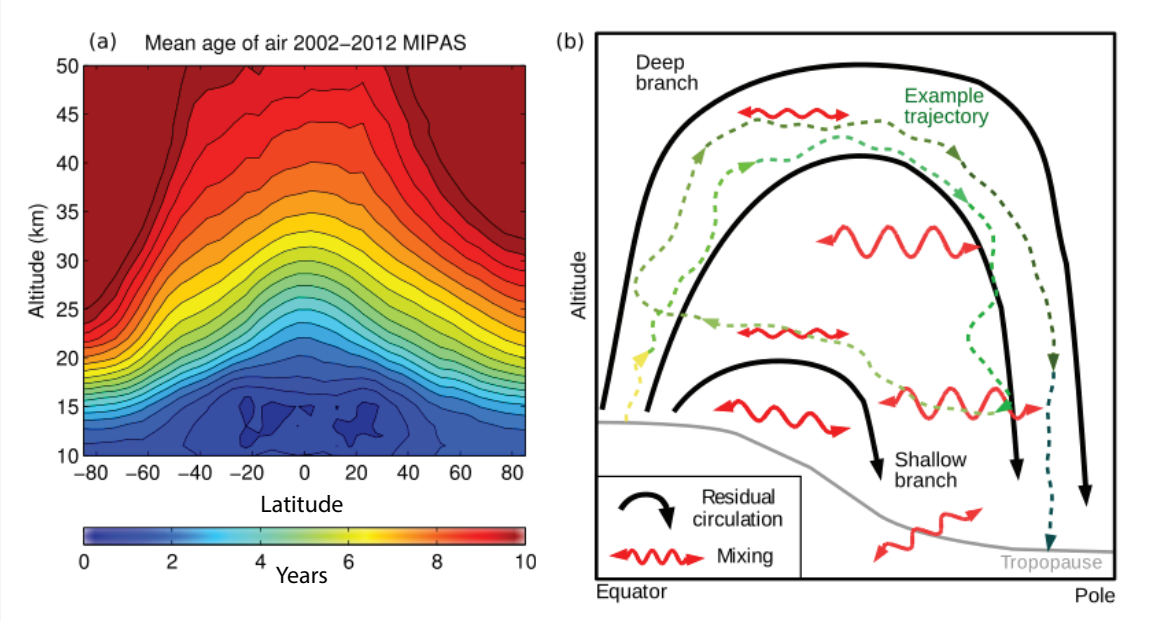

Box 5-2 Figure 1. (a) Climatology of annual mean age of air 2002–2012 from MIPAS SF_6 measurements and (b) schematic of the net stratospheric tracer transport circulation, including overturning circulation and mixing components. (a) Note that MIPAS mean age is overestimated at high latitudes due to an SF_6 mesospheric sink (Stiller et al., 2012). (a) Adapted from Haenel et al. (2015). (b) Adapted from Garny et al. (2014).

The AoA structure in **Box 5-2 Figure 1a** results from the combined effect of two components, as illustrated in **Box 5-2 Figure 1b:** slow mean advection by the overturning circulation (including shallow and deep branches; e.g., Birner and Boenisch, 2011) and rapid two-way quasi-isentropic irreversible mixing (see also Plumb, 2002; Shepherd, 2007). Accordingly, the AoA can be separated into the residual circulation transit timescale (RCTT) (Birner and Boenisch, 2011) and the time due to mixing processes (aging by mixing) (Garny et al., 2014). While the overturning circulation tends to steepen the meridional AoA gradients, mixing between the tropics and the extratropics causes recirculation of air parcels, increasing AoA throughout most of the stratosphere (see example trajectory in panel b).

Box 5-2, continued.

Furthermore, due to irreversible mixing, an air parcel traveling in the stratosphere does not maintain its identity, and the AoA at any location is fully described by a transit time distribution referred to as the age spectrum, which reflects a diversity of individual pathways followed by the elements forming the air mass (Hall and Plumb, 1994; Waugh and Hall, 2002). The mean age constitutes the first moment of the statistical distribution. Typical stratospheric age spectra feature long tails of old transit times due to aging by mixing, such that the mean age is usually longer than the modal age (peak of the age spectrum). Multiple peaks in the age spectrum reflect seasonal and interannual variability in the circulation (Ploeger and Birner, 2016). Understanding the separate contributions of the distinct transport mechanisms to the mean age and the age spectrum is key to constraining transport processes in models and their long-term trends, which are currently subject to large uncertainties.

AoA reduction in the NH lower stratosphere disappears for the most recent period. This could be related to an interruption in the acceleration of tropical upwelling in the lower stratosphere at the beginning of the 21st century (Aschmann et al., 2014), which is consistent with the observed reduced cooling of the tropical lower stratosphere over the first decade of the 21st century as compared to the previous two decades (see **Section 5.3.1.1**) (Aquila et al., 2016; Polvani et al., 2017; Randel et al., 2016; Khaykin et al., 2017). Different mechanisms have been proposed to explain the changes in tropical upwelling since around 2000, including ocean multi-decadal variability (Aschmann et al., 2014), the change in trend of atmospheric ODS concentrations since the late 1990s (see **Section 5.3.2.2**), and internal atmospheric variability (Garfinkel et al., 2017a). Moreover, the opposite sign of mean AoA trends in each hemisphere over the period 2002–2012 can be understood as a southward shift of the tropical upwelling region (Stiller et al., 2017); while the cause of this shift remains unclear, when its effects on AoA are removed, the remaining mean AoA trends are consistent with model predictions in the lower stratosphere (Stiller et al., 2017).

In addition to estimating long-term trends in the BDC, there are substantial uncertainties in estimates of the absolute strength of the overturning circulation among reanalyses (e.g., Abalos et al. (2015) estimate a 40% uncertainty). Using the meridional age gradient

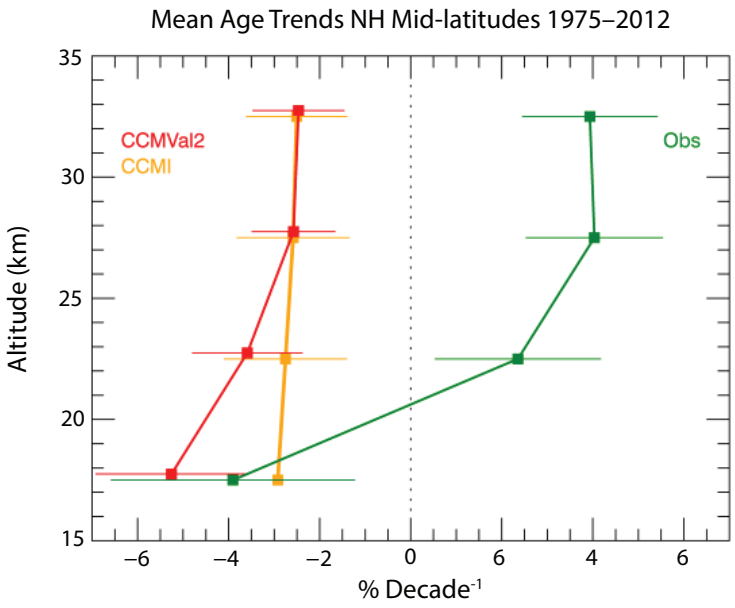

Figure 5-9. Profiles of trends in the Northern Hemisphere (NH) mid-latitude mean age of air (in percent per decade) from 1975 to 2012. Green symbols are trends derived from in situ tracer observations combined with a simple mechanistic model. Red symbols represent average trends from four ocean-coupled CCMVal2 models. Orange symbols represent average trends from nine ocean-coupled CCMI models. Error bars represent the standard deviation of the mean of all model trends at each level and, for observations, the 1σ uncertainty on the trend estimate at each level. Update to Ray et al. (2014).

as a metric of the strength of the stratospheric overturning circulation, good agreement is found between two different observational estimates at an altitude of 20 km (Neu and Plumb, 1999; Linz et al., 2016; Linz et al., 2017). The inferred value for the strength of the circulation is also shown to fall within the reanalysis uncertainty range and to agree with estimates from a climate model (Linz et al., 2017). In contrast, at higher levels, there is a 100% uncertainty in the circulation strength, with reanalyses and models showing significantly faster circulation than the observational estimate. This difference could be due to the fact that the AoA derived from SF_6 observations is overestimated, because this tracer has mesospheric sinks that lead to smaller concentrations of the tracer at high latitudes than if it were passively transported (e.g., Waugh and Hall, 2002; Haenel et al., 2015; Kovács et al., 2017). Nevertheless, the absolute strength of the overturning circulation remains highly uncertain in the middle and upper stratosphere (Linz et al., 2017).

5.3.2.2 Simulated Past and Future Changes of the BDC

The 2014 Ozone Assessment highlighted that chemistry–climate models robustly predict a long-term acceleration of the BDC in response to anthropogenic climate change (Hardiman et al., 2014; Palmeiro et al., 2014). This result stands for the new CCMI simulations (Morgenstern et al., 2018), while updated observational estimates still feature a near-zero trend or decelerating net transport circulation at mid-latitudes in the NH middle stratosphere (see **Figure 5-9**). The main recent advances in the analysis of trends in models have been through taking into account the potential contribution of large internal atmospheric variability on trends by assessing the role of the length of the period considered and through showing the importance of having several ensemble members for each simulation type. It was found that, while the BDC robustly accelerates over the last 55 years in chemistry–climate model simulations, when the period is limited to the last 25 years, some ensemble members show a slowing of tropical upwelling and an increase in NH mid-latitude mean AoA in the middle to upper stratosphere (Garfinkel et al., 2017a). It has also been found that the minimum record length needed to statistically distinguish a forced signal from the internal variability is about 30 years for a BDC trend of 2% per decade (Hardiman et al., 2017). This implies that shorter observational records do not necessarily reflect forced long-term trends. These results could potentially reconcile the modeled and observed AoA trends over shorter periods when most data have been collected, though discrepancies still remain with the longest observational records that began more than 40 years ago (**Figure 5-9**). On a wider perspective, one model study (Muthers et al., 2016) suggests that changes in mean AoA in the 20th and 21st centuries are unprecedented since the 1600s. However, this single-model result remains to be confirmed by other studies. Regarding future BDC trends, several CCMI models show the entire BDC being lifted as the tropopause rises (Oberländer-Hayn et al., 2016). Such close connection between the tropopause rise and the BDC acceleration may have implications for stratosphere–troposphere exchange (see **Section 5.3.3**).

A number of recent studies have highlighted the importance of assessing changes in isentropic eddy mixing in addition to the overturning circulation for interpreting long-term trends in the net stratospheric tracer transport and for comparing models to observations (Garny et al., 2014; Ray et al., 2014; Ploeger et al., 2015; Abalos et al., 2016; Miyazaki et al., 2016; Ray et al., 2016; Ploeger and Birner, 2016; Dietmüller et al., 2017). These studies build on a few previous studies addressing this issue (Ray et al., 2010; Li et al., 2012). They show that AoA trends derived from ERA-Interim reanalysis can be largely attributed to long-term trends in the isentropic mixing (Ploeger et al., 2015). Because isentropic mixing is a fundamental component of stratospheric tracer transport and its effect is integrated in AoA (see **Box 5-2**), it has to be adequately represented in models. Although two-way mixing and the mean overturning circulation are intrinsically coupled (both are driven by Rossby wave breaking), their combined effects on AoA, an integrated Lagrangian measure of transport, are not straightforward (Garny et al., 2014; Ploeger et al., 2015; Ploeger and Birner, 2016).

Previous model studies have examined the impact of ODS-driven ozone depletion and recovery on past and future BDC and AoA trends (e.g., Li et al., 2008; Oman et al., 2009; McLandress et al., 2010; Oberländer et al., 2013). Since the last Assessment, additional evidence from chemistry–climate model simulations has shown that Antarctic ozone depletion is the main driver of the observed BDC acceleration in the SH

summer over the past several decades (Keeble et al., 2014; Oberländer-Hayn et al., 2015; Garfinkel et al., 2017a; Polvani et al., 2018; Morgenstern et al., 2018; Li et al., 2018). **Figure 5-10a** shows the dominant role of ODSs in driving the SH polar downwelling acceleration until the year 2000. The changes in annual mean downwelling seen in **Figure 5-10a** predominantly reflect changes in austral summer (Polvani et al., 2018). Also shown in **Figure 5-10a** is a trend in polar downwelling in the 21st century of opposite sign, due to the ozone recovery (Oberländer et al., 2013; Polvani et al., 2018). The ODS influence on the BDC is not limited to the Antarctic region, and a number of recent modeling studies have quantified the global influence (Oberländer-Hayn et al., 2015; Polvani et al., 2017; Garfinkel et al., 2017a; Polvani et al., 2018). **Figure 5-10b** shows that, in a chemistry–climate model, a significant fraction (about 50%) of the past acceleration of the annual mean upwelling in the tropical lower stratosphere is attributed to ODSs. In the future, the decrease of ODSs and ozone recovery are expected to significantly reduce the GHG-driven BDC annual mean acceleration trends (**Figure 5-10b**). Finally, the ODS impact on the NH polar downwelling trends is negligible (**Figure 5-10c**). These results from a single chemistry–climate model remain to be tested in other models. Interestingly, recent modeling works have shown that the ozone hole, despite driving a strong acceleration of the downwelling over the boreal summer Antarctic lower stratosphere, leads to an increase in AoA in that region and season (Morgenstern et al., 2018; Li et al., 2018). This is attributed to the delay in the polar vortex breakup date, which implies that relatively old air remains isolated over this region. This result highlights the importance of considering changes in mixing for interpreting AoA trends.

The influence of ODS-induced ozone changes on the net overturning circulation occurs through changes in wave forcing associated with thermally driven changes in the background zonal wind. The wave forcing of the BDC cannot be viewed as predefined or fixed, as it may be affected by changes in radiation (Ming et al., 2016). Furthermore, there are important compensating processes between waves of different spatial scales, some of which cannot be directly represented in models and so are parameterized (e.g., Cohen et al., 2014; Sigmond and Shepherd, 2014).

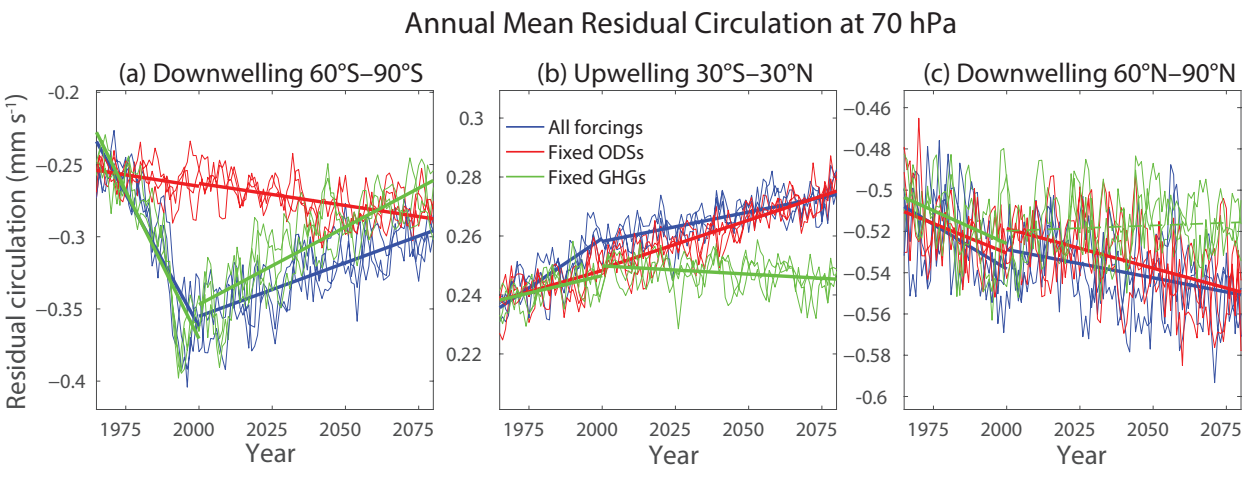

Figure 5-10. Time series of annual mean residual (overturning) circulation at 70 hPa over the (a) SH polar cap (60°S–90°S), (b) tropics (30°S–30°N), and (c) NH polar cap (60°N–90°N) for different runs from the Community Earth System Model (CESM) with Whole Atmosphere Community Climate Model (WACCM) as its atmospheric component. The thin colored lines represent all forcing runs (blue), runs with ODSs fixed to 1960 levels (red), and runs with GHGs fixed to 1960 levels (green). Three members are shown for each simulation type. Thick lines show the linear fit for each ensemble mean for the periods 1965–2000 and 2000–2080. Adapted from Polvani et al. (2018).

5.3.3 Stratosphere–Troposphere Exchange

Since ~90% of the total ozone column resides in the stratosphere, changes in stratosphere–troposphere exchange (STE) are critical to the evolution of the tropospheric ozone burden and thus air quality (e.g., Collins et al., 2003; Zeng and Pyle, 2005; Hegglin and Shepherd, 2009). Some of the factors affecting future changes in tropospheric ozone are addressed in **Section 3.4.4** of **Chapter 3** and in the recent IGAC Tropospheric Ozone Assessment Report (TOAR; see Young et al., 2018), which reports on the current understanding of tropospheric ozone in detail. Here we briefly assess the main advances since the 2014 Assessment regarding STE.

The 2014 Assessment discussed improvements to chemistry–climate models through the merging of tropospheric and stratospheric chemistry schemes, and it discussed the contribution of STE to the tropospheric ozone budget. The merged schemes resulted in improvements in modeled tropospheric ozone concentrations due to the inclusion of stratospheric ozone changes by ODSs and changes in the strength of the BDC (see **Section 5.3.2**). It was assessed that models consistently showed reduced ozone STE in the present compared to preindustrial times due to stratospheric ozone depletion, although the magnitude of the estimated change is model-dependent. On the other hand, model studies showed that concurrent ODS decreases and GHG increases in the future would lead to increased STE of ozone, with the magnitude of the change depending on the RCP scenario (see Section 4.5.3 in WMO (2014) and Section 11.3.5.1.2 in IPCC (2013)). Since the last Assessment, our qualitative understanding of the expected future changes in STE has not been modified. Stratospheric ozone influx into the troposphere is still expected to increase in the future, with the magnitude of the increase still model- and scenario-dependent, as discussed below.

STE typically occurs due to isentropic mixing, often during the formation of tropopause folds and cutoff lows associated with mid-latitude cyclonic disturbances, for example in the Atlantic and Pacific storm tracks (Stohl et al., 2003). New studies on STE have been conducted, quantifying its spatial and seasonal variability (e.g., Yang et al., 2016), investigating the mechanisms of ozone transport from the lowermost stratosphere to the surface (Škerlak et al., 2014; Lin et al., 2015; Albers et al., 2018), and giving quantitative observational constraints of the magnitude of tropospheric ozone changes due to STE (e.g., Neu et al., 2014). Stratosphere-to-troposphere ozone transport peaks in late spring and early summer in the Northern Hemisphere and shows little seasonality in the Southern Hemisphere (Yang et al., 2016). However, because it migrates seasonally in altitude following the subtropical jets, STE is strongest in winter in the Northern Hemisphere at the lower isentropes. This winter maximum is consistent with the peak of stratospheric ozone influence observed near the surface (Škerlak et al., 2014).

Nonetheless, difficulties remain in estimating the magnitude of STE. Large uncertainties have been reported in the magnitude, geographic distributions, seasonality, and long-term changes of STE, depending on the definition of the tropopause and the reanalysis dataset used (Boothe and Homeyer, 2017). In addition, it has been shown that the use of monthly mean residual circulation vertical velocities yields large errors in the estimated magnitude of ozone STE, resulting in different magnitude estimates in comparison to other methodologies (Hsu and Prather, 2014).

Ozone STE is controlled by the amount of ozone available in the lowermost stratosphere and also by the frequency and location of stratospheric intrusion events. Because these are governed by different mechanisms and their relative importance remains unclear, the variability of ozone STE, and in particular the relationship with El Niño–Southern Oscillation (ENSO), is still under discussion (Neu et al., 2014; Hess et al., 2015; Lin et al., 2015; Olsen et al., 2016; Albers et al., 2018). New research since the last Assessment provides more evidence that both the acceleration of the BDC (see **Section 5.3.2.2**) and stratospheric ozone recovery (see **Chapter 3**) will tend to increase the future global tropospheric ozone burden through enhanced STE. Two new studies find a substantial correlation between the strength of the BDC, STE, and tropospheric ozone during the observed period using satellite observations (Neu et al., 2014) and chemistry–climate model simulations constrained by observed SSTs and validated against observed ozone variability (Hess et al., 2015). The covariability between STE and tropospheric ozone from observations was used to deduce that the projected strengthening of the BDC alone (that is, without accounting for ozone recovery)

could lead to an increase in zonal mean tropospheric ozone of 2% by the end of the 21st century (Neu et al., 2014). A larger increase in mid-tropospheric ozone of 6% by 2100 due to BDC strengthening was obtained in one model study (Hess et al., 2015). The threefold difference between the two estimates highlights considerable quantitative uncertainty in the future evolution of ozone STE.

Several studies have estimated the role of STE for future tropospheric ozone using chemistry–climate model simulations that include the effects of climate change, in general agreeing that STE increases contribute importantly to future tropospheric ozone abundances. These studies examine the influence of the stratosphere on the tropospheric ozone through STE by including a stratospheric ozone tracer (no chemical ozone production in the troposphere) in the simulations (Banerjee et al., 2016; Meul et al., 2018). **Figure 5-11** shows the changes in the stratospheric ozone tracer due to climate change and ODS reduction, as a diagnostic of the impact of changes in STE on tropospheric ozone between 2000 and 2100 (Banerjee et al., 2016). A strengthened BDC under climate change following the RCP-8.5 scenario has its strongest effect on tropospheric ozone in the tropics and subtropics (**Figure 5-11a**), while stratospheric ozone recovery from declining long-lived ODSs has a larger role in the mid-latitudes and extratropics (**Figure 5-11b**). These results are consistent with recent estimates that the stratosphere-to-troposphere transport of ozone will increase more than 50% by 2100 under an RCP-8.5 scenario (Meul et al., 2018). Such increases in stratospheric ozone influx into the troposphere are consistent with those inferred in a multi-model study (Young et al., 2013) and model sensitivity studies (Kawase et al., 2011; Abalos et al., 2017). These results highlight STE as an important factor for determining future changes in tropospheric ozone, although its quantitative role remains uncertain due to the limited number of studies and the variations across current model results.

Future changes in tropospheric ozone will be determined by a complex interplay between chemical and transport processes. While all studies agree that STE changes will tend to increase future tropospheric ozone, the relative importance of STE versus tropospheric chemistry for future tropospheric ozone trends remains an open question. A strong sensitivity to GHG scenario, as reported in the last Assessment, is supported by new model results, with studies finding a net decrease in the global burden of tropospheric ozone in 2100 compared to that in 2000 in the RCP-6.0 scenario (Sekiya and Sudo, 2014; Revell et al., 2015) and an increase in the RCP8.5 scenario (Banerjee et al., 2016; Meul et al., 2018). A major source of uncertainty in projections of tropospheric ozone is the future evolution of methane concentrations, which are much larger in the RCP8.5 scenario than in the others. However, scenario dependence is not the only source of uncertainty in future tropospheric ozone. A study using new simulations from multiple chemistry–climate models finds considerable disagreement among models in tropospheric ozone even when the same scenario is considered, with much of the model spread being likely due to the uncertainty in stratospheric transport and STE trends (Morgenstern et al., 2018). A more detailed discussion of future tropospheric ozone changes is given in **Chapter 3, Section 3.4.4**.

5.3.4 Stratospheric Winds

5.3.4.1 Polar Vortices

The characteristics of stratospheric wintertime polar vortices, such as their strength and duration, have a large impact on polar stratospheric ozone variability and can also affect tropospheric climate. Observed and projected variability and long-term changes in polar vortex characteristics are discussed in **Chapter 4**. Here, we briefly review polar vortex changes with a focus on their implications for the troposphere.

Previous assessments reported an observed strengthening of the Antarctic polar vortex during austral spring and a delay in the vortex breakup date resulting from diabatic cooling associated with ozone loss. **Figure 4-3** in **Chapter 4** shows that the trend toward later breakup dates did not continue during recent years, which were instead characterized by a large variability in breakup dates ranging between mid-November and mid-December. This year-to-year variability is linked to variability in planetary wave activity, which is mostly driven by internal climate dynamics. No recent studies have analyzed projected changes in the Antarctic vortex and, in line with previous Assessments, it is expected that ozone recovery will lead to a weakening of the polar vortex

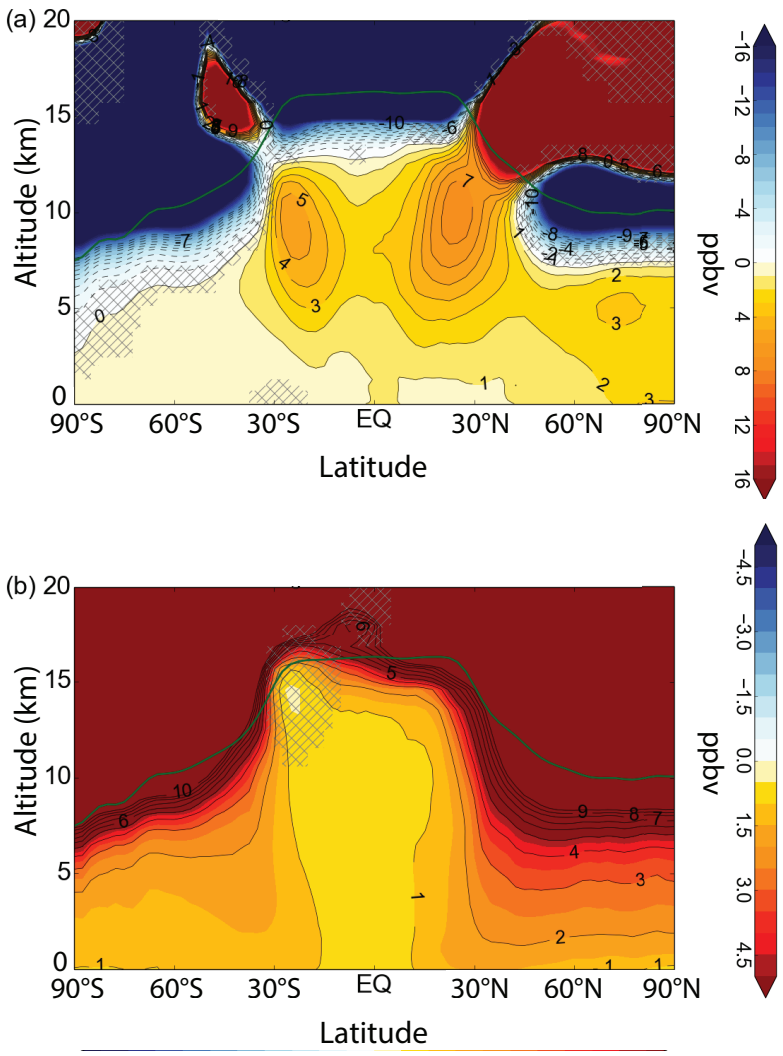

Figure 5-11. Modeled changes in ozone mixing ratio [ppbv] between 2000 and 2100 due to (a) changes in physical climate (GHGs, sea surface temperatures, and sea ice) following the RCP-8.5 scenario and (b) changes in ODS concentrations. Shown are changes for a stratospheric ozone tracer that is constrained to stratospheric values above the tropopause but that evolves freely in the troposphere and undergoes only tropospheric loss processes (i.e., there is no tropospheric ozone production). The inclusion of a separate stratospheric ozone tracer in the model simulations allows separation of the STE contribution from the changes due to tropospheric processes. Adapted from Banerjee et al. (2016).

and a return to earlier breakup dates. A trend toward later breakup dates of the Antarctic vortex may reappear in the late 21st century as a result of tropical upper-tropospheric warming driven by increased GHG concentrations and associated strengthening of the meridional temperature gradient near the tropopause (Wilcox and Charlton-Perez, 2013).

The large interannual variability in the Arctic polar vortex effectively masks any trends driven by changes in external forcings including ODSs and ozone, though there has been a shift toward weaker vortices in mid-winter since 1990 (consistent with the temperature changes discussed in **Section 5.3.1**) (Garfinkel et al., 2017b). It has been suggested in a number of studies that a loss of Arctic sea ice can lead to a weakening of the stratospheric vortex (e.g., Kim et al., 2014), and one study argued that the observed ice loss has shifted the vortex toward Eurasia (Zhang et al., 2016). However, another study demonstrated that the observed shift is also consistent with unforced decadal variability (Seviour, 2017). Two studies (Garfinkel et al., 2017b; Kretschmer et al., 2018) presented evidence that the weakening of the Arctic polar vortex since 1990 contributed to the hiatus in GHG-induced near-surface warming over Eurasia in boreal winter; however, the vortex weakening itself was not attributed to external forcing, implying that it is likely a result of internal variability.

Several new studies have analyzed future dynamical changes in the Arctic vortex and their implications

for surface climate. Coupled climate models disagree about the sign of the projected vortex changes (Simpson et al., 2018), although weakening of the polar night jet has been reported to be a preferred response across the CMIP5 multi-model ensemble (Manzini et al., 2014) and single-model large ensemble (Peings et al., 2017) by the end of the 21st century under a high GHG scenario. Nevertheless, episodes of a cold and strong polar vortex are projected to occur throughout the 21st century (Bednarz et al., 2016). While simulated future vortex changes are small in comparison to the observed large interannual variability, the intermodel spread in vortex changes is a significant component of uncertainty in future tropospheric climate change (Manzini et al., 2014; Zappa and Shepherd, 2017; Simpson et al., 2018).

The mechanisms of the projected changes in the Arctic polar vortex remain unclear. While projected Arctic amplification and sea ice loss can contribute to vortex weakening in coupled model simulations, as discussed above (Kim et al., 2014; Manzini et al., 2018), the weakening is also found in atmosphere-only model simulations omitting sea ice loss as a response to global SST warming (Karpechko and Manzini, 2017). The lack of understanding of the mechanisms, together with large intermodel spread in projections, indicates that our confidence in projected Arctic vortex changes is low.

5.3.4.2 Quasi-Biennial Oscillation Disruption and Implications

The influence of the Quasi-Biennial Oscillation (QBO) on stratospheric ozone is relatively well understood (**Chapter 3**, **Section 3.2.1.2**). However, the disruption of the QBO that took place in 2016 (see **Chapter 3** for a discussion of its effects on ozone) raised questions about how well we understand the QBO's generating mechanisms, the response of the QBO to climate change, and how the QBO will affect future ozone evolution.

During early 2016, a downward propagation of the eastward QBO phase was unexpectedly interrupted by the appearance of a westward jet at 40 hPa (Osprey et al., 2016; Newman et al., 2016). Several papers have concluded that the immediate cause of the interruption was a flux of easterly momentum associated with a pulse of planetary waves propagating from the NH extratropics (Osprey et al., 2016; Coy et al., 2017; Barton and McCormack, 2017; Watanabe et al., 2017). There is evidence that the strong 2015–2016 El Niño was implicated in forcing the wave pulse (Barton and McCormack, 2017; Hirota et al., 2018), and one study also suggests a role for the very low Arctic sea ice concentrations in that year (Hirota et al., 2018). The effect of the QBO interruption on ozone was consistent with our existing understanding of QBO–ozone linkages (see **Chapter 3, Section 3.2.1.2**). The interruption was not predicted by operational seasonal prediction models (Osprey et al., 2016), but it was reproduced retrospectively by an atmospheric model driven by observed SSTs (Watanabe et al., 2017). Although such an event is unprecedented in the more than 60 years of QBO observations (Newman et al., 2016), analogous events are found in model simulations (Osprey et al., 2016), and the effect of the anomalous wave flux on the QBO is consistent with our understanding of QBO generating mechanisms. Since the disruption in 2016, the QBO has recovered to its expected eastward phase. Analysis of simulations of future QBO, corroborated by observational evidence, suggests that QBO amplitude in the lower stratosphere will decrease (Kawatani and Hamilton, 2013; Schirber et al., 2015; Naoe et al., 2017) as a result of a projected increase in the mean tropical upwelling (see **Section 5.3.2.2**) and that the amplitude of QBO-induced ozone variability will consistently decrease in the lower stratosphere; in the upper stratosphere, it will increase due to ozone recovery (Naoe et al., 2017). However, this result is based on only a few available studies. Furthermore, our current understanding of changes in wave forcing contributing to the QBO is incomplete, which prevents firm conclusion about future QBO changes or whether QBO interruptions can occur more frequently in future climate.

5.4 EFFECTS OF CHANGES IN STRATOSPHERIC OZONE ON THE TROPOSPHERE AND SURFACE

The influence of stratospheric ozone change on SH tropospheric and surface climate has been analyzed and investigated in an increasingly mature body of research. A key result is that ozone depletion is assessed to be the dominant driver of austral summer (December–January–February; DJF) atmospheric circulation changes ranging from subpolar to tropical latitudes over the period in which stratospheric

ozone was rapidly decreasing. We focus here on what has been learned since the 2014 Ozone Assessment (Arblaster and Gillett et al., 2014). This includes improved quantification of the forced response to ozone in the context of natural internal variability and improved understanding of the role of recent changes in SSTs in driving observed SH circulation changes. We also highlight a growing body of evidence that suggests that the Southern Ocean response to ozone depletion is timescale-dependent. The effects of ozone depletion on the climate of the Southern Hemisphere, which span from the stratosphere to the oceans, are summarized in the schematic shown in **Figure 5-12**. We begin by assessing the effects of stratospheric ozone changes on the tropospheric circulation, followed by an assessment of the resultant impacts on surface climate, the ocean, and sea ice.

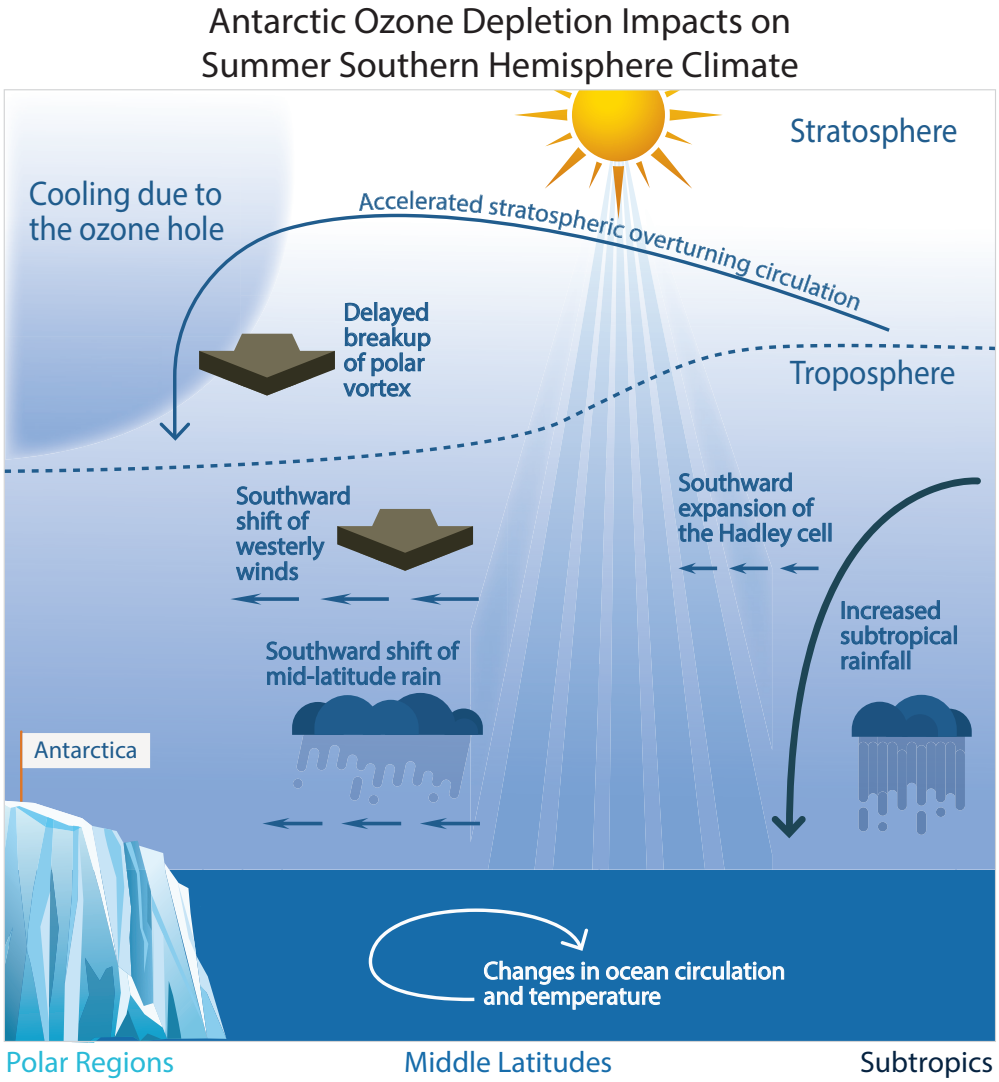

Figure 5-12. Schematic illustration of Southern Hemisphere climate impacts in austral summer associated with Antarctic ozone depletion. Ozone depletion has cooled the Antarctic stratosphere, leading to a delayed breakup of the stratospheric polar vortex and an accelerated Brewer–Dobson circulation. Impacts extended into the troposphere: A region of strong westerly winds and associated rainfall shifted southward, affecting the ocean circulation. The subtropical edge of the tropical circulation also expanded poleward, leading to reduced precipitation in mid-latitudes and enhanced precipitation in the subtropics. Update to Figure 4-22 in Arblaster and Gillett et al. (2014).

5.4.1 Tropospheric Circulation Effects

As described in **Section 5.3.1**, the primary effect of Antarctic stratospheric ozone depletion is to produce a strong cooling in the lower stratosphere over the Antarctic in austral spring. Over the period in which ozone depletion was increasing from 1960 to around 2000, large changes were observed in the SH mid-latitude and tropical circulations in austral summer: The SH tropospheric mid-latitude maximum in zonal winds (that is, the jet) shifted poleward; the Southern Annular Mode (SAM) index, which corresponds to opposite-signed changes in sea level pressure over high latitudes and mid-latitudes, shifted more into its positive phase (i.e., decreased sea level pressure over high latitudes); and the subtropical edge of the Hadley Cell shifted poleward. We first review the observational evidence for these changes and then discuss model simulations that causally link these changes to ozone depletion. An assessment of the current understanding of the mechanisms through which this shift occurs appears in **Section 5.4.2**.

5.4.1.1 The Southern Hemisphere: Observations

The SH general circulation includes a band of strong westerly winds, which are associated with the storm track (that is, synoptic-scale eddies and rainfall in the mid-latitudes). The latitude of the maximum zonal mean westerly winds in the lower troposphere is referred to as the mid-latitude near-surface jet (or for brevity, jet) and is climatologically centered around 52°S. Global monitoring of the location of the near-surface jet is available only since 1987 from the launch of the Special Sensor Microwave Imager (Goodberlet et al., 1989). Since then, a series of satellite microwave radiometers and scatterometers have continually observed near-surface wind speed. Measurements from the various satellite missions can then be combined into a gridded dataset, either with a reanalysis product or in a stand-alone product such as the Cross-Calibrated Multi-Platform (CCMP) ocean surface wind vector analyses (Atlas et al., 2011). Before 1987, winds were observed by available radiosondes and (after 1979) estimated from satellite measurements. Modern reanalysis products such as ERA-Interim and MERRA more accurately capture variability and trends in near-surface winds, wind stress, and the SAM after 1979 than earlier reanalyses (Swart et al., 2015) when compared to station data (for the SAM) and satellite data (for near-surface winds). The recent evolution of the latitude of the near-surface jet in CCMP is shown in **Figure 5-13**. Trends in the jet are strongest in DJF and are statistically significant at the 95% confidence level in that season (Swart et al., 2015), consistent with the findings of previous assessments. Since 2000, the jet in DJF has shifted equatorward, though trends are not statistically significant. Trends are weaker and not statistically significant in other seasons, with the exception of a significantly stronger jet in May (Ivy et al., 2017a).

The SAM is the leading mode of variability in the SH extratropical circulation and, as mentioned above, corresponds to opposite-signed changes in sea level pressure between subpolar latitudes and mid-latitudes. The SAM index generally tracks changes in the characteristics of the mid-latitude jet (as evidenced by the large correlation on interannual timescales in **Figure 5-13**), with the positive phase corresponding to a poleward jet shift, though the variations in the SAM can also be associated with variations in the strength of the mid-latitude jet (Monahan and Fyfe 2006; Swart et al., 2015; Solomon and Polvani, 2016).

The SAM index can be calculated from station pressure observations, which are available for a longer period than Southern Ocean surface wind observations as they do not rely on satellite retrievals. Hence the SAM has historically been used to quantify changes in the large-scale mid-latitude circulation. After 1979, there is generally good agreement between the SAM index calculated from station observations and that calculated from reanalyses, whereas prior to 1979, some reanalyses are known to have deficiencies (Marshall, 2003) and tend to simulate trends that are too strong (Swart et al., 2015).

Figure 5-13 shows the historical evolution of the SAM index from station observations of sea level pressure (based on an update of Marshall, 2003). The largest seasonal trends over the period in which ozone depletion was increasing (through 2000) are found in DJF and MAM (March–April–May), and these changes dominate the response in the annual mean. Since 2000, the SAM has stayed mostly in its positive phase (with respect to the 1971–2000 period). Evidence from paleoclimate reconstructions of the SAM index derived from networks of surface temperature proxies and from multiple studies suggests that the current

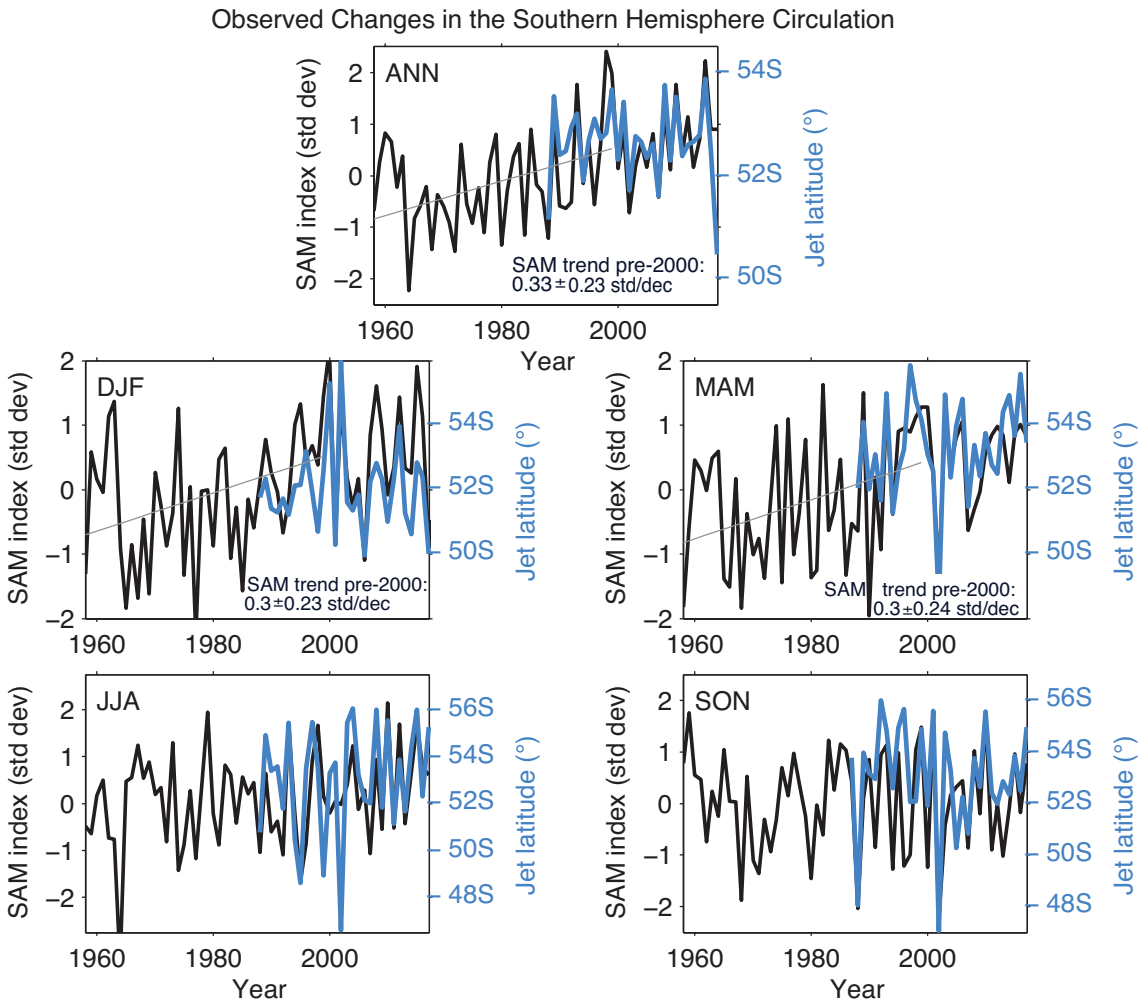

Figure 5-13. SAM index (black) and mid-latitude jet positions (blue) time series from 1958–2017 for the four seasons and annual mean. The SAM index is normalized by its standard deviation and is defined as in Marshall (2003). The jet position is based on the maximum of CCMP satellite-based surface wind speed (Atlas et al., 2011) (available for download at http://www.remss.com/measurements/ccmp), which starts in 1987. A linear trend line of the SAM changes before 2000 is shown when statistically significant, and the slope of the best fit line and its corresponding 95% uncertainty bounds are shown.

period of prolonged positive summer SAM conditions is unprecedented over at least the past 600 years (Villalba et al., 2012; Abram et al., 2014; Dätwyler et al., 2017). Reconstructions for the summer season (Dätwyler et al., 2017) are very robust across multiple methods and datasets, but some discrepancies exist in the magnitude of reconstructed low frequency SAM changes during the preindustrial period for the annually averaged SAM.

On interannual timescales, the position/strength of the mid-latitude jet and the Hadley Cell edge are correlated (Kang and Polvani, 2011; Ceppi and Hartmann, 2013; Staten and Reichler, 2014), raising the question of whether the subtropical Hadley Cell edge would also have shifted poleward. Recent studies have confirmed that the subtropical edge of the Hadley Cell has expanded poleward, confirming the results of the previous Assessment (Garfinkel et al., 2015a; Lucas and Nguyen, 2015; Davis and Birner, 2017; Solomon et al., 2017; Kim et al., 2017). This poleward shift is most pronounced in austral summer in the Atlantic and Indian Ocean sectors (Choi et al., 2014; Kim et al., 2017), the same region in which the upper-tropospheric polar

jet has shifted poleward most sharply (Manney and Hegglin, 2018). Quantifying the rate of the observed Hadley Cell expansion has been challenging, however. Different studies have used a wide variety of metrics to track Hadley Cell width, and two recent studies (Davis and Birner, 2017; Solomon et al., 2017) suggest that metrics based on upper-tropospheric quantities are only weakly correlated with metrics based on mid-tropospheric and surface processes, though another study (Mantsis et al., 2017) suggests that in CMIP5 models, a metric based on outgoing longwave radiation is well correlated with mid-tropospheric metrics. Furthermore, different reanalysis products do not agree as to the rate of expansion even when a common definition of a single metric is applied. For example, one study (Garfinkel et al., 2015a) compared five different reanalysis products (including MERRA output from two different stages in the assimilation cycle) and found that the trends in different reanalysis products (or even from two different stages in the assimilation cycle of the same reanalysis system) can be significantly different at the 90% confidence level in the Southern Hemisphere over the period 1980 to 1999, with rates of expansion ranging from 1 degree per decade to 0.3 degree per decade (**Figure 5-14**). Differences are even larger over the period from 1980 to 2009. Thus, while the Hadley Cell expansion is robust, its magnitude has large uncertainty, which is partly related to disagreement among applied metrics for the Hadley Cell edge. The development of a robust observational metric (or a set of metrics) of Hadley Cell width is still an area of active research.

5.4.1.2 The Southern Hemisphere: Model Simulations of the Past

We now assess modeling studies that have attempted to pin down the cause of the observed changes in the SH circulation, and we begin with the period in which ozone depletion was increasing, between the 1960s and 2000. The cleanest way to establish the importance of ozone for past changes in the SH circulation is to perform model simulations of the historical period both with and without ozone depletion. The 2014 Assessment described several such studies and concluded that ozone depletion is very likely the dominant driver of the changes in the SAM in summer. Since the previous Assessment, one modeling study has supported the conclusion that ozone depletion has led to a change in the summer SAM by comparing integrations with and without ozone depletion (Keeble et al., 2014). An additional study has also concluded that summertime Hadley Cell trends are strong in CMIP5 models only when ozone depletion is included (Tao et al., 2016) (**Figure 5-15**). A third study compared the summertime tropospheric response to ozone depletion from 1960 to 2000 in a suite of climate model simulations of varying configurations (for example, prescribed SSTs versus the inclusion of a coupled ocean, as well as prescribed ozone concentrations versus the inclusion of interactive chemistry) and found a consistent widening of the Hadley Cell and poleward shift of the jet in austral summer (Seviour et al., 2017a). **Figure 5-15** summarizes the trends in both the SAM and the subtropical Hadley Cell edge as simulated in the CMIP5 multi-model mean. Both the positive SAM trend and the poleward expansion of the Hadley Cell maximize in austral summer during the period from the early 1970s to around 2005, when the models are forced with all external climate drivers, including anthropogenic (ozone depletion, increasing GHG concentrations, and aerosols) and natural (solar cycle and volcanoes) factors. The separate contribution of ozone depletion and GHGs can be seen in both variables, with ozone playing a dominant role in austral summer and GHGs playing a major role during the other seasons. Overall, the majority of studies that have compared simulations forced with ozone depletion to simulations forced with no ozone depletion have concluded that ozone is the dominant forcing of changes in the SH circulation over the period in which ozone depletion was increasing.

Two studies that compared simulations with and without ozone disagreed with this consensus and concluded that ozone depletion was not the dominant cause of recent changes in the Southern Hemisphere in austral summer (Staten et al., 2012; Quan et al., 2014). However, there are methodological issues with both studies (Waugh et al., 2015): They both used prescribed ozone fields that underrepresent the magnitude of observed Antarctic ozone depletion, thus leading to a weakened response to ozone. Specifically, one of the studies (Quan et al., 2014) used ozone forcing (Lamarque et al., 2012) which underestimates observed ozone depletion by a factor of two (Figure 2f of Eyring et al., 2013). The other study (Staten et al., 2012) implicitly assumes that there was negligible ozone

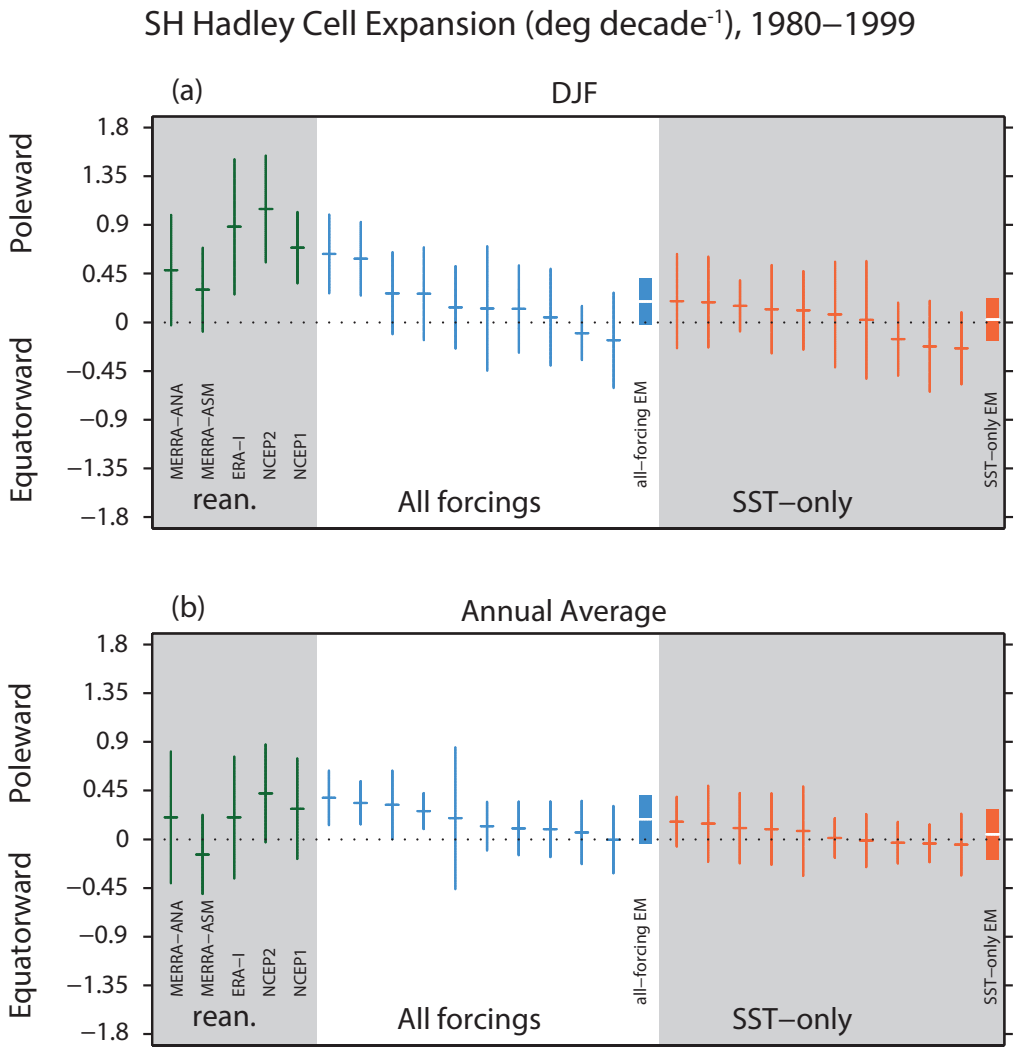

Figure 5-14. Poleward expansion of the SH Hadley Cell as determined by the zero crossing of the 500 hPa stream function in five reanalysis products and in each member of an ensemble of Goddard Earth Observing System Chemistry-Climate Model (GEOSCCM) simulations and in the ensemble mean (EM) in (a) DJF and (b) the annual average from 1980 to 1999. Integrations forced with time-varying ODS and GHG concentrations in addition to observed SSTs are in blue, while integrations with fixed ODS and GHG concentrations are in orange. Vertical lines or bars represent the 95% confidence interval on the trend as deduced by a Student's t test, and the center horizontal line indicates the trend. The uncertainty for the ensemble-mean trends are indicated by a rectangle, while that of individual ensemble members/reanalysis are indicated by a vertical line. The ensemble members for each ensemble are ordered by their expansion trend before they are plotted for clarity. Adapted from Garfinkel et al. (2015).

depletion between 1870 and 1979, as they use 1979 ozone values for their "preindustrial/1870" simulations, yet significant ozone loss occurred before this (Eyring et al., 2013) (see **Chapter 4**); hence the difference between their "preindustrial" simulation and 2000 simulation has too weak an ozone change. The net effect is that SST- and GHG-induced changes are considered over the period 1870 to 2000 as compared to ozone induced-changes from 1979 to 2000, which necessarily underestimates the relative impact of ozone on surface climate compared to other drivers.

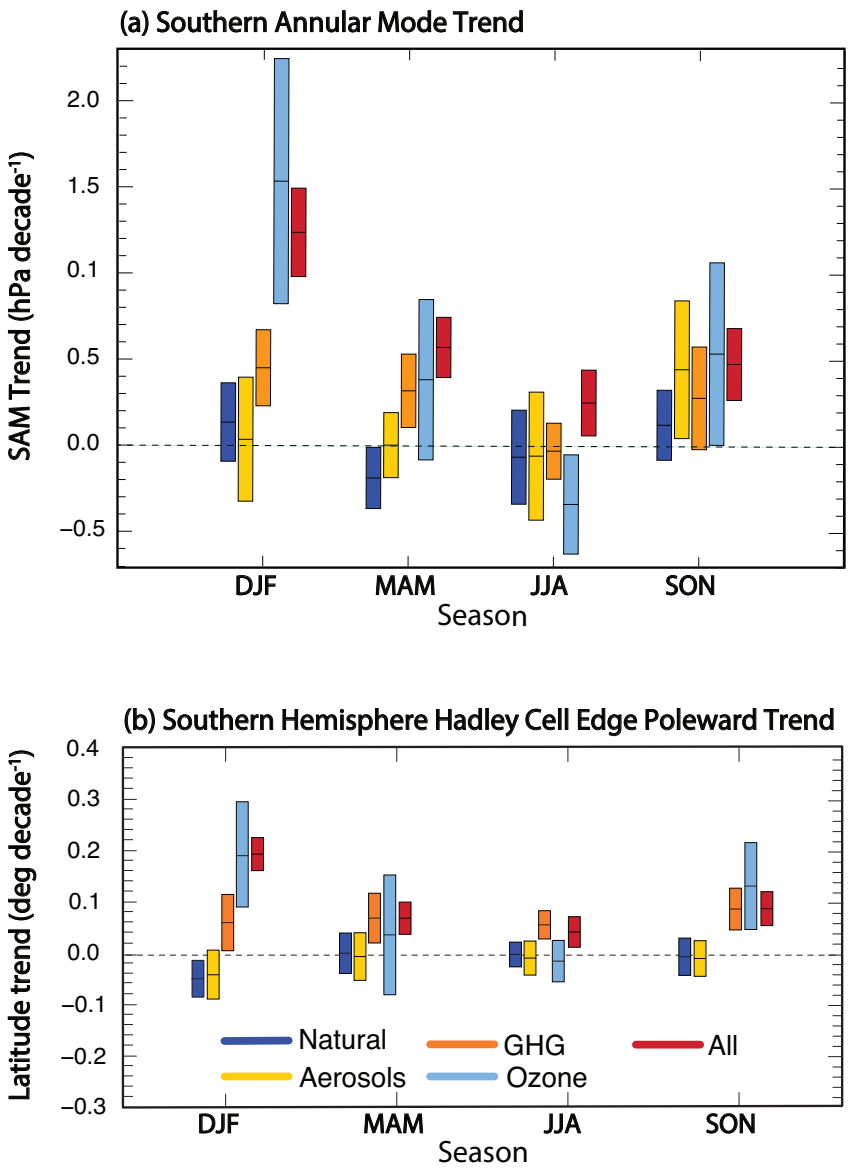

Figure 5-15. Seasonal-mean trends in the (a) SAM index for the period 1971–2006 and (b) the latitude of the poleward edge of the SH Hadley circulation at 500 hPa for the period 1970–2005 (1970–2000 for ozone only), derived from CMIP5 historical simulations. Positive trends indicate poleward expansion and negative values indicate equatorward retreat. Error bars are 90% confidence level. Units are (a) hPa per decade and (b) degree per decade. The colors denote model experiments including the following forcings: all anthropogenic and natural (red); greenhouse gases only (orange); tropospheric and stratospheric ozone only (light blue); natural (solar and volcanic) only (dark blue); and anthropogenic aerosols only (gold). Adapted from Gillett et al. (2013) and Tao et al. (2016).

The weight of the evidence from studies that have compared the impact of ozone depletion to other forcings in a methodologically appropriate manner clearly points to stratospheric ozone depletion as the dominant driver of the changes in the summer SAM over the period in which an ozone hole was formed (prior to 2000).

The trends in tropospheric zonal wind in CCMI models from 1960 to 2000, when forced with natural and anthropogenic forcings including ozone depletion, are similar to those in reanalysis data (**Figure 5-16a–c**; Son et al., 2018). Trends are somewhat weaker in CMIP5 models (**Figure 5-16d;** Rea et al., 2018); however, the weaker trends are most pronounced in those CMIP5 models that did not use interactive chemistry (**Figure 5-16f**; as noted by Eyring et al., 2013); trends in CMIP5 models that used interactive chemistry are quantitatively similar to those simulated by the CCMI models and observations (**Figure 5-16e**). While the observed zonal wind trend is generally consistent with the forced response to ozone depletion, the wind field by itself does not provide a unique fingerprint of ozone depletion due to the large internal variability in the climate system (Schneider et al., 2015).

Although there is uncertainty in the magnitude of the Hadley Cell widening (see **Section 5.4.1.3**), studies agree that the widening has continued (e.g., Mantsis et al., 2017). At the same time, the SAM has mostly

stayed in its positive phase, though the jet latitude has shifted somewhat equatorward from its 2000 position in austral summer (**Figure 5-13**). As discussed in **Chapter 4**, SH polar ozone depletion peaked around 2000 and has slowly begun its recovery, and hence ozone cannot be the sole driver of changes in the Southern Hemisphere since 2000. Rather, several studies have concluded that recent changes in tropical and subtropical SSTs (due to both internal variability and GHG-induced warming), and in particular decadal variability associated with the Pacific Decadal Oscillation (also known as the Interdecadal Pacific Oscillation), drove recent changes in SH circulation (Allen et al., 2014; Waugh et al., 2015; Garfinkel et al., 2015b; Franzke et al., 2015; Nguyen et al., 2015; Clem et al., 2016; Schneider et al., 2015; Allen and

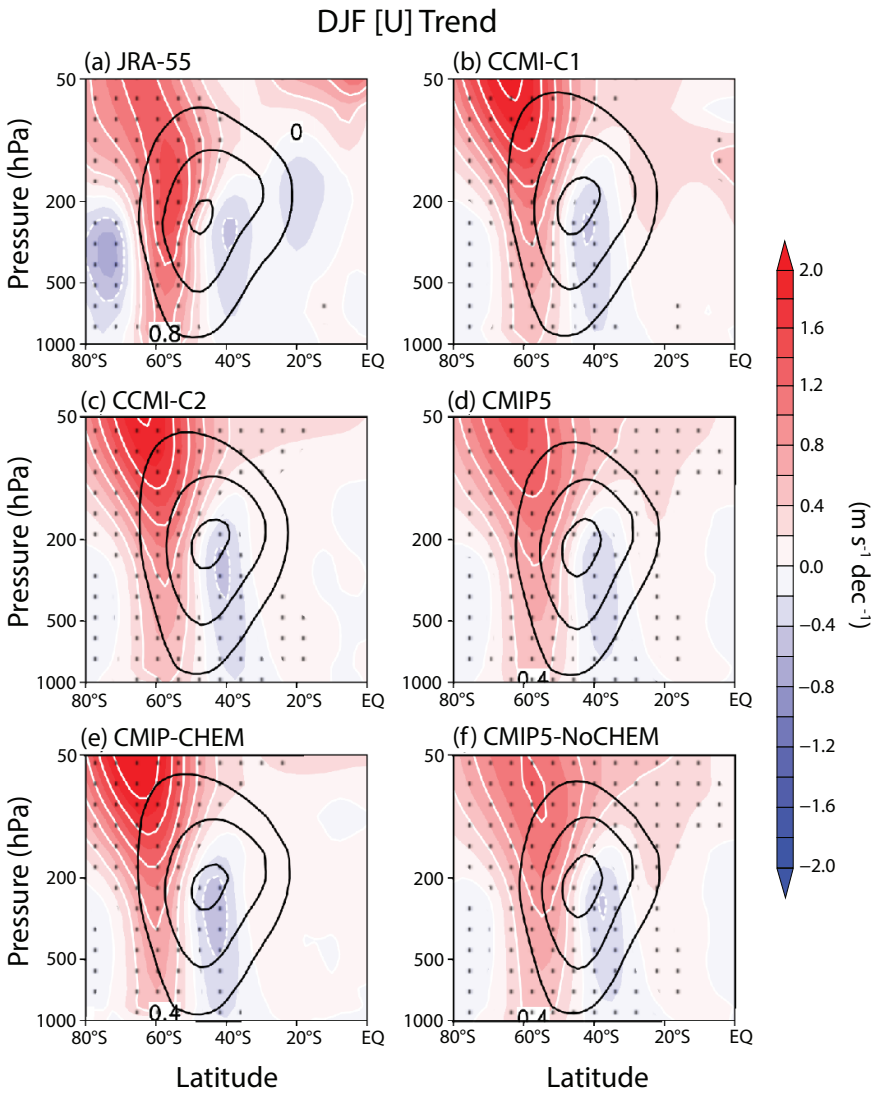

Figure 5-16. Long-term mean (thin black contour) and linear trend (color) of zonal-mean DJF zonal winds over 1960–2000 (the period of ozone loss) for (a) Japanese 55-year Reanalysis (JRA-55); (b, c) CCMI models in REF-C1 and REF-C2 simulations, respectively; and (d, e, f) CMIP5 models. The positive (negative) trends on the poleward (equatorward) flanks of the mean jet characterize a poleward shift of the jet. A comparison between CMIP5 models with and without chemistry is shown in panels e and f. The JRA-55 is the most recent reanalysis product to cover the full period of ozone loss; trends in other reanalysis products analyzed over a shorter period are quantitatively similar (e.g., Son et al., 2010). Contour interval of climatological wind is 10 m s^{-1} starting from 10 m s^{-1} at the outer-most contour. Adapted from Son et al. (2018).

Kovilakam 2017; Mantsis et al., 2017; Fogt et al., 2017; Amaya et al., 2018).

As discussed in **Section 5.4.1.1**, significant trends in the strength of the tropospheric mid-latitude jet, are also evident in May, in addition to summer; however, unlike in summer, a role of ozone depletion in the May trends is unclear. While ozone trends and stratospheric cooling have been observed in late fall, implying that they might have contributed to the tropospheric trends in May, similar stratospheric changes have also been observed earlier in fall and in summer but without concurrent significant trends in the tropospheric circulation. Furthermore, observational and modeling studies suggest a stronger role of observed changes in tropical SSTs in forcing SH tropospheric circulation changes in autumn, especially after 2000, when the ozone forcing has begun to recover (Schneider et al., 2015; Clem et al., 2016). Finally, SAM trends in autumn are not robust in modeling studies, with some studies finding positive trends (Stone et al., 2016) (see **Figure 5-15**) and others finding no trend (Swart et al., 2015; Tao et al., 2016), implying the trends may not be attributed to external forcing.

Finally, there is no consensus on the importance of changes in aerosol concentrations for changes in the SH tropospheric circulation: Some studies find that historical changes in aerosols largely canceled the effect of GHGs on the SAM in the last half of the 20th century in CMIP5 models (e.g., Fyfe et al., 2012; Gillett et al., 2013), while others find a relatively weak role for aerosols in CMIP5 models for both the SAM and the Hadley Cell changes (Steptoe et al., 2016; Tao et al., 2016). This discrepancy could be due to differences in the number of models considered by each study.

5.4.1.3 The Southern Hemisphere: Magnitude of Past Changes in Models

Modeled ensemble-mean trends in the jet position and SAM are somewhat weaker than those observed in several atmosphere–ocean and chemistry–climate model ensembles (see **Figure 5-16**) (Swart et al., 2015; Rea et al., 2018; Iglesias-Suarez et al., 2016; Purich et al., 2016a; Son et al., 2018). Climate models, on average, have been shown to underestimate trends in the *strength* of the SH mid-latitude jet (Swart and Fyfe, 2012; Swart et al., 2015; Purich et al., 2016a). These underestimations have important implications for understanding changes to SH surface wind stress and hence attribution of the trends in ocean circulation and sea ice (**Section 5.4.4**). Similarly, the ensemble, or multi-model, mean response of the Hadley Cell to historical forcings in climate models is weaker than observed, as noted in the previous Assessment (Quan et al., 2014; Garfinkel et al., 2015a). Recent research has suggested that this difference might not reflect any model biases but rather could be due to internal variability contributing to the observed trend, while averaging over an ensemble damps any such contribution from internal variability (Garfinkel et al., 2015a; Davis and Birner, 2017; Mantsis et al., 2017). Namely, the multi-model-mean trends illustrate the forced component in these circulation changes, while the reanalysis trends indicate one particular realization impacted by natural variability. For Hadley Cell expansion, individual climate simulations that include observed time-varying SSTs, ozone, and GHG concentrations can simulate trends as large as those evident in reanalysis and observational products (Garfinkel et al., 2015a; Allen and Kovilakam, 2017; Davis and Birner, 2017) (see **Figure 5-14**). According to these results, the magnitude of the forced response is comparable to the magnitude of the internal variability (**Figure 5-14**). In fact, CMIP5 models with neither time-varying GHGs nor ozone can simulate 20-year expansion trends larger than those inferred from satellite data (Mantsis et al., 2017). Similarly, individual simulations of the past climate covering the period of ozone depletion can reproduce the magnitude of the trends in the SH mid-latitude jet evident in reanalyses, implying that any discrepancy between multi-model mean and observed trends is within the uncertainty due to internal variability (Schneider et al., 2015; Swart et al., 2015; Rea et al., 2018).

There are some known model deficiencies, outlined below, that can affect the magnitude of simulated SH tropospheric circulation trends. On the one hand, in the case of models that prescribe ozone as a boundary condition rather than internally simulate it, the magnitude of simulated tropospheric circulation response to ozone depletion can be affected by unrealistic ozone forcing. For example, ozone depletion in the CMIP5 ozone forcing is weaker than observed, and it has been suggested that this may lead to an underestimation of the response in the extratropical SH circulation (**Figure 5-16d**; Young et al., 2014). In addition, a monthly-mean and zonal-mean ozone dataset misses the maximum amplitude of the ozone hole,

which may lead to an underestimated tropospheric response (Crook et al., 2008; Waugh et al., 2009; Neely et al., 2014). On the other hand, the response of the mid-latitude jet to ozone forcing does not depend on whether the atmosphere is interactively coupled with the ocean in a model or is forced with prescribed SSTs (Sigmond et al., 2010; Seviour et al., 2017a; Son et al., 2018) (see **Figure 5-16**).

Other model deficiencies that can affect simulation of tropospheric response to ozone forcing include a lack of fully resolved stratospheric dynamics (Rea et al., 2018) and an orientation of the simulated polar vortex that is too zonal (Dennison et al., 2017), both of which may lead to underestimation of the tropospheric response. By contrast, a delay in springtime breakdown of the polar vortex present in many climate models (SPARC, 2010) may lead to an overly strong response (Sheshadri and Plumb, 2016; Lin et al., 2017) (see **Section 5.4.2**).

In addition to the stratospheric biases, most current climate models exhibit an equatorward bias in the position of the SH mid-latitude jet in summer as compared to reanalysis data (Wilcox et al., 2012; Swart and Fyfe, 2012), due in part to biases in the cloud distribution (Ceppi et al., 2012), though this bias is reduced in CCMI models (Son et al., 2018). The 2014 Assessment noted that the magnitude of the simulated tropospheric response to the ozone hole may depend on the severity of this bias, with models that exhibit a more equatorward climatological jet bias also showing a larger poleward shift of the jet in response to ozone depletion (e.g., Sigmond and Fyfe, 2014). New studies, however, do not find similar relationships in the CCMI simulations (Son et al., 2018), nor in CMIP5 models when limited to the austral summer season (Simpson and Polvani, 2016), nor in ozone-only forced simulations (Seviour et al., 2017a), suggesting that the relationship between a larger climatological jet bias and a larger response to ozone depletion is not robust.

Considering the contribution of internal variability to uncertainty in simulated tropospheric circulation response to ozone depletion, new modeling studies using a large single-model ensemble (Solomon and Polvani, 2016) and long control simulations (Thomas et al., 2015) suggest that the internal variability of the SH mid-latitude jet is smaller than its forced response to combined anthropogenic forcing during the 20th century as well as its projected response during the 21st century (Solomon and Polvani, 2016), in agreement with the previous Assessment. One study reported that during the period 1980–2004, the forced component exceeds internal variability in the case of a poleward jet shift but not for the SAM trend (Thomas et al., 2015). For the SAM, a stronger forcing over a longer period is needed for a robust positive trend to emerge over internal variability (Gillett et al., 2013; see **Figure 5-15**), consistent with the previous Assessment.

Overall, we assess with high confidence that stratospheric ozone depletion is the dominant external driver of changes in the SH summer tropospheric circulation before the year 2000; however, existing model deficiencies preclude a quantitative separation of the magnitudes of the forced (mostly due to ozone) and unforced components of the observed trends.

5.4.1.4 The Southern Hemisphere: Model Simulations of the Future

The role of ozone in future changes in the SH large-scale atmospheric circulation has received comparatively little attention since the 2014 Assessment, with studies generally finding results consistent with those reported in 2014. Ozone recovery will have impacts opposite to those associated with ozone depletion (Solomon and Polvani, 2016; Dennison et al., 2016) and hence will mitigate some of the poleward shift of the jet due to projected increases in concentrations of GHGs. The degree of mitigation is dependent on the rate of increase in GHGs (Iglesias-Suarez et al., 2016; Tao et al., 2016; Rea et al., 2018). Some of the GHG-induced poleward shift will be compensated by the effect of GHGs on ozone (i.e., super-recovery; Morgenstern et al., 2014; see also **Chapter 3**). Uncertainty in the magnitude of the mitigation for a given scenario can be reduced if careful attention is paid to jet biases and to the magnitude of lower-stratospheric temperature trends over Antarctica (Wenzel et al., 2016), as well as to biases in present-day sea ice concentration for each model (Bracegirdle et al., 2018).

5.4.1.5 The Northern Hemisphere

The last Ozone Assessment found no robust linkages between stratospheric ozone depletion and tropospheric circulation in the Northern Hemisphere, though a weak positive Northern Annular Mode

trend is evident in CMIP5 models forced with ozone concentrations. While there has been little work since 2014 focusing on changes on decadal timescales, several studies have explored whether interannual variability in late spring ozone concentrations may modulate surface climate (**Section 5.4.3**).

5.4.2 Mechanisms for Stratosphere–Troposphere Dynamical Coupling

As described in **Section 5.4.1**, stratospheric ozone loss in the Southern Hemisphere has led to a poleward shift in the tropospheric mid-latitude jet. We now discuss progress toward understanding the dynamical mechanisms for this observed downward coupling. As stated in the previous Assessment, it is well established that the impact of stratospheric ozone depletion on the troposphere occurs through a cooling of the lower polar stratosphere, which is associated with anomalously strong westerly winds and a positive anomaly in stratospheric potential vorticity. It is well accepted that the balanced response in the troposphere to this positive potential vorticity anomaly is an acceleration of the zonal flow on the poleward flank of the jet (e.g., Hartley et al., 1998; Thompson et al., 2006), consistent with the sign of the observed change. However, this balanced response is too weak to explain the magnitude of the observed circulation shift.

Studies with idealized atmospheric models in particular suggest that eddy feedbacks amplify the impact of stratospheric cooling and so play a critical role in the mechanism, as discussed in the last Assessment. The relative roles of synoptic and planetary waves, with zonal wavenumbers greater than 3 and less than 3, respectively, have been the subject of two recent idealized modeling studies (Yang et al., 2015; Smith and Scott, 2016). These point to both categories of waves being important for the amplification of the tropospheric circulation response, as are substantial nonlinear eddy–eddy interactions (consistent with Orr et al., 2012). Specifically, these studies indicate that the tropospheric response cannot be due solely to the imposed radiative cooling modifying tropospheric synoptic waves alone and that planetary scale waves are crucial in the downward influence. It is very difficult to tease out the nature of these interactions, however, as it is likely impossible to clarify how the changes in waves have modified the zonal-mean flow after the zonal-mean flow has already changed (Garfinkel et al., 2013; Garfinkel and Waugh, 2014).

While the SH tropospheric response to ozone depletion in December is simulated by the climate models, it is unclear based on the current literature whether the response can be quantitatively explained by the strengthened stratospheric westerly winds and the delay in the breakdown of the stratospheric polar vortex only. Two studies (Sun et al., 2014; Byrne et al., 2017) conclude that the delay in the breakdown can account for the tropospheric impacts, but a third study (Sheshadri et al., 2014) argues that it cannot account for the full impact (though it does contribute). Finally, the onset date for the vortex breakdown is generally too late in the current climate models (e.g., Wilcox and Charlton-Perez, 2013), in part due to too-weak gravity wave drag in the polar stratosphere near 60°S (McLandress et al., 2012; Geller et al., 2013; Garcia et al., 2017; Garfinkel and Oman, 2018), and this bias impacts the magnitude and seasonality of the tropospheric response to ozone depletion (Sheshadri and Plumb, 2016; Lin et al., 2017).

5.4.3 Surface Impacts

The last Assessment noted that extratropical rainfall in the Southern Hemisphere is tied to the position of the mid-latitude jet and, for the first time, suggested that recent changes in both extratropical and subtropical austral summer rainfall may be related to ozone depletion. However, only a few studies were available, and most either did not isolate the effect of ozone depletion from other anthropogenic forcings and/or they used simplified models or experiments. Subsequent studies have sought to understand the dynamical mechanisms for the subtropical rainfall increase in summer. One study (Hendon et al., 2014), attribute it to a poleward shift of the subtropical dry zone. Understanding the extratropical rainfall response is hampered by the quality of observational products, with little in situ data and changes in satellite products leading to substantial differences across reanalysis results. Nonetheless, a weighted average across five reanalyses suggests the changes in summer from 1979 to 2010 are dynamically consistent with increases in synoptic eddy activity (Solman and Orlanski, 2016), which is primarily associated with ozone depletion. Also, one study (Bai et al., 2016), using maximum covariance analysis and principal component analysis to attribute increases in SH extratropical rainfall, found

a predominant role of ozone depletion over GHGs. However, a firm conclusion about the role of ozone depletion cannot be reached based on these statistical studies only, because statistical relationships are not typically able to determine causality.

Since the last Assessment, a small number of studies have investigated links between regional rainfall changes and ozone depletion. In particular, there has been a focus on the significant increase of austral summer rainfall in southeastern South America (SESA) over the past 50 to 100 years. This region, which includes northern Argentina, Uruguay, southern Brazil and Paraguay, has experienced one of the largest increases in rainfall worldwide (Gonzalez et al., 2014). Most studies using ensembles of climate models or single-model ensembles attribute this increase to anthropogenic forcing (Vera and Díaz, 2015; Díaz and Vera, 2017; Zhang et al., 2016; Wu and Polvani, 2017); however, they disagree on whether the increase is driven by GHG increases (Zhang et al., 2016) or by ozone depletion (Yu and Polvani, 2017). One study (Zhang et al., 2016) notes that its model may underestimate the rainfall response to ozone depletion and aerosols, which somewhat undermines its attribution of the rainfall increase to GHGs. Internal decadal variability due to changes in SSTs was also likely an important driver of the rainfall changes (Zhang et al., 2016), which could explain why the multi-model rainfall increase due to anthropogenic forcing is weaker than that observed (Vera and Díaz, 2015; Díaz and Vera, 2017). Hence, there is a wide range of conclusions for the attribution of rainfall increases in the SESA region, with a large sensitivity to the model and time period analyzed.

Other regional rainfall changes have received relatively little attention since the last Assessment. An imprint of ozone depletion has been identified in changes of the position of the South Pacific Convergence Zone (SPCZ) over the 1961–1996 period, with increases in rainfall on the northern edge and decreases to the south (Brönnimann et al., 2017). Projections by chemistry–climate models suggest that these changes will reverse as a result of ozone recovery. One study suggested the role of ozone in recent winter rainfall declines in southwestern Australia (Delworth et al., 2014), although another study argued that ozone depletion is unlikely to be an important factor in this season (Karoly, 2014). In East Africa, the SAM has been identified as the leading cause of changes in summer rainfall, surface temperature, and the diurnal temperature range, implying the role of ozone during the period of depletion (Manatsa et al., 2013, 2015, 2016). A small anthropogenic component was also found in long-term drying trends in Chile since the late 1970s, but the contribution of ozone depletion has not been isolated (Boisier et al., 2016). Given that these are single studies on each region, it is difficult to make an overall assessment of their significance.

Research since the last Assessment to tease out the impact of ozone recovery on future rainfall trends has been limited by the lack of ozone-only simulations for the 21st century under the CMIP5 framework. One study (Lim et al., 2016) discusses future rainfall changes related to the SAM, finding a robust impact of SAM changes on SH summer rainfall, with a positive SAM opposing the thermodynamically driven projected changes in the subtropics to mid-latitudes while enhancing the increases in the high latitudes. Ozone recovery would drive a more negative SAM and the reverse of these impacts on rainfall.

In terms of surface temperature changes, the previous Assessment found that the largest surface temperature response was over the high-latitude Southern Ocean (see **Section 5.4.4**) rather than Antarctica. While a contribution of ozone depletion to Antarctic surface temperature trends has been shown in a number of previous studies (e.g., McLandress et al., 2011), recent studies have emphasized an important role for natural variability in explaining some of the observed temperature changes over the Antarctic Peninsula and West Antarctica in recent decades (Jones et al., 2016; Turner et al., 2016; Smith and Polvani, 2017). One study (Smith and Polvani, 2017) analyzes the AMIP5 and CMIP5 models, as well as the observed relationship between the SAM and surface warming over Antarctica, concluding that the pattern of warming matches neither anthropogenically forced trends nor trends congruent with the SAM and that internal variability likely played a key role. Similarly, another study (Turner et al., 2016) notes both the regional and seasonal sensitivity of the temperature changes and the dominant processes involved, concluding that while ozone depletion likely contributed to warming of the eastern Antarctic Peninsula during summer, the warming across the peninsula is not inconsistent with natural variability, particularly when placed in

the context of paleoclimate records, which show previous multidecadal periods of strong warming (Jones et al., 2016). Another study (Chiodo et al., 2017) also finds a negligible radiative impact of ozone depletion on Antarctic surface temperatures, suggesting that the high albedo of the snow-covered surface simply reflects any increases in shortwave radiation. Hence, while these studies do not rule out that the ozone depletion has likely contributed to Antarctic surface temperature trends in some regions and seasons, as was previously suggested, they do show that the large natural variability of the region and the sparsity of data and large model biases in the Antarctic and Southern Ocean regions (e.g., Eyring et al., 2013; Marshall and Bracegirdle, 2014; Purich et al., 2016a; see also **Figure 5-16**) impact our confidence in attribution and projection studies there.

Several additional impacts of stratospheric ozone depletion have now been documented. For example, one study (Dennison et al., 2015), using a single chemistry–climate model, finds that ozone depletion leads to an increased frequency of extreme anomalies and increased persistence of the SAM in the stratosphere and stronger, more persistent stratosphere–troposphere coupling. Additionally, another study (Dennison et al., 2016) finds that ozone depletion leads to an increase in blocking frequency—as defined by persistent positive anomalies in 500 hPa geopotential heights—in the South Atlantic region and little change in the South Pacific in their model, consistent with ERA-Interim reanalysis trends over the satellite era. Though this indicates a potential impact of stratospheric ozone on blocking-induced heat waves and rainfall patterns, this result would need to be substantiated with additional models, particularly given well-known model biases in underestimating blocking frequency (Ummenhofer et al., 2013).

5.4.3.1 Interannual Variability

The last Assessment noted two studies (Son et al., 2013; Bandoro et al., 2014) linking interannual variability of Antarctic ozone anomalies in spring to SH summer surface temperature and rainfall changes. Recent modeling studies, using a range of approaches, have examined the possible connection between Arctic spring ozone and surface climate and have obtained mixed results. One study (Cheung et al., 2014) probed whether the extreme Arctic ozone depletion of 2011 had an effect on tropospheric climate with the UK Met Office operational weather forecasting model. It found no improvement in spring tropospheric forecast skill when forcing the model with more realistic ozone concentrations as compared to climatological ozone. Another study (Karpechko et al., 2014) found a relationship between the 2011 low-Arctic stratospheric ozone anomalies and tropospheric climate in atmospheric general circulation model simulations, but it noted that specifying the ozone anomalies in isolation of SST anomalies did not result in a significant surface impact. A third study (Smith and Polvani, 2014) found that the prescribed ozone forcing needed for a robust tropospheric response in its simulations appeared to be larger than that historically observed.

In contrast, a coupled chemistry–climate simulation study (Calvo et al., 2015) found a robust stratospheric–tropospheric response in low versus high ozone years: a positive phase of the North Atlantic Oscillation (NAO), a poleward shift of the North Atlantic tropospheric jet, and corresponding regional surface temperature anomalies. This study used an ensemble of simulations driven by historically observed ODSs, and the link between stratospheric ozone and tropospheric circulation was found only during the recent period of high ODSs, suggesting the importance of chemistry feedback on the dynamics. The fully coupled approach of this study (Calvo et al., 2015) allows consistency between the evolving ozone distributions and dynamical conditions, which may explain the differences between its conclusions and those of studies prescribing ozone concentrations. Future work is needed to evaluate whether differences in the ozone forcings, as well as other inter-model differences, among the various studies have contributed to the range of conclusions.

Two recent observational studies have also suggested that interannual variability in ozone can modify surface climate. The first study (Ivy et al., 2017b) finds that extreme Arctic stratospheric ozone anomalies in March are associated with NH tropospheric climate in spring (March–April) in specific regions of the Northern Hemisphere; the effects are generally consistent with those found in a chemistry-climate model (Calvo et al., 2015). Finally, another study (Xie et al., 2016) suggests that Arctic stratospheric ozone anomalies influence the North Pacific Oscillation (NPO)

and that an anomalous NPO modulates subtropical SSTs. This subtropical SST anomaly might then lead to improved predictability of ENSO, though future work is needed to confirm many aspects of this chain of associations (Garfinkel, 2017). However, it is well known that a delayed or advanced final warming of the Arctic stratospheric vortex can lead to surface impacts (Black and McDaniel, 2007; Ayarzagüena et al., 2009; Hardiman et al., 2011), and distinguishing the dynamical impact of the final warming from the radiative impact of the ozone anomaly that typically accompanies a final warming also requires additional work.

Thus, our assessment is that interannual variability in springtime Antarctic and Arctic ozone may be important for surface climate, but work remains to better quantify this connection.

5.4.4 Ocean and Ice Impacts

5.4.4.1 Ocean Impacts

As discussed above, observations show trends in the SAM and low-level tropospheric winds that are largest during austral summer (**Figures 5-13** and **5-15**), and these summertime trends have been mainly attributed to stratospheric ozone depletion. A positive SAM trend implies a poleward shift and/or strengthening of the surface wind stress, which plays a fundamental role in the ocean circulation. Westerly wind stress acts to drive northward transport in the underlying ocean (via Ekman transport), creating a region of divergence and upwelling on the poleward side of the surface wind maximum and a region of convergence and downwelling equatorward of the surface wind maximum (e.g., Arblaster and Gillett et al., 2014). The previous Assessment reported that observations indicate a strengthening of the horizontal and vertical circulations in the Southern Ocean, of which a substantial part was likely caused by ozone-induced westerly wind trends. These wind trends were also linked to subsurface warming below and north of the Antarctic Circumpolar Current (ACC), but the relative importance of the wind trends and other forcings (notably warming due to increased GHGs) had not been quantified.

Since the last Assessment, more evidence has appeared indicating a substantial role for ozone depletion in recent trends of the Southern Ocean circulation. For austral summer, one study (Solomon et al., 2015) showed that modeled trends in the vertical ocean circulation are mainly attributable to ozone depletion, while a different study (Wang et al., 2014) showed that ozone recovery acts to mitigate future GHG-induced changes in the horizontal ocean circulation. Observed changes in the thermal structure of the Southern Ocean (**Figure 5-17**) are dominated by a warming that maximizes along the northern flank of the ACC, around 40–50°S, with the largest warming in the upper 1,000 m (Armour et al., 2016; Schneider and Deser, 2018). Two noticeable exceptions are the regions with subsurface cooling north of 35°S (Armour et al., 2016) and widespread SST cooling that occurred since the late 1970s in the region south of 50°S (Fan et al., 2014; Jones et al., 2016; Armour et al., 2016; Schneider and Deser, 2018). The high-latitude surface cooling is intimately linked to the observed increase in Antarctic sea ice over that period (Parkinson and DiGirolamo, 2016) and will be discussed in **Section 5.4.4.2**.

Focusing first on the region between 30–60°S, a modeling study identified increasing GHGs as the main driver of the warming in this region, with ozone depletion playing a secondary role (Solomon et al., 2015). This appears consistent with a recent study (Armour et al., 2016) that suggests that the structure of upper ocean warming, with delayed warming south of the ACC and enhanced warming to the north, is fundamentally shaped by the mean (climatological) meridional circulation in the Southern Ocean. This study finds that wind-driven upwelling of water that has not been warmed by GHGs slows the warming south of the ACC, while the GHG-induced heat is taken up and transported northward and then stored just north of the ACC. This mechanism does not rely on changes in the meridional ocean circulation, possibly explaining why ozone-induced atmospheric circulation changes play a secondary role in accounting for recent Southern Ocean warming.

In conjunction with these warming trends, the Southern Ocean has also experienced freshening (i.e., a decline in salinity), with the exception of a strong salinification trend north of 45°S in the upper 500 m (**Figure 5-17**). A recent modeling study suggests that 30% of the modeled Southern Ocean freshening can be attributed to ozone depletion (Solomon et al., 2015). Sources of the freshening are believed

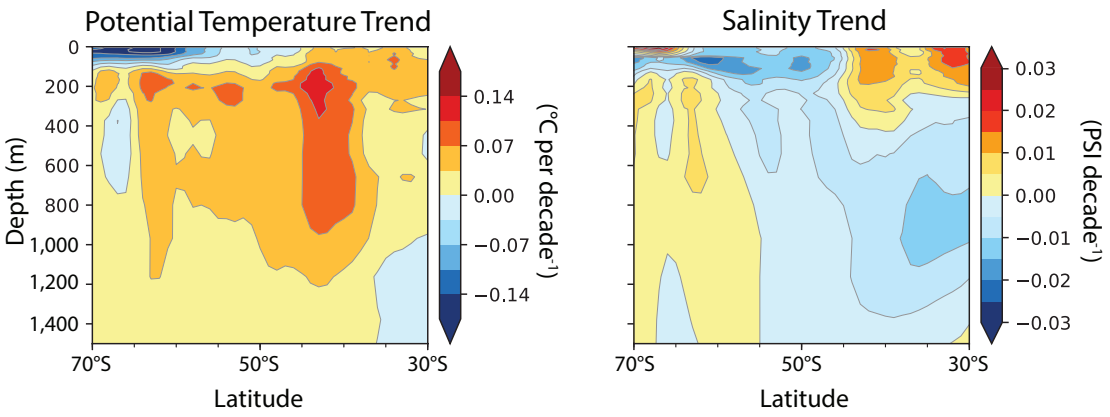

Figure 5-17. Observed 1979–2013 trend in annual-mean, zonal-mean ocean potential temperature and salinity from the Met Office Hadley Centre's EN4 dataset (Good et al., 2013).

to be located in the high latitudes and may include GHG- and ozone-induced changes in high-latitude precipitation minus evaporation (Fyfe et al., 2012), a wind-driven increase in northward freshwater transport by sea ice (Haumann et al., 2016), and basal melting of Antarctic ice shelves (Bintanja et al., 2013). Note that the melting of ice shelves was not considered by this study (Solomon et al., 2015).

Finally, we note that unforced internal variability of the Southern Ocean may have played a role in observed trends. While its magnitude is highly uncertain, some studies suggest that it is potentially large (Latif et al., 2013; Zhang et al., 2017).

5.4.4.2 Sea Ice Impacts

We now turn to the observed high-latitude (south of 50°S) surface cooling and the associated increase in Antarctic sea ice since 1979. New studies suggest that these trends reflect multi-decadal variability, with opposite trends in SSTs observed over the 1950–1978 period (Fan et al., 2014) and a recently recovered satellite-based estimate of Antarctic sea ice extent suggesting a decreasing sea ice trend from the mid-1960s to 1979 (Meier et al., 2013; Armour and Bitz, 2015; Gagné et al., 2015). The magnitude and sign of the ozone hole contribution to Southern Ocean temperature and Antarctic sea ice trends since 1979 have been topics of much discussion. In the last Assessment, it was reported that all climate model simulations that isolated the impact of stratospheric ozone depletion (including time-slice simulations in models with and without resolved ocean eddies, a fully coupled chemistry–climate model, and all six CMIP5 models with ozone-only simulations available) simulated decreased sea ice extent associated with ozone-induced changes in the Southern Ocean circulation, suggesting that ozone depletion had not contributed to the observed high-latitude ocean cooling and increase in Antarctic sea ice. The 2014 Assessment also cautioned that due to inconsistencies between the observed and modeled sea ice trends, confidence in the simulated response to the formation of the ozone hole was limited.

New modeling studies have corroborated the findings of the last Assessment that a realistic, time-evolving ozone hole leads to Antarctic sea ice decline and thus cannot explain the observed increase in sea ice since 1979 (Solomon et al., 2015) nor the regional patterns of Antarctic sea ice trends (Landrum et al., 2017). However, other recent studies have highlighted discrepancies between modeled and observed sea ice trends since 1979 (Gagné et al., 2015; Hobbs et al., 2015; Rosenblum and Eisenman, 2017), which may be related to model biases in the ocean mean state (Kostov et al., 2016, 2018; Schneider and Deser, 2018), Southern Ocean deep convection (Behrens et al., 2016), the weaker simulation of recent wind trends (Purich et al., 2016a), the underestimation of the zonal asymmetries in the atmospheric circulation (Haumann et al., 2014), the underestimation of historical surface freshening (Purich et al., 2018), and the lack of an interactive ice shelf component (Pauling et al., 2017). These studies 1) confirm that the confidence in the

simulated response to ozone depletion is still limited and 2) argue that the conclusion that the ozone hole has not contributed to recent high-latitude ocean and sea ice trends may be preliminary.

Despite these persistent model uncertainties, significant advances have been made in the understanding of processes responsible for the modeled ocean and sea ice response to ozone depletion. Idealized model simulations where the stratospheric ozone concentrations were instantaneously changed from pre-ozone hole to ozone hole conditions (Ferreira et al., 2015) demonstrated that the high-latitude ocean response entails two timescales (**Figures 5-18** and **Figure 5-19**). On the shorter timescales (months to years), the response is characterized by ocean cooling at the surface associated with increased northward Ekman transport of colder high-latitude waters. This is consistent with well-known correlations between month-to-month variations in the SAM, SST and sea ice extent. On longer timescales (years to decades), this surface cooling is then replaced by warming associated with enhanced upwelling of relatively warm waters beneath the mixed layer (see also Marshall et al., 2014). This two-timescale behavior was also seen in a different coupled climate model with significantly different characteristics of ocean convection (Seviour et al., 2016, 2017b) (**Figure 5-19c**). It should be noted that part of the initial cooling response in **Figure 5-19c** may be a reflection of the initial conditions: As a corresponding ensemble of control simulations was not available, the unforced time evolution of the SSTs was estimated indirectly. Furthermore, in spite of a relatively long cooling phase, the sea ice did not expand in those simulations. Nonetheless, based on the initial cooling of SSTs in response to instantaneous ozone forcing, some have argued that ozone

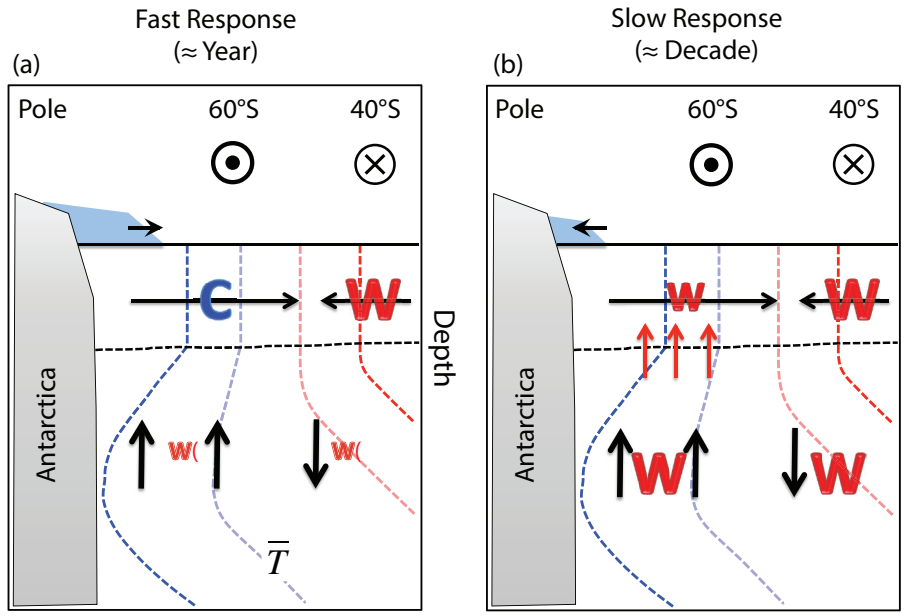

Figure 5-18. Schematic of the two-timescale response of the ocean and sea ice to a stepwise ozone hole as simulated by climate models. The dot at 60°S and × at 40°S indicate the dipole in surface wind stress associated with the strengthened SAM in response to ozone depletion. (a) The fast response is dominated by surface cooling associated with increased northward Ekman transport, whereas (b) in the slow response this cooling is replaced by warming, which is the result of enhanced upwelling of relatively warm waters from beneath the mixed layer. Blue patches represent the sea ice cover (expanding in the fast response and contracting in the slow response). Adapted from Ferreira et al. (2015).

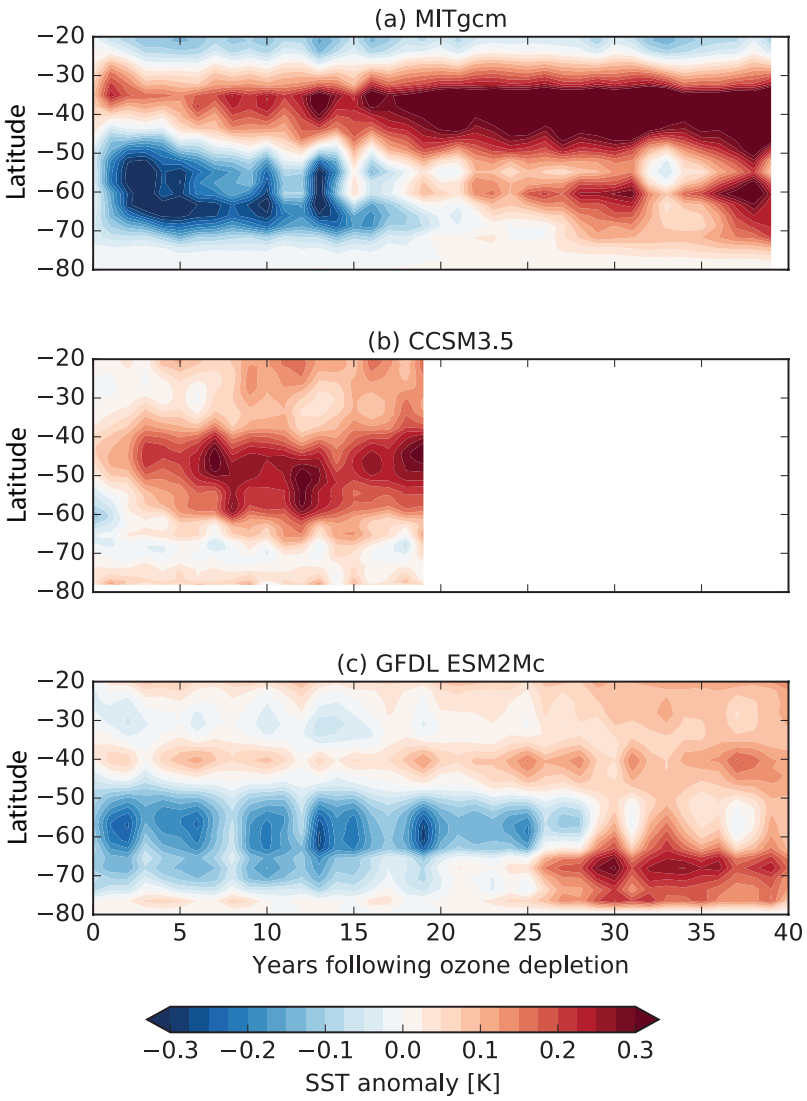

Figure 5-19. Zonal-mean and annual-mean SST response to a stepwise ozone depletion in three coupled models: (a) MITgcm, with an idealized Double-Drake configuration, and two comprehensive models, (b) CCSM3.5 and (c) GFDL ESM2Mc. All three models show a two-timescale response, consisting of a cooling followed by a warming in the Southern Ocean region (50–70°S). However, their magnitude and timescales vary greatly. The net cooling lasts approximately 20 years in the MITgcm, 3 years in CCSM3.5, and 30 years in GFDL ESM2Mc. Adapted from Ferreira et al. (2015) and Seviour et al. (2016).

depletion could drive a transient expansion of sea ice (Marshall et al., 2014; Ferreira et al., 2015). The impact of a realistically prescribed (i.e., time-varying) ozone hole on Antarctic sea ice trends critically depends on the timescale of transition from the initial cooling to subsequent warming. Unfortunately, this timescale is not well constrained, varying greatly between the three models with the prescribed stepwise ozone perturbation (**Figure 5-19**). Other attempts to quantify the impact of the ozone hole on Antarctic sea ice are more indirect and rely on statistical techniques (such as convolution theorem) to extract the SST or sea ice response to a hypothetical step increase in the SAM index. Consistent with the idealized ozone experiments, these studies find a large intermodel spread between CMIP5 models in the SST response: In response to a SAM increase, some models simulate a short transition time from initial cooling to

subsequent warming, while other models continue to cool for at least 20 years (Kostov et al., 2016, 2018). This intermodel spread has been related to biases in the models' mean ocean stratification and to dynamical processes, including oceanic (parameterized) eddy fluxes, mixed layer dynamics, and air–sea interactions (Ferreira et al., 2015; Kostov et al., 2016). This technique has also been applied to Antarctic sea ice, revealing a large range in modeled transition timescale from initial sea ice expansion to subsequent sea ice contraction in response to a step function in the SAM (Holland et al., 2016). Applying the modeled sea ice response function to SAM variability but driven by the observed SAM time series, one study (Holland et al., 2016) suggests that for the multi-model mean, the observed variations in the SAM have driven a modest sea ice decline. While these studies based on the convolution theorem are generally consistent with the idealized ozone forcing perturbations, it remains to be demonstrated that the convolution theorem can accurately predict the sea ice response to the SAM in each model.

The new studies that have quantified the response to an instantaneous ozone perturbation or SAM increase have provided important, novel insights into the physical processes involved in the sea ice response to ozone depletion. It should be emphasized, however, that these idealized experiments are tools to probe the physics of the climate system and that they were not meant to represent the real ozone hole, as its formation and the corresponding SAM increase have occurred over several decades. Nonetheless, these studies suggest that when forced with the real, time-varying ozone hole, models with a long cooling timescale would simulate increased sea ice. However, this does not seem to be consistent with the fact that all studies that have analyzed climate model experiments forced with realistic, time-varying ozone depletion consistently find decreasing sea ice.

It also needs to be emphasized that the modest increase in Antarctic sea ice extent is the result of near-canceling regional trends, with the strongest sea ice increase in the Ross Sea and strongest decrease in the Bellingshausen and Amundsen Seas (Turner et al., 2015; Hobbs et al., 2016). This pattern in the sea ice trends is qualitatively consistent with a deepening of the Amundsen Sea Low (ASL). There is some evidence that the ozone hole has contributed to these atmospheric circulation trends (England et al., 2016) in the summer months, but it has also been noted that the observed ASL trends are within the bounds of modeled internal variability (Turner et al., 2015). An increasing body of evidence suggests that the ozone hole is not the main driver of ASL trends and points to decadal variations in the tropical Pacific (Meehl et al., 2016; Purich et al., 2016b; Schneider and Deser, 2018), or possibly the Atlantic (Li et al., 2014), as the likely drivers.

We further note that during the austral spring (September, October, November; SON) of 2016, unprecedented retreat of Antarctic sea ice was observed that was 46% faster than the mean rate of loss in spring over the satellite era (Turner et al., 2017). This led to record-low sea ice extent anomalies, well exceeding 3 standard deviations of the observed 1979–2016 ice extent (Stuecker et al., 2017). This observation contrasts sharply with the long-term increasing sea ice trend discussed above. Studies have linked the unprecedented retreat to record negative values of the SAM (Turner et al., 2017; Doddridge and Marshall, 2017; Stuecker et al., 2017) and extratropical SST anomalies forced by the extreme 2015–2016 El Niño (Stuecker et al., 2017). These studies suggest that the unprecedented retreat was the result of tropically forced and internal SH atmospheric variability (and hence that it was unrelated to the slow, long-term warming simulated by the models), but more studies are needed to come to robust conclusions.

In conclusion, since the last Assessment, significant progress has been made regarding the understanding of processes involved in the response of Antarctic sea ice to ozone depletion, which is now believed to entail a fast surface cooling followed by a slow, long-term surface warming. However, the role that the ozone hole has played in observed Antarctic sea ice changes remains unclear. While the conclusion of the last Assessment that the ozone hole cannot explain recent trends in Antarctic sea ice is supported by new modeling studies, confidence in this result remains low. This is because climate models generally do not reproduce observed Antarctic sea ice trends since 1979 and because new studies have identified several systematic biases. Future progress could be made by model improvements and repetition of realistic ozone-only simulations performed with more coupled climate models.

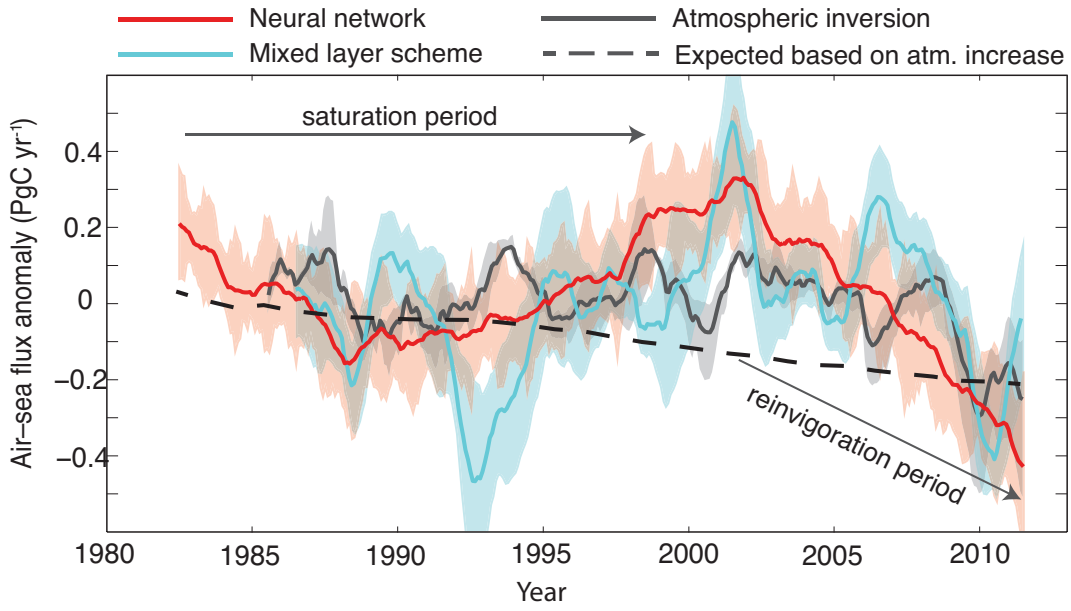

Figure 5-20. Evolution of the Southern Ocean carbon sink based on (red and blue lines and shading) two methods to interpolate surface ocean observations and (black solid line and gray shading) an atmospheric inversion method. The expected uptake based on the growth of atmospheric CO_2 alone is shown by the dashed black line. Negative values indicate anomalous uptake by the ocean. Adapted from Landschützer et al. (2015).

5.4.4.3 Ocean Carbon

The Southern Ocean plays a crucial role in the global carbon cycle, as it accounts for about 40% of the global oceanic uptake of anthropogenic CO_2 (Khatiwala et al., 2009; Frölicher et al., 2015). The strength of the carbon sink is mainly dependent on the air–sea gradients of CO_2. In the absence of other changes, the increase in anthropogenic CO_2 in the atmosphere would lead to increased air–sea gradients and hence to an increased carbon sink (dashed black line in **Figure 5-20**). It was previously suggested that the carbon sink had slowed down (Le Quéré et al., 2007) and that this slowdown was partly related to ozone-induced changes in the surface winds, which bring up carbon-rich water and hence reduce the air–sea gradient of CO_2. These results relied on atmospheric inversion methods (which estimate carbon fluxes from atmospheric CO_2 measurements) and forward ocean models. The realism of this slowdown has been debated in the literature, as inversion models have been shown to depend on data selection (Law et al., 2008) and the coarse resolution ocean models employed in most studies do not represent critical processes such as mesoscale eddies (Swart et al., 2014). Furthermore, the last Assessment reported that for the 1990–2009 period, estimates of the trends in the carbon sink depended on the analysis, with atmospheric inversions generally showing a slowdown in the uptake and ocean biogeochemical models indicating no slowdown (Lenton et al., 2013).

Since the last Assessment, further evidence has appeared suggesting that the apparent slowdown of the carbon sink is not robust (Landschützer et al., 2015, Munro et al., 2015) (**Figure 5-20**). These studies employed observations of the surface ocean CO_2 measurements and hence did not rely on imperfect ocean biogeochemical models. While they confirmed earlier studies that the carbon sink slowed down between the 1980s and early 2000s, they also found a remarkable reversal with a reinvigoration of the sink between 2002 and 2012 (**Figure 5-20**). Averaged over the Southern Ocean, these decadal variations were found to be reasonably robust to the method used to interpolate

the sparse measurements in space and time, though significant uncertainties remain on smaller spatial scales (Ritter et al., 2017). As shown in **Figure 5-20**, the strength of the carbon sink is now thought to be comparable to that expected based on atmospheric CO_2 increases alone. These results suggest that atmospheric circulation changes (whether driven by ozone or not) have not had a considerable impact on the net strength of the Southern Ocean carbon sink.

5.4.5 Changes in Radiative Forcing and Feedbacks

Since the last Assessment, there have been no major published updates to the estimated preindustrial to present-day ozone radiative forcing (RF) due to the effects of long-lived ODSs on stratospheric and tropospheric ozone abundances. However, one study (Hossaini et al., 2015) highlighted 1) that halogenated very short-lived substances (VSLSs) of both anthropogenic and natural origin tend to destroy ozone in the lower stratosphere more efficiently than long-lived ODSs and 2) that since the ozone radiative effect per molecule is stronger in the lower stratosphere than in the upper stratosphere, this may be important for the global radiative balance. This study estimated a global radiative effect from the stratospheric ozone changes in response to observed VSLSs (bromine [Br], chlorine [Cl], and iodine species) of −0.08 W m^{-2}. Although the study found no trend in the influence of VSLSs on global ozone between 1979 and 2013, the influence of brominated VSLSs on global ozone in the preindustrial (i.e., with low anthropogenic Cl) was ~30% smaller than present day owing to the coupling between Br and Cl chemical cycles. The study therefore estimated an indirect ozone RF from VSLSs of −0.014 W m^{-2}, which is about one-tenth of the study's estimated total ozone RF due to long-lived ODSs.

New studies since the last Assessment have quantified the stratospheric and tropospheric ozone RF due to the projected major drivers of atmospheric ozone concentrations over the 21st century: declining halogenated ODS concentrations, climate change due to anthropogenic forcing, changes to tropospheric ozone precursor species including methane, and changes to chemically active greenhouse gases (nitrous oxide [N_2O]). One study (Banerjee et al., 2018) used a chemistry–climate model to estimate the 21st-century ozone RF due to the projected decline in long-lived halogenated ODSs. It found a total (stratosphere and troposphere) ozone RF between 2000 and 2100 of 0.07 W m^{-2}. This is in quantitative agreement with another study (Iglesias-Suarez et al., 2018) that used a different chemistry–climate model and estimated the ozone RF due to future ODSs to be 0.129 ± 0.081 W m^{-2}. Thus, the future decline in ODSs over the 21st century will induce a small indirect positive RF from ozone. However, this positive RF is substantially smaller than the negative direct RF due to declining atmospheric ODSs as a result of the Montreal Protocol and its Amendments (see **Chapter 6**).

A number of modeling studies published since the last Assessment have examined the impact of changes in ozone in response to an abrupt increase in CO_2 on estimates of the equilibrium climate sensitivity (ECS)—the equilibrium change in global mean near-surface temperature in response to a doubling in CO_2. As discussed in **Chapters 3** and **4**, CO_2 affects stratospheric ozone abundances through effects on transport and chemistry (via changes to stratospheric temperatures). New estimates of the effect of ozone changes on ECS in different chemistry–climate models range from no change (Marsh et al., 2016) to a reduction in ECS of about 20% (Nowack et al., 2014), with some studies finding a decrease in ECS of a smaller magnitude (Dietmüller et al., 2014; Muthers et al., 2014). The differences in the relative importance of ozone changes for inferred ECS are likely to be related to the distribution and magnitude of ozone and stratospheric water vapor changes simulated in the individual models. We therefore conclude that ozone changes and their associated effect on climate feedbacks in response to increased CO_2 are more likely to reduce than to increase ECS; however, there is currently large quantitative uncertainty in the magnitude of this feedback.

5.5 CLIMATE IMPACTS OF THE MONTREAL PROTOCOL

5.5.1 World Avoided by the Montreal Protocol

World-avoided simulations evaluate the environmental and climate impacts that have been avoided as a result of the successful regulation of ODS emissions under the Montreal Protocol. This is generally done by a comparison of climate model simulations with

and without ODS emissions regulations. In the scenarios with unregulated ODSs, the ODSs are generally assumed to increase at a constant rate of 3–3.5% per year (e.g., Prather et al., 1996; Velders et al., 2007; Newman et al., 2009; Garcia et al., 2012). As reported in the 2014 Assessment, chemistry–climate models suggest that continued accumulation of ODSs in the atmosphere in the absence of the Montreal Protocol would have led to a collapse of the global ozone layer by the mid-21st century, with devastating environmental implications (Newman et al., 2009; Garcia et al., 2012). The last Assessment also reported on the additional (mostly unanticipated) benefits of ODS regulations for mitigation of global climate change. Specifically, it was reported that by later this century, unregulated ODS increases could have led to global surface temperature increases comparable to temperature increases caused by other greenhouse gases (Velders et al., 2007) and could have almost doubled changes in the hydrological cycle (precipitation minus evaporation) over the next few decades.

While new literature on this topic since the last Assessment is limited, such studies have highlighted other aspects of the climate benefits of the Montreal Protocol. One modeling study found that in the world-avoided scenario, the projected increase in the potential intensity of tropical cyclones is nearly three times larger in 2065 than in a scenario accounting for warming due to other greenhouse gases only (Polvani et al., 2016). Two other studies have attempted to quantify the implications of the avoided temperature and precipitation changes from restricting ODS emissions for global sea level rise (SLR). One study found that under an idealized scenario in which the emissions of gases regulated under the Montreal Protocol had instead been eliminated in 2050, additional thermal SLR of between 4–14 cm would be expected in the 21st century (Zickfeld et al., 2017), with the large range coming from the uncertainty in ocean heat uptake efficiencies in climate models. The other study found that by 2065, thermal SLR avoided by the Montreal Protocol is about 5 cm, but note that part of that SLR is balanced by changes in the hydrological cycle over Antarctica (Previdi and Polvani, 2017).

5.5.2 Projected Climate Impacts of the Kigali Amendment

Other new studies have simulated future climate impacts that will be avoided if nations adhere to the phasedown of hydrofluorocarbons (HFCs) under the Kigali Amendment. In the simulations without HFC regulations, a wide range of HFC scenarios is typically considered (**Chapter 2, Section 2.3.1**). As discussed in **Chapter 2**, these new studies indicate that the anticipated phasedown of HFCs is expected to avoid up to 0.4 K of global mean surface warming by 2100. The atmospheric impacts of HFC regulations have been further quantified using a 2-D (latitude–pressure) interactive chemistry, radiation, and dynamics model (Hurwitz et al., 2015, 2016). These studies found that unregulated increases in HFCs would result in a warming of the troposphere and stratosphere. In a business-as-usual HFC emissions scenario, the tropical lower stratosphere in 2050 was up to 0.41 K warmer than in a scenario with zero HFC emissions (Hurwitz et al., 2015). In that same business-as-usual scenario, the 10–16 km global mean temperature was projected to increase by 0.11–0.13 K between 2015 and 2050, while HFC mitigation scenarios similar to those proposed under the Kigali Amendment were found to avoid most of that warming (Hurwitz et al., 2016). In a business-as-usual scenario, HFCs were also found to impact the atmospheric circulation, slightly enhancing the Brewer–Dobson circulation above 18 km (resulting in a small decrease of the stratospheric mean age of air by −0.3%) and weakening the Hadley Cell circulation below 18 km (Hurwitz et al., 2015). More studies are needed to confirm this result with more comprehensive models.

REFERENCES

Abalos M., B. Legras, F. Ploeger, and W.J. Randel, Evaluating the advective Brewer-Dobson circulation in three reanalyses for the period 1979-2012, *J. Geophys. Res. Atmos., 120,* 7534–7554, doi:10.1002/2015JD023182, 2015.

Abalos M., B. Legras, and E. Shuckburgh, Interannual variability in effective diffusivity in the upper troposphere / lower stratosphere from reanalysis data, *Q. J. R. Meteorol. Soc.*, *142,* 1847–1861, doi:10.1002/qj.2779, 2016.

Abalos M., W.J. Randel, D.E. Kinnison, and R. Garcia, Using the artificial tracer e90 to examine present and future UTLS transport in WACCM, *J. Atmos. Sci.*, *74*, doi:10.1175/JAS-D-17-0135.1, 2017.

Abram, N.J., R. Mulvaney, F. Vimeux, S.J. Phipps, J. Turner, and M.H. England, Evolution of the Southern Annular Mode during the past millennium, *Nat. Clim. Change*, *4*, 564–569, doi:10.1038/nclimate2235, 2014.

Albers, J.R., J. Perlwitz, A.H. Butler, T. Birner, G.N. Kiladis, Z.D. Lawarence, G.L. Manney, A.O. Langford, and J. Dias, Mechanisms governing interannual variability of stratosphere to troposphere ozone transport, *J. Geophys. Res. Atmos.*, *123*, 234–260, doi:10.1002/2017JD026890, 2018.

Allen, R.J., and M. Kovilakam, The role of natural climate variability in recent tropical expansion, *J. Clim.*, 30, 6329–6550, doi:10.1175/JCLI-D-16-0735.1, 2017.

Allen, R.J., J.R. Norris, and M. Kovilakam, Influence of anthropogenic aerosols and the Pacific Decadal Oscillation on tropical belt width, *Nat. Geosci., 7*, 270–274, doi:10.1038/ngeo2091, 2014.

Amaya, D.J., N. Siler, S.P. Xie, and A.J. Miller, The interplay of internal and forced modes of Hadley Cell expansion: Lessons from the global warming hiatus, *Clim. Dyn.*, 51, 305–319, doi:10.1007/s00382-017-3921-5, 2018.

Anderson, J.G., D.M. Wilmouth, J.B. Smith, and D.S. Sayres, UV dosage levels in summer: Increased risk of ozone loss from convectively injected water vapor, *Science*, *337*, 835–839, doi:10.1126/science.1222978, 2012.

Anderson, J.G., D.K. Weisenstein, K.P. Bowman, C.R. Homeyer, J.B. Smith, D.M. Wilmouth, D.S. Sayres, J.E. Klobas, S.S. Leroy, J.A. Dykema, and S.C. Wofsy, Stratospheric ozone over the United States in summer linked to observations of convection and temperature via chlorine and bromine catalysis, *Proc. Natl. Acad. Sci.*, *114* (25), E4905–E4913, doi:10.1073/pnas.1619318114, 2017.

Anderson, J.G. and C.E. Clapp, Coupling free radical catalysis, climate change, and human health, *Phys. Chem. Chem. Phys., 20,* 10569–10587, doi:10.1039/C7CP08331A, 2018.

Aquila, V., W.H. Swartz, D.W. Waugh, P.R. Colarco, S. Pawson, L.M. Polvani, and R.S. Stolarski, Isolating the roles of different forcing agents in global stratospheric temperature changes using model integrations with incrementally added single forcings, *J. Geophys. Res.*, *20* (16), doi:10.1002/2015JD023841, 2016.

Arblaster, J.M., N.P Gillett (Lead Authors), N. Calvo, P.M. Forster, L.M. Polvani, S.-W. Son, D.W. Waugh, and P.J. Young, Stratospheric ozone changes and climate, Chapter 4 in *Scientific Assessment of Ozone Depletion: 2014*, Global Ozone Research and Monitoring Project–Report No. 55, World Meteorological Organization, Geneva, Switzerland, 2014.

Armour, K.C., and C.M. Bitz, Observed and projected trends in Antarctic sea ice, *U.S. Clivar Var.*, *13*, 12–19, doi:10.1175/BAMS-D-11-00244.1, 2015.

Armour, K.C., J. Marshall, J.R. Scott, A. Donohoe, and E.R. Newsom, Southern Ocean warming delayed by circumpolar upwelling and equatorward transport, *Nat. Geosci., 9*, 549–554, doi:10.1038/ngeo2731, 2016.

Aschmann, J., J.P. Burrows, C. Gebhardt, A. Rozanov, R. Hommel, M. Weber, and A.M. Thompson, On the hiatus in the acceleration of tropical upwelling since the beginning of the 21st century, *Atmos. Chem. Phys.*, *14*, 12803–12814, doi:10.5194/acp-14-12803-2014, 2014.

Atlas, R., R.N. Hoffman, J. Ardizzone, S.M. Leidner, J.C. Jusem, D.K. Smith, and D. Gombos, A cross-calibrated, multiplatform ocean surface wind velocity product for meteorological and oceanographic applications, *Bull. Am. Meteorol. Soc.*, *92* (2), 157–174, doi:10.1175/2010BAMS2949.1,2011.

Avery, M.A., S.M. Davis, K.H. Rosenlof, H. Ye, and A.E. Desser, Large anomalies in lower stratospheric water vapour and ice during the 2015–2016 El Niño, *Nat. Geosci., 10*, 405–409, doi:10.1038/ngeo2961, 2017.

Ayarzagüena, B., and E. Serrano, Monthly characterization of the tropospheric circulation over the Euro-Atlantic area in relation with the timing of stratospheric final warmings, *J. Clim., 22* (23), 6313–6324, doi:10.1175/2009JCL13565.1, 2011.

Bai, K., N.-B. Chang, and W. Gao, Quantification of relative contribution of Antarctic ozone depletion to increased austral extratropical precipitation during 1979–2013, *J. Geophys. Res.*, *121* (4), 1459–1474, doi:10.1002/2015JD024247, 2016.

Baldwin M., and M. Dameris (Lead Authors), J. Austin, S. Bekki, B. Bregman, N. Butchart, E. Cordero, N. Gillett, H.-F. Graf, C. Granier, D. Kinnison, S. Lal, T. Peter, W. Randel, J. Scinocca, D. Shindell, H. Struthers, M. Takahashi, D. Thompson, Climate-Ozone Connections, Chapter 5 in *Scientific Assessment of Ozone Depletion: 2006*, Global Ozone Research and Monitoring Project–Report No. 50, World Meteorological Organization, Geneva, Switzerland, 2007.

Bandoro, J., S. Solomon, A. Donohoe, D.W. Thompson, and B.D. Santer, Influences of the Antarctic ozone hole on Southern Hemispheric summer climate change, *J. Clim.*, *27* (16), 6245–6264, doi:10.1175/JCLI-D-13-00698.1, 2014.

Banerjee, A., A.C. Maycock, A.T. Archibald, N.L. Abraham, P. Telford, P. Braesicke, and J.A. Pyle, Drivers of changes in stratospheric and tropospheric ozone between year 2000 and 2100, *Atmos. Chem. Phys.*, *16*, 2727–2746, doi:10.5194/acp-16-2727-2016, 2016.

Banerjee, A., A.C. Maycock, and J.A. Pyle, Chemical and climatic drivers of radiative forcing due to changes in stratospheric and tropospheric ozone over the 21st century, *Atmos. Chem. Phys.*, *18*, 2899–2911, doi:10.5194/acp-2017-741, 2018.

Barton, C.A., and J.P. McCormack, Origin of the 2016 QBO disruption and its relationship to extreme El Niño events, *Geophys. Res. Lett.*, *44*, 11,150–11,157, doi:10.1002/2017GL075576, 2017.

Bednarz, E.M., A.C. Maycock, N.L. Abraham, P. Braesicke, O. Dessens, and J.A. Pyle, Future Arctic ozone recovery: The importance of chemistry and dynamics, *Atmos. Chem. Phys.*, *16*, 12159–12176, doi:10.5194/acp-16-12159-2016, 2016.

Behrens, E., G. Rickard, O. Morgenstern, T. Martin, A. Osprey, and M. Joshi, Southern Ocean deep convection in global climate models: A driver for variability of subpolar gyres and Drake Passage transport on decadal timescales, *J. Geophys. Res. Oceans*, 121, 3905–3925, doi:10.1002/2015JC011286, 2016.

Betts, R.A., C.D. Jones, J.R. Knight, R.F. Keeling, and J.J. Kennedy, El Niño and a record CO_2 rise, *Nat. Clim. Change*, *6*, 806–810, doi:10.1038/nclimate3063, 2016.

Bintanja, R., G.J. van Oldenborgh, S.S. Drijfhout, B. Wouters, and C.A. Katsman, Important role for ocean warming and increased ice-shelf melt in Antarctic sea ice expansion, *Nat. Geosci.*, *6*, 376–379, doi:10.1038/ngeo1767, 2013.

Birner, T., and H. Bönisch, Residual circulation trajectories and transit times into the extratropical lowermost stratosphere, *Atmos. Chem. Phys.*, *11*, 817–827, doi:10.5194/acp-11-817-2011, 2011.

Black, R.X., and B.A. McDaniel, The dynamics of Northern Hemisphere stratospheric finalwarming events, *J. Atmos. Sci.*, *64*, 2932-2946, doi:10.1175/JAS3981.1, 2007.

Blunden, J., and D.S. Arndt, editors, State of the Climate in 2016, *Bull. Am. Meteorol. Soc.*, *98* (8), Si–S277, doi:10.1175/2017BAMSStateoftheClimate.1, 2017.

Bohlinger, P., B.-M. Sinnhuber, R. Ruhnke, and O. Kirner, Radiative and dynamical contributions to past and future Arctic stratospheric temperature trends, *Atmos. Chem. Phys.*, *14*, 1679–1688, doi:10.5194/acp-14-1679-2014, 2014.

Boisier, J.P., R. Rondanelli, R.D. Garreaud, and F. Muñoz, Anthropogenic and natural contributions to the Southeast Pacific precipitation decline and recent megadrought in central Chile, *Geophys. Res. Lett., 43*, 413–421, doi:10.1002/2015GL067265, 2016.

Boothe, A.C., and C.R. Homeyer, Global large-scale stratosphere–troposphere exchange in modern reanalyses, *Atmos. Chem. Phys.*, *17*, 5537–5559, doi:10.5194/acp-17-5537-2017, 2017.

Bracegirdle, T.J., P. Hyder, and C.R. Holmes, CMIP5 diversity in southern westerly jet projections related to historical sea ice area: Strong link to strengthening and weak link to shift, *J. Clim.*, *31*, 195–211, doi:10.1175/JCLI-D-17-0320.1, 2018.

Brewer, A.W., Condensation Trails, *Weather*, *1*, 34–40, doi:10.1002/j.1477-8696.1946.tb00024.x, 1946.

Brinkop, S., M. Dameris, P. Jöckel, H. Garny, S. Lossow, and G. Stiller, The millennium water vapour drop in chemistry–climate model simulations, *Atmos. Chem. Phys.*, *16*, 8125–8140, doi:10.5194/

acp-16-8125-2016, 2016.

Brönnimann, S., M. Jacques-Coper, E. Rozanov, A.M. Fischer, O. Morgenstern, G. Zeng, H. Akiyoshi, and Y. Yamashita, Tropical circulation and precipitation response to ozone depletion and recovery, *Environ. Res. Lett.*, *12* (6), doi:10.1088/1748-9326/aa7416, 2017.

Butchart, N., The Brewer-Dobson circulation, *Rev. Geophys., 52*, 157–184, doi:10.1002/2013RG000448, 2014.

Byrne, N.J., T.G. Shepherd, T. Woollings, and R.A. Plumb, Nonstationarity in Southern Hemisphere Climate Variability Associated with the Seasonal Breakdown of the Stratospheric Polar Vortex. *J. Clim.,* 30, 7125–7139, doi:10.1175/JCLI-D-17-0097.1, 2017.

Calvo, N., L.M. Polvani, and S. Solomon, On the surface impact of Arctic stratospheric ozone extremes. *Environ. Res. Lett.*, *10*, 094003, doi:10.1088/1748-9326/10/9/094003, 2015.

Ceppi, P., Y.-T. Hwang, D.M.W. Frierson, and D.L. Hartmann, Southern Hemisphere jet latitude biases in CMIP5 models linked to shortwave cloud forcing, *Geophys. Res. Lett., 39*, L19708, doi:10.1029/2012GL053115, 2012.

Ceppi, P., and D.L. Hartmann, On the speed of the eddy-driven jet and the width of the Hadley cell in the Southern Hemisphere, *J. Clim.*, *26* (10), 3450–3465, doi:10.1175/JCLI-D-12-00414.1, 2013.

Cheung, J.C.H., J.D. Haigh, and D.R. Jackson, Impact of EOS MLS ozone data on medium-extended range ensemble weather forecasts, *J. Geophys. Res. Atmos.*, *119*, 9253–9266, doi:10.1002/2014JD021823, 2014.

Chiodo, G., L.M. Polvani, and M. Previdi, Large increase in incident shortwave radiation due to the ozone hole offset by high climatological albedo over Antarctica, *J. Clim.*, *30*, 4883–4890, doi:10.1175/JCLI-D-16-0842.1, 2017.

Choi, J., S.-W. Son, J. Lu, and S.-K. Min, Further observational evidence of Hadley cell widening in the Southern Hemisphere, *Geophys. Res. Lett.*, *41*, 2590–2597, doi:10.1002/2014GL059426, 2014.

Christy, J.R., R.W. Spencer, W.B. Norris, and W.D. Braswell, Error estimates of version 5.0 of MSU-AMSU bulk atmospheric temperature, *J. Atmospheric Ocean. Technol.*, *20* (5), 613–629, doi:10.1175/1520-0426, 2003.

Clem, K.R., J.A. Renwick, and J. McGregor, Relationship between eastern tropical Pacific cooling and recent trends in the Southern Hemisphere zonal-mean circulation, *Clim. Dyn.*, *49,* 113–129, doi:10.1007/s00382-016-3329-7, 2016.

Cohen, N.Y., E.P. Gerber, and O. Bühler, What Drives the Brewer–Dobson Circulation?, *J. Atmos. Sci.*, *71*, 3837–3855, doi:10.1175/JAS-D-14-0021.1, 2014.

Collins, W.J., R.G. Derwent, B. Garnier, C.E. Johnson, M.G. Sanderson, and D.S. Stevenson, Effect of stratosphere-troposphere exchange on the future tropospheric ozone trend, *J. Geophys. Res.*, *108*, 8528–8537, doi:10.1029/2002JD002617, 2003.

Coy, L., P.A. Newman, S. Pawson, and L.R. Lait, Dynamics of the disrupted 2015/16 quasi-biennial oscillation, *J. Clim.*, *30*, 5661–5674, doi:10.1175/JCLI-D-16-0663.1, 2017.

Crook, J.A., N.P. Gillett, and S.P. Keeley, Sensitivity of Southern Hemisphere climate to zonal asymmetry in ozone, *Geophys. Res. Lett.*, *35* (7), doi:10.1029/2007GL032698, 2008.

Dätwyler, C., R. Neukom, N.J. Abram, A.E. Gallant, M. Grosjean, M. Jacques-Coper, D.J. Karoly, and R. Villalba, Teleconnection stationarity, variability and trends of the Southern Annular Mode (SAM) during the last millennium, *Clim. Dyn.*, *51* (5/6), 2321–2339, doi:10.1007/s00382-017-4015-0, 2017.

Davis, N., and T. Birner, On the discrepancies in tropical belt expansion between reanalyses and climate models and among tropical belt width metrics, *J. Clim.*, *30*, 1211–1231, doi:10.1175/JCLI-D-16-0371.1, 2017.

Delworth, T.L., and F. Zeng, Regional rainfall decline in Australia attributed to anthropogenic greenhouse gases and ozone levels, *Nat. Geosci.*, *7*, 583–587, doi:10.1038/ngeo2201, 2014.

Dennison, F.W., A.J. McDonald, and O. Morgenstern, The effect of ozone depletion on the Southern Annular Mode and stratosphere-troposphere couplin, *J. Geophys. Res. Atmos.*, 120 (13), 6305–6312, doi:10.1002/2014JD023009, 2015.

Dennison, F.W., A.J. McDonald, and O. Morgenstern, The influence of ozone forcing on blocking in the Southern Hemisphere, *J. Geophys. Res. Atmos.*, *121* (24), 14,358–14,371, doi:10.1002/2016JD025033, 2016.

Dennison, F., A. McDonald, and O. Morgenstern, The evolution of zonally asymmetric austral ozone in a chemistry–climate model, *Atmos. Chem.*

Phys., *17* (22), 14075–14084, doi:10.5194/acp-17-14075-2017, 2017.

Dessler, A.E., H. Ye, T. Wang, M.R. Schoeberl, L.D. Oman, A.R. Douglass, A.H. Butler, K.H. Rosenlof, S.M Davis, and R.W. Portmann, Transport of ice into the stratosphere and the humidification of the stratosphere over the 21st century, *Geophys. Res. Lett.*, *45*, 2323–2329, doi:10.1002/2016GL06799, 2016.

Diallo, M., B. Legras, and A. Chédin, Age of stratospheric air in the ERA-Interim, *Atmos. Chem. Phys., 12*, 12133–12154, doi:10.5194/acp-12-12133-2012, 2012.

Díaz, L.B., and C.S. Vera, Austral summer precipitation interannual variability and trends over Southeastern South America in CMIP5 models, *Int. J. Climatol.*, *35* (10), 3172–3177, doi:10.1002/joc.4153, 2017.

Dietmüller, S., M. Ponater, and R. Sausen, Interactive ozone induces a negative feedback in CO_2-driven climate change simulations, *J. Geophys. Res. Atmos.*, *119*, 1796–1805, doi:10.1002/2013JD020575, 2014.

Dietmüller, S., H. Garny, F. Plöger, P. Jöckel, and D. Cai, Effects of mixing on resolved and unresolved scales on stratospheric age of air, *Atmos. Chem. Phys.*, *17*, 7703–7719, doi:10.5194/acp-17-7703-2017, 2017.

Ding, Q., and Q. Fu, A warming tropical central Pacific dries the lower stratosphere, *Clim. Dyn.*, 1–15, doi:10.1007/s00382-017-3774-y, 2017.

Dlugokencky, E.J., L.P. Steele, P.M. Lang, and K.A. Masarie, The growth rate and distribution of atmospheric methane, *J. Geophys. Res., 99*, 17,021–17,043, doi:10.1029/94JD01245, 1994.

Doddridge, E.W., & J. Marshall, Modulation of the seasonal cycle of Antarctic sea ice extent related to the Southern Annular Mode. *Geophy. Res. Lett.*, *44*, 9761–9768, doi:10.1002/2017GL074319, 2017.

Douglass, A.R., R.S. Stolarski, S.E. Strahan, and L.D. Oman, Understanding differences in upper stratospheric ozone response to changes in chlorine and temperature as computed using CCMVal-2 models, *J. Geophys. Res.*, *117*, D16306, doi:10.1029/2012JD017483, 2012.

Engel, A., T. Möbius, H. Bönisch, U. Schmidt, R. Heinz, I. Levin, E. Atlas, S. Aoki, T. Nakazawa, S. Sugawara, F. Moore, D. Hurst, J. Elkins, S. Schauffler, A. Andrews, and K. Berine, Age of stratospheric air unchanged within uncertainties over the past 30 years, *Nat. Geosci.*, *2*, 28–31, doi:10.1038/GEO388, 2009.

Engel, A., H. Bönisch, M. Ullrich, R. Sitals, O. Membrive, F. Danis, and C. Crevoisier, Mean age of stratospheric air derived from AirCore observations, *Atmos. Chem. Phys.*, *17*, 6825–6838, doi:10.5194/acp-17-6825-2017, 2017.

England, M.R., L.M. Polvani, K.L. Smith, L. Landrum, and M.M. Holland, Robust response of the Amundsen Sea Low to stratospheric ozone depletion, *Geophys. Res. Lett.*, *43*, 8207–8213, doi:10.1002/2016GL070055, 2016.

Eyring, V., J.M. Arblaster, I. Cionni, J. Sedlacek, J. Perlwitz, P.J. Young, S. Bekki, D. Bergmann, P. Cameron-Smith, W. Collins, G. Faluvegi, K.-D. Gottschaldt, L. Horowitz, D. Kinnison, J.-F. Lamarque, D.R. Marsh, D. Saint-Martin, D. Shindell, K. Sudo, S. Szopa, and S. Watanabe, Long-term changes in tropospheric and stratospheric ozone and associated climate impacts in CMIP5 simulations, *J. Geophys. Res.*, *118* , 5029–5060, doi:10.1002/jgrd.50316, 2013.

Fan, T., C. Deser, and D. Schneider, Recent sea ice trend in the context of Southern Ocean surface climate variations since 1950, *Geophys. Res. Lett., 41*, 2419–2426, doi:10.1002/2014GL059239, 2014.

Ferraro, A.J., M. Collins, and F.H. Lambert, A hiatus in the stratosphere, *Nat. Clim. Change.*, *5*, 497–498, doi:10.1038/nclimate2624, 2015.

Ferreira, D., J. Marshall, C.M. Bitz, S. Solomon, and A. Plumb, Antarctic ocean and sea ice response to ozone depletion: A two-time-scale problem, *J. Clim.*, *28*, 1206–1226, doi:10.1175/JCLI-D-14-00313.1, 2015.

Fogt, R.L., C.A. Goergens, J.M. Jones, D.P. Schneider, J.P. Nicolas, D.H. Bromwich, and H.E. Dusselier, A twentieth century perspective on summer Antarctic pressure change and variability and contributions from tropical SSTs and ozone depletion, *Geophys. Res. Lett.*, *44*, 9918–9927, doi:10.1002/2017GL075079, 2017.

Franzke, C.L.E., T.J. O'Kane, D.P. Monselesan, J.S. Risbey, and I. Horenko, Systematic attribution of observed southern hemispheric circulation trends to external forcing and internal variability, *Nonlin. Process. Geophys. 22*, 513–525, doi:10.5194/npg-22-513-2015, 2015.

Frölicher, T.L., J.L. Sarmiento, D.J. Paynter, J.P. Dunne, J.P. Krasting, and M. Winton, Dominance of the

Southern Ocean in anthropogenic carbon and heat uptake in CMIP5 models, *J. Clim.*, *28*, 862–886, doi:10.1175/JCLI-D-14-00117.1, 2015.

Fu, Q., S. Solomon, and P. Lin, On the seasonal dependence of tropical lower-stratospheric temperature trends, *Atmos. Chem. Phys.*, *10*, 2643–2653, doi:10.5194/acp-10-2643-2010, 2010.

Fu, Q., P. Lin, S. Solomon, and D.L. Hartmann, Observational evidence of strengthening of the Brewer-Dobson circulation since 1980, *J. Geophys. Res. Atmos.*, *120*, 10,214–10,228, doi:10.1002/2015JD023657, 2015.

Fueglistaler S., M. Abalos, T.J. Flannaghan, P. Lin, W.J. Randel, Variability and trends in dynamical forcing of tropical lower stratospheric temperatures, *Atmos. Chem. Phys., 14*, 13439–13453, doi:10.5194/acp-14-13439-2014, 2014.

Fyfe, J.C., N.P. Gillett, and G.J. Marshall, Human influence on extratropical Southern Hemisphere summer precipitation, *Geophys. Res. Lett.*, *39*, L23711, doi:10.1029/2012GL054199, 2012.

Gagné, M.-È., N.P. Gillett, and J.C. Fyfe, Observed and simulated changes in Antarctic sea ice extent over the past 50 years, *Geophys. Res. Lett.*, *42*, 90–95, doi:10.1002/2014GL062231, 2015.

Garcia, R.R., W.J. Randel, and D.E. Kinnison, On the determination of age of air trends from atmospheric trace species, *J. Atmos. Sci.*, 68, 139–154, doi:10.1175/2010JAS3527, 2011.

Garcia, R.R., D.E. Kinnison, and D.R. Marsh, "World avoided" simulations with the whole atmosphere community climate dodel, *J. Geophys. Res., 117*, D23303, doi:10.1029/2012JD018430, 2012.

Garcia, R.R., A.K. Smith, D.E. Kinnison, Á.D.L. Cámara, and D.J. Murphy, Modification of the gravity wave parameterization in the whole atmosphere community climate model: Motivation and results, *J. Atmos. Sci.*, *74* (1), 275–291, doi:10.1175/JAS-D-16-0104.1, 2017.

Garfinkel, C.I., D.W. Waugh, and E.P. Gerber, The effect of tropospheric jet latitude on coupling between the stratospheric polar vortex and the troposphere, *J. Clim.*, *26* (6), 2077–2095, doi:10.1175/JCLI-D-12-00301.1, 2013.

Garfinkel, C.I., and D.W. Waugh, Tropospheric Rossby wave breaking and variability of the latitude of the eddy-driven jet, *J. Clim.*, *27* (18), 7069–7085, doi:10.1175/JCLI-D-14-00081.1, 2014.

Garfinkel, C.I., M. Hurwitz, and L.D. Oman, Effect of recent sea surface temperature trends on the Arctic stratospheric vortex, *J. Geophys. Res. Atmos.*, *120*, 5404–5416, doi:10.1002/2015JD023284, 2015a.

Garfinkel, C.I., D.W. Waugh, and L.M. Polvani, Recent Hadley cell expansion: the role of internal atmospheric variability in reconciling modeled and observed trend, *Geophys. Lett., Res.*, *42,* doi:10.1002/2015GL066942, 2015b.

Garfinkel C.I., V. Aquila, D.W. Waugh, and L.D. Oman, Time-varying changes in the simulated structure of the Brewer–Dobson Circulation, *Atmos. Chem. Phys.*, *17*, 1313–1327, doi:10.5194/acp-17-1313-2017, 2017a.

Garfinkel, C.I., S.W. Son, K. Song, V. Aquila, and L.D. Oman, Stratospheric variability contributed to and sustained the recent hiatus in Eurasian winter warming, *Geophys. Res. Lett.*, *44*, doi:10.1002/2016GL072035, 2017b.

Garfinkel, C.I., Might stratospheric variability lead to improved predictability of ENSO events?, *Environ. Res. Lett.*, *12* (3), doi:10.1088/1748-9326/aa60a4, 2017.

Garfinkel, C.I., and L.D. Oman, Effect of gravity waves from small islands in the Southern Ocean on the Southern Hemisphere atmospheric circulation, *J. Geophys. Res. Atmos.*, *122*, doi:10.1002/2017JD027576, 2018.

Garfinkel, C.I., A. Gordon, L.D. Oman, F. Li, S. Davis, and S. Pawson, Nonlinear response of tropical lower stratospheric temperature and water vapor to ENSO, *Atmos. Chem. Phys.*, *18* 4597–4615, doi:10.5194/acp-2017-520, 2018.

Garny, H., T. Birner, H. Bönisch, and F. Bunzel, The effects of mixing on age of air, *J. Geophys. Res. Atmos.*, *119*, 7015–7034, doi:10.1002/2013JD021417, 2014.

Geller, M.A., M.J. Alexander, P.T. Love, J. Bacmeister, M. Ern, A. Hertzog, E. Manzini, P. Preusse, K. Sato, A.A. Scaife, and T. Zhou, A Comparison between gravity wave momentum fluxes in observations and climate models, *J. Clim.*, *26*, 6383–6405, doi:10.1175/JCLI-D-12-00545.1, 2013.

Gillett, N.P., J.C. Fyfe, and D.E. Parker, Attribution of observed sea level pressure trends to greenhouse gas, aerosol, and ozone changes, *Geophys. Res. Lett.*, *40* (10), 2302–2306, doi:10.1002/grl.50500, 2013, 2013.

Gonzalez, P., L.M. Polvani, R. Seager, and G. Correa, Stratospheric ozone depletion: A key driver

of recent precipitation trends in south eastern South America, *Clim. Dyn.*, *42* (7/8), 1775–1792, doi:10.1007/s00382-013-1777-x, 2014.

Good, S.A., M.J. Martin, and N.A. Rayner, EN4: Quality controlled ocean temperature and salinity profiles and monthly objective analyses with uncertainty estimates, *J. Geophys. Res. Ocean.*, *118*, 6704–6716, doi:10.1002/2013JC009067, 2013.

Goodberlet, M.A., C.T. Swift, and J.C. Wilkerson, Remote sensing of ocean surface winds with the Special Sensor Microwave/Imager, *J. Geophys. Res. Ocean.*, *94* (C10), 14547–14555, doi:10.1029/JC094iC10p14547, 1989.

Gray, L.J., J. Beer, M. Geller, J.D. Haigh, M. Lockwood, K. Matthes, U. Cubasch, D. Fleitmann, G. Harrison, L. Hood, J. Luterbacher, G.A. Meehl, D. Shindell, B. van Geel, and W. White, Solar influences on climate, *Rev. Geophys.*, *48* (4), doi:10.1029/2009RG000282, 2010.

Haenel, F.J., G.P. Stiller, T. Clarmann, B. Funke, E. Eckert, N. Glatthor, U. Grabowski, S. Kellmann, M. Kiefer, A. Linden, and T. Reddmann, Reassessment of MIPAS age of air trends and variability, *Atmos. Chem. Phys.*, *15*, 13161–13176, doi:10.5194/acp-15-13161-2015, 2015.

Haigh, J.D., The Sun and the Earth's climate, *Living Rev. Solar Phys.*, *4* (2), doi:10.12942/lrsp-2007-2, 2007.

Haimberger, L., C. Tavolato, and S. Sperka, Homogenization of the global radiosonde temperature dataset through combined comparison with reanalysis background series and neighboring stations, *J. Clim.*, *25*, 8108–8131, doi:10.1175/JCLI-D-11-00668.1, 2012.

Hall, T.M., and R.A. Plumb, Age as a diagnostic of stratospheric transport, *J. Geophys. Res.*, *99* (D1), 1059–1070, doi:10.1029/93JD03192, 1994.

Hardiman, S.C., N. Butchart, A.J. Charlton-Perez, T.A. Shaw, H. Akiyoshi, A. Baumgaertner, S. Bekki, P. Braesicke, M. Chipperfield, M. Dameris, R.R. Garcia, M. Michou, S. Pawson, E. Rozanov, and K. Shibata, Improved predictability of the troposphere using stratospheric final warmings, *J. Geophys. Res. Atmos.*, *116* (D18), doi:10.1029/2011JD015914, 2011.

Hardiman, S.C., N. Butchart, and N. Calvo, The morphology of the Brewer-Dobson circulation and its response to climate change in CMIP5 simulations, *Q. J. R. Meteorol. Soc.*, *140* (683), 1958–1965, doi:10.1002/qj.2258, 2014.

Hardiman, S.C., P. Lin, A.A. Scaife, N.J. Dunstone, and H.-L. Ren, The influence of dynamical variability on the observed Brewer-Dobson circulation trend, *Geophys. Res. Lett.*, *44*, 2885–2892, doi:10.1002/2017GL072706, 2017.

Hartley, D.E., J.T. Villarin, R.X. Black, and C.A. Davis, A new perspective on the dynamical link between the stratosphere and troposphere, *Nature*, *39,* 471–474, doi:10.1038/35112, 1998.

Hathaway, D.H., The Solar Cycle, *Living Rev. Solar Phys.*, *12* (4), doi:10.1007/lrsp-2015-4, 2015.

Haumann, F.A., D. Notz, and H. Schmidt, Anthropogenic influence on recent circulation-driven Antarctic sea ice changes, *Geophys. Res. Lett.*, *41*, 8429–8437, doi:10.1002/2014GL061659, 2014.

Haumann, F.A., N. Gruber, M. Münnich, I. Frenger, and S. Kern, Sea-ice transport driving Southern Ocean salinity and its recent trends, *Nature*, *537*, 89–92, doi:10.1038/nature1910, 2016.

Hegglin, M.I., and T.G. Shepherd, Large climate-induced changes in ultraviolet index and stratosphere-to-troposphere ozone flux, *Nat. Geosci.*, *2*, 687–691, doi:10.1038/ngeo604, 2009.

Hegglin, M.I., D.A. Plummer, and T.G. Shepherd, Vertical structure of stratospheric water vapour trends derived from merged satellite data, *Nat. Geosci.*, *7*, 768–776, doi:10.1038/ngeo2236, 2014.

Hendon, H.H., E.-P. Lim, and H. Nguyen, Seasonal variations of subtropical precipitation associated with the southern annular mode, *J. Clim.*, *27*, 3446–3460, doi:10.1175/JCLI-D-13-00550.1, 2014.

Hess, P., D. Kinnison, and Q. Tang, Ensemble simulations of the role of the stratosphere in the attribution of northern extratropical tropospheric ozone variability, *Atmos. Chem. Phys.*, *15*, 2341–2365, doi:10.5194/acp-15-2341-2015, 2015.

Hirota, N., H. Shiogama, H. Akiyoshi, T. Ogura, M. Takahashi, Y. Kawatani, M. Kimoto, and M. Mori, The influences of El Niño and Arctic sea-ice on the QBO disruption in February 2016, *npj Clim. and Atmos. Sci.*, *1* (10), doi:10.1038/s41612-018-0020-1, 2018.

Hobbs, W.R., N.L. Bindoff, and M.N. Raphael, New perspectives on observed and simulated Antarctic sea ice extent trends using optimal fingerprinting techniques, *J. Clim.*, *28*, 1543–1560, doi:10.1175/JCLI-D-14-00367.1, 2015.

Hobbs, W.R., R. Massom, S. Stammerjohn, P. Reid, G. Williams, and W. Meier, A review of recent changes in Southern Ocean sea ice, their drivers and forcings, *Glob. Planet. Chang.*, *143*, 228–250, doi:10.1016/j.gloplacha.2016.06.008, 2016.

Holland, M.M., L. Landrum, Y. Kostov, and J. Marshall, Sensitivity of Antarctic sea ice to the Southern Annular Mode in coupled climate models, *Clim. Dyn.*, *49* (5/6), doi:10.1007/s00382-016-3162-z., 2016.

Hossaini, R., M.P. Chipperfield, S.A. Montzka, A. Rap, S. Dhomse, and W. Feng, Efficiency of short-lived halogens at influencing climate through depletion of stratospheric ozone, *Nat. Geosci.*, *8*, 186–190, doi:10.1038/ngeo2363, 2015.

Hsu, J., and M.J. Prather, Is the residual vertical velocity a good proxy for stratosphere-troposphere exchange of ozone?, *Geophys. Res. Lett.*, *41*, 9024–9032, doi:10.1002/2014GL061994, 2014.

Hurst, D.F., S.J. Oltmans, H. Vömel, K.H. Rosenlof, S.M. Davis, E.A. Ray, E.G. Hall, and A.F. Jordan, Stratospheric water vapor trends over Boulder, Colorado: Analysis of the 30-year Boulder record, *J. Geophys. Res.*, *116*, D02306, doi:10.1029/2010JD015065, 2011.

Hurst, D.F., A. Lambert, W.G. Read, S.M. Davis, K.H. Rosenlof, E.G. Hall, A.F. Jordan, and S.J. Oltmans, Validation of Aura Microwave Limb Sounder stratospheric water vapor measurements by the NOAA frost point hygrometer, *J. Geophys. Res.*, *119*, 1612–1625, doi:10.1002/2013JD020757, 2014.

Hurst, D.F., W.G. Read, H. Vömel, H.B. Selkirk, K.H. Rosenlof, S.M. Davis, E.G. Hall, A. Jordan, S.J. Oltmans, Recent divergences in stratospheric water vapor measurements by frost point hygrometers and the Aura Microwave Limb Sounder, *Atmos. Meas. Tech.*, *9*, 447–4457, doi:10.5194/amt-2016-157, 2016.

Hurwitz, M.M., E.C. Fleming, P.A. Newman, F. Li, E. Mlawer, K. Cady-Pereira, and R. Bailey, Ozone depletion by hydrofluorocarbons, *Geophys. Res. Lett.*, *42*, 8686–8692, doi:10.1002/2015GL065856, 2015.

Hurwitz, M.M., E.L. Fleming, P.A. Newman, F. Li, and Q. Liang, Early action on HFCs,mitigates future atmospheric change, *Environ. Res. Lett.*, *11*, 114019, doi:10.1088/1748-9326/11/11/114019, 2016.

Iglesias-Suarez, F., P.J. Young, and O. Wild, Stratospheric ozone change and related climate impacts over 1850–2100 as modelled by the ACCMIP ensemble, *Atmos. Chem. Phys.*, *16* (1), 343–363, doi:10.5194/acp-16-343-2016, 2016.

Iglesias-Suarez, F., D.E. Kinnison, A. Rap, O. Wild, and P.J. Young, Key drivers of ozone change and its radiative forcing over the 21st century, *Atmos. Chem. Phys.*, *18* (9), 6121–6139, doi:10.5194/acp-2017-939, 2018.

IPCC (Intergovernmental Panel on Climate Change), *Climate Change 2013: The Physical Science Basis. Contribution of Working Group I to the Fifth Assessment Report of the Intergovernmental Panel on Climate Change*, edited by T.F. Stocker, D. Qin, G.-K. Plattner, M. Tignor, S.K. Allen, J. Boschung, A. Nauels, Y. Xia, V. Bex, and P.M. Midgley, 1535 pp., Cambridge University Press, Cambridge, United Kingdom, 2013.

Ivy, D.J., S. Solomon, and H.E. Rieder, Radiative and dynamical influences on polar stratospheric temperature trends, *J. Clim.*, doi:10.1175/JCLI-D-15-0503.1, 2016.

Ivy, D.J., C. Hilgenbrink, D. Kinnison, R.A. Plumb, A. Sheshadri, S. Solomon, and D.W.J. Thompson, Observed Changes in the southern hemispheric circulation in May, *J. Clim.*, *30* (2), 527–536, doi:10.1175/JCLI-D-16-0394.1, 2017a.

Ivy, D.J., S. Solomon, N. Calvo, and D.W.J. Thompson, Observed connections of Arctic stratospheric ozone extremes to Northern Hemisphere surface climate, *Environ. Res. Lett.*, *12* (2), 024004, doi:10.1088/1748-9326/aa57a4/, 2017b.

Jones, J.M., S.T. Gille, H. Goosse, N.J. Abram, P.O. Canziani, D.J. Charman, K.R. Clem, X. Crosta, C. de Lavergne, I. Eisenman, M.H. England, R.L. Fogt, L.M. Frankcombe, G.J. Marshall, V. Masson-Delmotte, A.K. Morrrison, A.J. Orsi, M.N. Raphael, J.A. Renwick, D.P. Schneider, G.R. Simpkins, E.R. Steig, B. Stenni, D. Swingedouw, and T.R. Vance, Assessing recent trends in high-latitude Southern Hemisphere surface climate, *Nat. Clim. Change*, *6*, 917–926, doi:10.1038/nclimate3103, 2016.

Kang, S.M., and L.M. Polvani, The interannual relationship between the latitude of the eddy-driven jet and the edge of the Hadley cell, *J. Clim.*, *24* (2), 563–568, doi:10.1175/JCLI-D-12-00414.1, 2011.

Karoly, D.J., Climate change: Human-induced rainfall changes, *Nat. Geosci.*, *7*, 551–552, doi:10.1038/ngeo2207, 2014.

Karpechko, A.Yu., J. Perlwitz, and E. Manzini. A model study of tropospheric impacts of the Arctic ozone depletion 2011, *J. Geophys. Res. Atmos.*, *119* (13),

7999–8014, doi:10.1002/2013JD021350, 2014.

Karpechko, A.Yu., and E. Manzini, Arctic stratosphere dynamical response to global warming, *J. Clim.*, *30* (17), 7071–7086, doi:10.1175/JCLI-D-16-0781.1, 2017.

Kawase, H., T. Nagashima, K. Sudo, and T. Nozawa, Future changes in tropospheric ozone under Representative Concentration Pathways (RCPs), *Geophys. Res. Lett.*, *38*, L05801, doi:10.1029/2010GL046402, 2011.

Kawatani, Y., and K. Hamilton, Weakened stratospheric quasibiennial oscillation driven by increased tropical mean upwelling, *Nature*, *497*, 478–481, doi:10.1038/nature12140, 2013.

Keeble, J., P. Braesicke, N.L. Abraham, H.K. Roscoe, and J.A. Pyle, The impact of polar stratospheric ozone loss on Southern Hemisphere stratospheric circulation and climate, *Atmos. Chem. Phys.*, *14*, 13705–13717, doi:10.5194/acp-14-13705-2014, 2014.

Keeley, S.P.E., N.P. Gillett, D.W.J. Thompson, S. Solomon, and P.M. Forster, Is Antarctic climate most sensitive to ozone depletion in the middle or lower stratosphere?, *Geophys. Res. Lett.*, *34*, L22812, doi:10.1029/2007GL031238, 2007.

Khatiwala, S., F. Primeau, and T. Hall, Reconstruction of the history of anthropogenic CO_2 concentrations in the ocean, *Nature*, *462*, 346–349, doi:10.1038/nature08526, 2009.

Khaykin, S.M., B.M. Funatsu, A. Hauchecorne, S. Godin-Beekmann, C. Claud, P. Keckhut, A. Pazmino, H. Gleisner, J.K. Nielsen, S. Syndergaard, and K.B. Lauritsen, Postmillennium changes in stratospheric temperature consistently resolved by GPS radio occultation and AMSU observations, *Geophys. Res. Lett.*, *44*, 7510–7518, doi:10.1002/2017GL074353, 2017.

Kim, B.M., S.-W. Son, S.-K. Min, J.-H. Jeong, S.-J. Kim, X. Zhang, T. Shim, and J.-H. Yoon, Weakening of the stratospheric polar vortex by Arctic sea-ice loss, *Nat. Commun., 5*, 4646, doi:10.1038/ncomms5646, 2014.

Kim, J., K.M. Grise, and S.-W. Son, Thermal characteristics of the cold-point tropopause region in CMIP5 models, *J. Geophys. Res. Atmos.*, *118*, 8827–8841, doi:10.1002/jgrd.50649, 2013.

Kim, J.-S., J.-S. Kug, J.-H. Yoon, and S.-J. Jeong, Increased atmospheric CO_2 growth rate during El Niño driven by reduced terrestrial productivity in the CMIP5 ESMs, *J. Clim.*, *29*, 8783–8805, doi:10.1175/JCLI-D-14-00672.1, 2016.

Kim, Y.-H., S.-K. Min, S.-W. Son, and J. Choi, Attribution of the local Hadley cell widening in the Southern Hemisphere, *Geophys. Res. Lett.*, *44*, 1015–1024, doi:10.1002/2016GL072353, 2017.

Klobas, J.E., D.M. Wilmouth, D.K. Weisenstein, J.G. Anderson, and R.J. Salawitch, Ozone depletion following future volcanic eruptions, *Geophys. Res. Lett.*, *44*, 7490–7499, doi: 10.1002/2017GL073972, 2017.

Konopka, P., F. Ploeger, M. Tao, and M. Riese, Zonally resolved impact of ENSO on the stratospheric circulation and water vapor entry values, *J. Geophys. Res. Atmos.*, *121* (19), 11,486–11,501, doi:10.1002/2015JD024698, 2016.

Kostov, Y., J. Marshall, U. Hausmann, K.C. Armour, D. Ferreira, and M.M. Holland, Fast and slow responses of Southern Ocean sea surface temperature to SAM in coupled climate models, *Clim. Dyn.*, 1–15, doi:10.1007/s00382-016-3162-z, 2016.

Kostov, Y., D. Ferreira, K.C. Armour, and J. Marshall, Contributions of greenhouse gas forcing and the southern annular mode to historical Southern Ocean surface temperature trends, *Geophys. Res. Lett.*, *45*, doi:10.1002/2017GL074964, 2018.

Kovács, T., W. Feng, A. Totterdill, J.M.C. Plane, S. Dhomse, J.C. Gómez-Martín, G.P. Stiller, F.J. Haenel, C. Smith, P.M. Forster, R.R. García, D.R. Marsh, and M.P. Chipperfield, Determination of the atmospheric lifetime and global warming potential of sulfur hexafluoride using a three-dimensional model, *Atmos. Chem. Phys.*, *17*, 883–898, doi:10.5194/acp-17-883-2017, 2017.

Kremser, S., L.W. Thomason, M. Hobe, M. Hermann, T. Deshler, C. Timmreck, M. Toohey, A. Stenke, J.P. Schwarz, R. Weigel, S. Fueglistaler, F.J. Prata, J.-P. Vernier, H. Schlager, J.E. Barnes, J.-C. Antuna-Marrero, D. Fairlie, M. Palm, E. Mahieu, J. Notholt, M. Rex, C. Bingen, F. Vanhellemont, A. Bourassa, J.M.C. Plane, D. Klocke, S.A. Carn, L.R. Neely, A.D. James, L. Rieger, J.C. Wilson, and B. Meland, Stratospheric aerosol - Observations, processes, and impact on climate, *Rev. Geophys.*, *54*, 278–335, doi:10.1002/2015RG000511, 2016.

Kretschmer, M., D. Coumou, L. Agel, M. Barlow, E. Tziperman, and J. Cohen, More-persistent weak stratospheric polar vortex states linked to cold extremes, *Bull. Am. Meteorol. Soc.*, *99*, 49–60, doi:10.1175/BAMS-D-16-0259.1, 2018.

Lamarque, J.F., L.K. Emmons, P.G. Hess, D.E. Kinnison, S. Tilmes, F. Vitt, and J.J. Orlando, CAM-chem: Description and evaluation of interactive atmospheric chemistry in the community Earth system model, *Geosci. Model Dev.*, *5* (2), 369–411, doi:10.5194/gmd-5-369-2012, 2012.

Landrum, L.L., M.M. Holland, M.N. Raphael, and L.M. Polvani, L., Stratospheric ozone depletion: An unlikely driver of the regional trends in Antarctic sea ice in austral fall in the late twentieth century, *Geophys. Res. Lett.*, *44*, 11,062–11,070, doi:10.1002/2017GL075618, 2017.

Landschützer, P., N. Gruber, F.A. Haumann, C. Rodenbeck, D.D. Bakker, N. Metzl, C. Sweeney, T. Takahasi, B. Tilbrook, and R. Wanninkhof, The reinvigoration of the Southern Ocean carbon sink, *Science, 349*, 1221–1224, doi:10.1126/science.aab2620, 2015.

Langematz, U., S. Meul, K. Grunow, E. Romanowsky, S. Oberländer, J. Abalichin, and A. Kubin, Future Arctic temperature and ozone: The role of stratospheric composition changes, *J. Geophys. Res. Atmos.*, *119*, 2092–2112, doi:10.1002/2013JD021100, 2014.

Lanzante, J.R., S.A. Klein, and D.J. Seidel, Temporal homogenization of monthly radiosonde temperature data, Part I: Methodology, *J. Clim.*, *16*, 224–240, doi:10.1175/1520-0442(2003)016<0224:THOMRT>2.0.CO;2, 2003.

Latif, M., T. Martin, and W. Park, Southern Ocean sector centennial climate variability and recent decadal trends, *J. Clim., 26*, 7767–7782, doi:10.1175/JCLI-D-12-00281.1, 2013.

Law, R.M., R.J. Matear, and R.J. Francey, Comment on "Saturation of the Southern Ocean CO_2 sink due to recent climate change", *Science*, *319* (5863), doi:10.1126/science.1149077, 2008.

Le Quéré, C., C. Rodenbeck, E.T. Buitenhuis, T.J. Conway, R. Langenfelds, A. Gomez, C. Labuschagne, M. Ramonet, T. Nakazawa, N. Metzl, N. Gillett, and M. Heimann, Saturation of the Southern Ocean CO_2 sink due to recent climate change, *Science*, *316*, 1735–1738, doi:10.1126/science.1136188, 2007.

Le Quéré, C., R.M. Andrew, P. Friedlingstein, S. Sitch, J. Pongratz, A.C. Manning, J.I. Korsbakken, G.P. Peters, J.G. Canadell, R.B. Jackson, T.A. Boden, P.P. Tans, O.D. Andrews, V.K. Arora, D.C.E. Bakker, L. Barbero, M. Becker, R.A. Betts, L. Bopp, F. Chevallier, L.P. Chini, P. Ciais, C.E. Cosca, J. Cross, K. Currie, T. Gasser, I. Harris, J. Hauck, V. Haverd, R.A. Houghton, C.W. Hunt, T. Ilyina, A.K. Jain, E. Kato, M. Kautz, R.F. Keeling, K. Klein Goldewijk, A. Körtzinger, P. Landschützer, N. Lefèvre, A. Lenton, S. Lienert, I. Lima, D. Lombardozzi, N. Metzl, F. Millero, P.M.S. Monteiro, D.R. Munro, J.E.M.S. Nabel, S.I. Nakaoka, Y. Nojiri, X.A. Padin, A. Peregon, B. Pfeil, D. Pierrot, B. Poulter, G. Rehder, J. Reimer, C. Rödenbeck, J. Schwinger, R. Séférian, I. Skjelvan, B.D. Stocker, H. Tian, B. Tilbrook, F.N. Tubiello, I.T. van der Laan-Luijkx, G.R. van der Werf, S. van Heuven, N. Viovy, N. Vuichard, A.P. Walker, A.J. Watson, A.J. Wiltshire, S. Zaehle, and D. Zhu, Global carbon budget 2017, *Earth Syst. Sci. Data, 10*, 405–448, doi:10.5194/essd-10-405-2018, 2018.

Lenton, A., B. Tilbrook, R.M. Law, D. Bakker, S.C. Doney, N. Gruber, M. Ishii, M. Hoppema, N.S. Lovenduski, R.J. Matear, B.I. McNeil, N. Metzl, S.E. Mikaloff Fletcher, P.M.S. Monteiro, C. Rödenbeck, C. Sweeney, and T. Takahashi, Sea-air CO_2 fluxes in the Southern Ocean for the period 1990–2009, *Biogeosci., 10*, 4037–4054, doi:10.5194/bg-10-4037-2013, 2013.

Li, F., J. Austin, and J. Wilson, The strength of the Brewer–Dobson Circulation in a changing climate: Coupled chemistry–climate model simulations, *J. Clim.*, *21*, 40–57, doi:10.1175/2007JCLI1663.1, 2008.

Li, F., D.W. Waugh, A.R. Douglass, P.A. Newman, S.E. Strahan, J. Ma, J.E. Nielsen, and Q. Liang, Long-term changes in stratospheric age spectra in the 21st century in the Goddard Earth Observing System Chemistry-Climate Model (GEOSCCM), *J. Geophys. Res.*, *117*, D20119, doi:10.1029/2012JD017905, 2012.

Li, F., P. Newman, S. Pawson, and J. Perlwitz, Effects of greenhouse gas increase and stratospheric ozone depletion on stratospheric mean age of air in 1960–2010, *J. Geophys. Res. Atmos.*, *123* (4), 2098–2110, doi:10.1002/2017JD027562, 2018.

Li, X., D.M. Holland, E.P. Gerber, and C. Yoo, Impacts of the north and tropical Atlantic Ocean on the Antarctic Peninsula and sea ice, *Nature*, *505*, 538–542, doi:10.1038/nature12945, 2014.

Lim, E.P., H.H. Hendon, J.M. Arblaster, F. Delage, H. Nguyen, S.K. Min, and M.C. Wheeler, The impact of the Southern Annular Mode on fu-

ture changes in Southern Hemisphere rainfall, *Geophys. Res. Lett.*, *43* (13), 7160–7167, doi:10.1002/2016GL069453, 2016.

Lin, M., A.M. Fiore, L.W. Horowitz, A.O. Langford, S.J. Oltmans, D. Tarasick, and H.E. Rieder, Climate variability modulates western U.S. ozone air quality in spring via deep stratospheric intrusions, *Nat. Commun.*, *6*, 7105, doi:10.1038/ncomms8105, 2015.

Lin, P., D. Paynter, L. Polvani, P. Correa, J. Gustavo, Y. Ming, and V. Ramaswamy, Dependence of model-simulated response to ozone depletion on stratospheric polar vortex climatology, *Geophys. Res. Lett.*, *17*, 14,593–14,629, doi:10.1002/2017GL073862, 2017.

Linz, M., R.A. Plumb, E.P. Gerber, and A. Sheshadri, The relationship between age of air and the diabatic circulation of the stratosphere, *J. Atmos. Sci.*, *73*, 4507–4518, doi:10.1175/JAS-D-16-0125.1, 2016.

Linz M., R.A. Plumb, E.P. Gerber, F.J. Haenel, G. Stiller, D.E. Kinnison, A. Ming, and J.L. Neu, The strength of the meridional overturning circulation of the stratosphere, *Nat. Geosci.*, *10*, 663–667, doi:10.1038/ngeo3013, 2017.

Long, C.S., M. Fujiwara, S. Davis, D.M. Mitchell, and C.J. Wright, Climatology and interannual variability of dynamic variables in multiple reanalyses evaluated by the SPARC Reanalysis Intercomparison Project (S-RIP), *Atmos. Chem. Phys.*, *17*, 14,593–14,629, doi:10.5194/acp-17-14593-2017, 2017.

Lucas, C., and H. Nguyen, Regional characteristics of tropical expansion and the role of climate variability, *J. Geophys. Res. Atmos.*, *120*, 6809–6824, doi:10.1002/2015JD023130, 2015.

Mahieu, E., M.P. Chipperfield, J. Notholt, T. Reddmann, J. Anderson, P.F. Bernath, T. Blumenstock, M.T. Coffey, S.S. Dhomse, W. Feng, B. Franco, L. Froidevaux, D.W.T. Griffith, J.W. Hannigan, F. Hase, R. Hossaini, N.B. Jones, I. Morino, I. Murata, H. Nakajima, M. Palm, C. Paton-Walsh, J.M. Russelll III, M. Schneider, C. Servais, D. Smale, and K.A. Walker, Recent Northern Hemisphere stratospheric HCl increase due to atmospheric circulation changes, *Nature*, *515*, 104–107, doi:10.1038/nature13857, 2014.

Manatsa, D., Y. Morioka, S.K. Behera, T. Yamagata, and C.H. Matarira, Link between Antarctic ozone depletion and summer warming over southern Africa, *Nat. Geosci.*, *6*, 934–939, doi:10.1038/ngeo1968, 2013.

Manatsa, D., Y. Morioka, S.K. Behera, T.D. Mushore, and R. Mugandani, Linking the southern annular mode to the diurnal temperature range shifts over southern Africa, *Int. J. Climatol.*, *35*, 4220–4236, doi:10.1002/joc.4281, 2015.

Manatsa, D., C. Mudavanhu, T.D. Mushore, and E. Mavhura, Linking major shifts in East Africa 'short rains' to the Southern Annular Mode, *Int. J. Climatol.*, *36*, 1590–1599, doi:10.1002/joc.4443, 2016.

Manney, G.L., and M.I. Hegglin, Seasonal and regional variations of long-term changes in upper-tropospheric jets from reanalyses, *J. Clim.*, *31* (1), 423–448, doi:10.1175/JCLI-D-17-0303.1, 2018.

Mantsis, D.F., S. Sherwood, R.J. Allen, and L. Shi, Natural variations of tropical width and recent trends, *Geophys. Res. Lett.*, *44*, 3825–3832, doi:10.1002/2016GL072097, 2017.

Manzini, E., A.Yu. Karpechoko, J. Anstey, M.P. Baldwin, R.X. Black, C. Cagnazzo, N. Calvo, A. Charlton-Perez, B. Christiansen, P. Davini, E. Gerber, M. Giorgetta, L. Gray, S.C. Hardiman, Y.-Y. Lee, D.R. March, B.A. McDaniel, A. Purich, A.A. Scaife, D. Shindell, S.-W. Son, S. Watanabe, and G. Zappa, Northern winter climate change: Assessment of uncertainty in CMIP5 projections related to stratosphere-troposphere coupling, *J. Geophys. Res. Atmos.*, *119*, 7979–7998, doi:10.1002/2013JD021403, 2014.

Manzini, E., A. Y., Karpechko, and L. Kornblueh, Nonlinear response of the stratosphere and the North Atlantic-European climate to global warming, *Geophys. Res. Lett.*, *45*, 4255–4263, doi:10.1029/2018GL077826, 2018.

Marsh, D.R., J.-F. Lamarque, A.J. Conley, and L.M. Polvani, Stratospheric ozone chemistry feedbacks are not critical for the determination of climate sensitivity in CESM1(WACCM), *Geophys. Res. Lett.*, *43*, 3928–3934, doi:10.1002/2016GL068344, 2016.

Marshall, G.J., Trends in the Southern Annular Mode from observations and reanalyses, *J. Clim.*, *16* (24), 4134–4143, doi: 10.1175/1520-0442(2003)016<4134:TITSAM>2.0.CO;2, 2003.

Marshall, G.J., and T. Bracegirdle, An examination of the relationship between the Southern Annular Mode and Antarctic surface air temperatures in the CMIP5 historical runs, *Clim. Dyn.*, *45* (5/6), 1513–1535, doi:10.1007/s00382-014-2406-z, 2014.

Marshall, J., K. Armour, J. Scott, Y. Kostov, U. Hausmann, D. Ferreira, T. Shepherd, T., and C. Bitz, The ocean's role in polar climate change: Asymmetric Arctic and Antarctic responses to greenhouse gas and ozone forcing, *Philos. Trans. Roy. Soc. A, 372*, doi:10.1098/rsta.2013.0040, 2014.

Masarie, K.A., and P.P. Tans, Extension and integration of atmospheric carbon dioxide data into a globally consistent measurement record, *J. Geopys. Res.*, *100*, 11,593–11,610, doi:10.1029/95JD00859, 1995.

Maycock, A.C., M.M. Joshi, K.P. Shine, S.M. Davis, and K.H. Rosenlof, The potential impact of changes in lower stratospheric water vapour on stratospheric temperatures over the past 30 years, *Q. J. R. Meteorol. Soc.*, *140*, 2176–2185, doi:10.1002/qj.2287, 2014.

Maycock, A.C., The contribution of ozone to future stratospheric temperature trends, *Geophys. Res. Lett.*, *43* (9), 4077–4658, doi:10.1002/2016GL068511, 2016.

Maycock, A.C., W.J. Randel, A.K. Steiner, A.Yu., Karpechko, J. Christy, R. Saunders, D.W.J. Thompson, C.-Z. Zou, A. Chrysanthou, N.L. Abraham, H. Akiyoshi, A.T. Archibald, N. Butchart, M. Chipperfield, M. Dameris, M. Deushi, S. Dhomse, G. Di Genova, P. Jöckel, D.E. Kinnison, O. Kirner, F. Ladstädter, M. Michou, O. Morgenstern, F. O'Connor, L. Oman, G. Pitari, D.A. Plummer, L.E. Revell, E. Rozanov, A. Stenke, D. Visioni, Y. Yamashita, and G. Zeng, Revisiting the mystery of recent stratospheric temperature trends, *Geophys. Res. Letts.*, *45*, 9919–9933, doi:10.1029/2018GL078035, 2018.

McLandress, C., A.I. Jonsson, D.A. Plummer, M.C. Reader, J.F. Scinocca, and T.G. Shepherd, Separating the dynamical effects of climate change and ozone depletion, Part I: Southern Hemisphere stratosphere, *J. Clim.*, *23*, 5002–5020, doi:10.1175/2010JCLI3586.1, 2010.

McLandress, C., T.G. Shepherd, J.F. Scinocca, D.A. Plummer, M. Sigmond, A.I. Jonsson, and M.C. Reader, Separating the dynamical effects of climate change and ozone depletion, Part II: Southern Hemisphere troposphere, J. Clim., 24, 1850–1868, doi:10.1175/2010JCLI3958.1, 2011.

McLandress, C., T.G. Shepherd, S. Polavarapu, and S.R. Beagley, Is missing orographic gravity wave drag near 60°S the cause of the stratospheric zonal wind biases in chemistry–climate models?, *J. Atmos. Sci.*, *69*, 802–818, doi:10.1175/JAS-D-11-0159.1, 2012.

McLandress, C., T.G. Shepherd, A.I. Jonsson, T. von Clarmann, and B. Funke, A method for merging nadir-sounding climate records, with an application to the global-mean stratospheric temperature data sets from SSU and AMSU, *Atmos. Chem. Phys., 15*, 9271–9284, doi:10.5194/acp-15-9271-2015, 2015.

Mears, C.A., F.J. Wentz, P. Thorne, and D. Bernie, Assessing uncertainty in estimates of atmospheric temperature changes from MSU and AMSU using a Monte-Carlo estimation technique, *J. Geophys. Res.*, *116*, D08112, doi:10.1029/2010JD014954, 2011.

Meehl, G.A., J.M. Arblaster, C.M. Bitz, C.T.Y. Chung, and H. Teng, Antarctic sea-ice expansion between 2000 and 2014 driven by tropical Pacific decadal climate variability, *Nat. Geosci., 9,* 590–595, doi:10.1038/ngeo2751, 2016.

Meier, W.N., D. Gallaher, and G.G. Campbell, New estimates of Arctic and Antarctic sea ice extent during September 1964 from recovered Nimbus I satellite imagery, *Cryosph.*, *7*, 699–705, doi:10.5194/tc-7-699-2013, 2013.

Meul, S., U. Langematz, P. Kröger, S. Oberländer-Hayn, and P. Jöckel, Future changes in the stratosphere-to-troposphere ozone mass flux and the contribution from climate change and ozone recovery, *Atmos. Chem. Phys.*, *18*, 7721–7738, doi:10.5194/acp-18-7721-2018, 2018.

Mills, M.J., A. Schmidt, R. Easter, S. Solomon, D.E. Kinnison, S.J. Ghan, R.R. Neely III, D.R. Marsh, A. Conley, C.G. Bardeen, and A. Gettelman, Global volcanic aerosol properties derived from emissions, 1990–2014, using CESM1(WACCM), *J. Geophys. Res. Atmos.*, *121*, 2332–2348, doi:10.1002/2015JD024290, 2016.

Ming, A., P. Hitchcock, and P. Haynes, The response of the lower stratosphere to zonally symmetric thermal and mechanical forcing, *J. Atmos. Sci., 73*, 1903–1922, doi:10.1175/JAS-D-15-0294.1, 2016.

Mitchell, D.M., Attributing the forced components of observed stratospheric temperature variability to external drivers, *Q. J. R. Meteorol. Soc.*, *142*, 1041–1047, doi:10.1002/qj.2707, 2016.

Miyazaki, K., T. Iwasaki, Y. Kawatani, C. Kobayashi, S. Sugawara, and M.I. Hegglin, Inter-comparison of stratospheric mean-meridional circulation and

eddy mixing among six reanalysis data sets, *Atmos. Chem. Phys.*, *16*, 6131–6152, doi:10.5194/acp-16-6131-2016, 2016.

Monahan, A.H., and J.C. Fyfe, On the nature of zonal jet EOFs, *J. Clim.*, *19*, 6409–6424, doi:10.1175/JCLI3960.1, 2006.

Morgenstern, O., G. Zeng, S.M. Dean, M. Joshi, N.L. Abraham, and A. Osprey, Direct and ozone-mediated forcing of the Southern Annular Mode by greenhouse gases, *Geophys. Res. Lett.*, *41* (24), 9050–9057, doi:10.1002/2014GL062140, 2014.

Morgenstern, O., M.I. Hegglin, E. Rozanov, F.M. O'Connor, N.L. Abraham, H. Akiyoshi, A.T. Archibald, S. Bekki, N. Butchart, M.P. Chipperfield, M. Deushi, S.S. Dhomse, R.R. Garcia, S.C. Hardiman, L.W. Horowitz, P. Jöckel, B. Josse, D. Kinnison, M. Lin, E. Mancini, M.E. Manyin, M. Marchand, V. Marécal, M. Michou, L.D. Oman, G. Pitari, D.A. Plummer, L.E. Revell, D. Saint-Martin, R. Schofield, A. Stenke, K. Stone, K. Sudo, T.Y. Tanaka, S. Tilmes, Y. Yamashita, K. Yoshida, and G. Zeng, Review of the global models used within Phase 1 of the Chemistry-Climate Model Initiative (CCMI), *Geosci. Model Dev.*, *10*, 639–671, doi:10.5194/gmd-10-639-2017, 2017.

Morgenstern, O., H. Akiyoshi, Y. Yamashita, D.E. Kinnison, R.R. Garcia, D.A. Plummer, J. Scinocca, G. Zeng, E. Rozanov, A. Stenke, L.E. Revell, G. Pitari, E. Mancini, E., G. Di Genova, S.S. Dhomse, and M.P. Chipperfield, Ozone sensitivity to varying greenhouse gases and ozone-depleting substances in CCMI-1 simulations, *Atmos. Chem. Phys.*, *18*, 1091–1114, doi:10.5194/acp-18-1091-2018, 2018.

Munro, D.R., N.S. Lovenduski, T. Takahashi, B.B. Stephens, T. Newberger, and C. Sweeney, Recent evidence for a strengthening CO_2 sink in the Southern Ocean from carbonate system measurements in the Drake Passage (2002–2015), *Geophys. Res. Lett.*, *42*, 7623–7630, doi:10.1002/2015GL065194, 2015.

Murphy, D.M., K.D. Froyd, J.P. Schwarz, and J.C. Wilson, Observations of the chemical composition of stratospheric aerosol particles, *Q. J. R. Meteorol. Soc.*, *140*, 1269–1278, doi:10.1002/qj.2213, 2014.

Muthers, S., J.G. Anet, A. Stenke, C.C. Raible, E. Rozanov, S. Brönnimann, T. Peter, F.X. Arfeuille, A.I. Shapiro, J. Beer, F. Steinhilber, Y. Brugnara, and W. Schmutz, The coupled atmosphere-chemistry-ocean model SOCOL-MPIOM, *Geosci. Model Dev.*, *7*, 2157–2179, doi:10.5194/gmd-7-2157-2014, 2014.

Muthers, S., A. Kuchar, A. Stenke, J. Schmitt, J.G. Anet, C.C. Raible, and T.F. Stocker, Stratospheric age of air variations between 1600 and 2100, *Geophys. Res. Lett.*, *43*, doi:10.1002/2016GL068734, 2016.

Myhre, G., D. Shindell, (Coordination and Lead Authors), F.-M. Bréon, W. Collins, J. Fuglestvedt, J. Huang, D. Koch, J.-F. Lamarque, D. Lee, B. Mendoza, T. Nakajima, A. Robock, G. Stephens, T. Takemura, and H. Zhang, Anthropogenic and natural radiative forcing, Chapter 8, in *Climate Change 2013: The Physical Science Basis. Contribution of Working Group I to the Fifth Assessment Report of the Intergovernmental Panel on Climate Change,* review editors D. Jacob, A.R. Ravishankara, and K. Shine, 659–740, Cambridge University Press, Cambridge, United Kingdom, doi:10.1017/ CBO9781107415324.018, 2013.

Naik, V., L.W. Horowitz, M.D. Schwarzkopf, and M. Lin, Impact of volcanic aerosols on stratospheric ozone recovery, *J. Geophys. Res. Atmos.*, *122*, 9515–9528, doi:10.1002/2016JD025808, 2017.

Naoe, H., M. Deushi, K. Yoshida, and K. Shibata, Future changes in the ozone quasi-biennial oscillation with increasing GHGs and ozone recovery in CCMI simulations, *J. Clim.*, *30*, 6977–6997, doi:10.1175/JCLI-D-16-0464.1, 2017.

Nash, J., and R. Saunders, A review of stratospheric sounding unit radiance observations for climate trends and reanalyses, *Q. J. R. Meteorol. Soc.*, *141*, 2103–2113, doi:10.1002/qj.2505, 2015.

Neely, R.R., III, O.B. Toon, S. Solomon, J.-P. Vernier, C. Alvarez, J.M. English, K.H. Rosenlof, M.J. Mills, C.G. Bardeen, J.S. Daniel, and J.P. Thayer, Recent anthropogenic increases in SO_2 from Asia have minimal impact on stratospheric aerosol, *Geophys. Res. Lett.*, *40*, doi:10.1002/grl.50263, 2013.

Neely, R.R., III, D.R. Marsh, K.L. Smith, S.M. Davis, and L.M. Polvani, Biases in Southern Hemisphere climate trends induced by coarsely specifying the temporal resolution of stratospheric ozone, *Geophys. Res. Lett.*, *41* (23), 8602–8610, doi:10.1002/2014GL061627, 2014.

Neu, J.L., and R.A. Plumb, Age of air in a leaky pipe model of stratospheric transport, *J. Geophys. Res.*, *104* (D16), 19243–19255, doi:10.1029/1999JD900251, 1999.

Neu, J.L., T. Flury, G.L. Manney, M.L. Santee, N.J. Livesey, and J. Worden, Tropospheric ozone variations governed by changes in stratospheric circulation, *Nat. Geosci.*, *7*, 340–344, doi:10.1038/ngeo2138, 2014.

Newman, P.A., L.D. Oman, A.R. Douglass, E.L. Fleming, S.M. Frith, M.M. Hurwitz, S.R. Kawa, C.H. Jackman, N.A. Krotkov, E.R. Nash, J.E. Nielsen, S. Pawson, R.S. Stolarski, and G.J.M. Velders, What would have happened to the ozone layer if chlorofluorocarbons (CFCs) had not been regulated?, *Atmos. Chem. Phys.*, *9*, 2113–2128, doi:10.5194/acp-9-2113-2009, 2009.

Newman, P.A., L. Coy, S. Pawson, and L.R. Lait, The anomalous change in the QBO in 2015–2016, *Geophys. Res. Lett.*, *43* (16), 8791–8797, doi:10.1002/2016GL070373, 2016.

Nguyen, H., C. Lucas, A. Evans, B. Timbal, and L. Hanson, Expansion of the Southern Hemisphere Hadley cell in response to greenhouse gas forcing, *J. Clim.*, *28* (20), 8067–8077, doi:10.1175/JCLI-D-15-0139.1, 2015.

Nowack, P.J., N.L. Abraham, A.C. Maycock, P. Braesicke, J.M. Gregory, M. Joshi, A. Osprey, and J.A. Pyle, A large ozone-circulation feedback and its implications for global warming assessments, *Nat. Clim. Change*, *5*, 41–45, doi:10.1038/nclimate2451, 2014.

Oberländer, S., U. Langematz, and S. Meul, Unraveling impact factors for future changes in the Brewer-Dobson circulation, *J. Geophys. Res. Atmos.*, *118*, 10,296–10,312, doi:10.1002/jgrd.50775, 2013.

Oberländer-Hayn, S., S. Meul, U. Langematz, J. Abalichin, and F. Haenel, A chemistry-climate model study of past changes in the Brewer-Dobson circulation, *J. Geophys. Res. Atmos.*, *120*, 6742–6757, doi:10.1002/2014JD022843, 2015.

Oberländer-Hayn, S., E.P. Gerber, J. Abalichin, H. Akiyoshi, A. Kerschbaumer, A. Kubin, M. Kunze, U. Langematz, S. Meul, M. Michou, O. Morgenstern, and L.D. Oman, Is the Brewer-Dobson circulation increasing or moving upward?, *Geophys. Res. Lett.*, *43*, 1772–1779, doi:10.1002/2015GL067545, 2016.

Olsen, M.A., K. Wargan, and S. Pawson, Tropospheric column ozone response to ENSO in GEOS-5 assimilation of OMI and MLS ozone data, *Atmos. Chem. Phys.*, *16*, 7091–7103, doi:10.5194/acp-16-7091-2016, 2016.

Oltmans, S.J., H. Vömel, D.J. Hofmann, K.H. Rosenlof, D. Kley, The increase in stratospheric water vapor from balloonborne, frostpoint hygrometer measurements at Washington, D.C., and Boulder, Colorado, *Geophys. Res. Lett.*, *2*, 3453–3457, doi:10.1029/2000GL012133, 2000.

Oman, L., D.W. Waugh, S. Pawson, R.S. Stolarski, and P.A. Newman, On the influence of anthropogenic forcings on changes in the stratospheric mean age, *J. Geophys. Res.*, *114*, D03105, doi:10.1029/2008JD010378, 2009.

Orr, A., T.J. Bracegirdle, J.S. Hoskings, T. Jung, J.D. Haigh, T. Phillips, and W. Feng, Possible dynamical mechanisms for Southern Hemisphere climate change due to the ozone hole, *J. Atmos. Sci.*, *69*, 2917–2932, doi:10.1175/JAS-D-11-0210.1, 2012.

Orr, A., T.J. Bracegirdle, J.S. Hoskings, W. Feng, H. Roscoe, and J.D. Haigh, Strong dynamical modulation of the cooling of the polar stratosphere associated with the Antarctic ozone hole, *J. Clim.*, *26*, 662–668, doi:10.1175/JCLI-D-12-00480.1, 2013.

Osprey, S.M., N. Butchart, J.R. Knight, A.A. Scaife, K. Hamilton, J.A. Anstey, V. Schenzinger, and C. Zhang, An unexpected disruption of the atmospheric quasi-biennial oscillation, *Science*, *353* (6306), 1424–1427, doi:10.1126/science.aah4156, 2016.

Ossó, A., Y. Sola, K.H. Rosenlof, B. Hassler, J. Bech, and J. Lorente, How robust are trends in the Brewer–Dobson circulation derived from observed stratospheric temperatures?, *J. Clim., 28*, 3024–3040, doi:10.1175/JCLI-D-14-00295.1, 2015.

Palmeiro, F.M., N. Calvo, and R.R. Garcia, Future changes in the Brewer-Dobson circulation under different greenhouse gas concentrations in WACCM4, *J. Atmos. Sci.*, *71*, 2962–2975, doi:10.1175/JAS-D-13-0289.1, 2014.

Parkinson, C.L., and N.E. DiGirolamo, New visualizations highlight new information on the contrasting Arctic and Antarctic sea-ice trends since the late 1970s, *Remote Sens. Environ.*, *183*, 198–204, doi:10.1016/j.rse.2016.05.020, 2016.

Pauling, A.G., I.J. Smith, P.J. Langhorne, and C.M. Bitz, Time-dependent freshwater input from ice shelves: Impacts on Antarctic sea ice and the Southern Ocean in an Earth system model, *Geophys. Res. Lett.*, *44*, 10,454–10,461, doi:10.1002/2017GL075017, 2017.

Peings Y., J. Cattiaux, S. Vavrus, and G. Magnusdottir, Late 21st century changes of the mid-latitude

atmospheric circulation in the CESM large ensemble, *J. Clim.*, *30*, 5943–5960, doi:10.1175/JCLI-D-16-0340.1, 2017.

Ploeger, F., M. Abalos, T. Birner, P. Konopka, B. Legras, R. Müller, and M. Riese, Quantifying the effects of mixing and residual circulation on trends of stratospheric mean age of air, *Geophys. Res. Lett.*, *42*, 2047–2054, doi:10.1002/2014GL062927, 2015.

Ploeger, F., and T. Birner, Seasonal and inter-annual variability of lower stratospheric age of air spectra, *Atmos. Chem. Phys.*, *16*, 10195–10213, doi:10.5194/acp-16-10195-2016, 2016.

Plumb, R.A., Stratospheric transport, *J. Met. Soc. Japan*, *80*, 793–809, doi:10.2151/jmsj.80.793, 2002.

Polvani, L.M., S.J. Camargo, and R.R. Garcia, The importance of the Montreal Protocol in mitigating the potential intensity of tropical cyclones, *J. Clim.*, *29*, 2275–2289, doi:10.1175/JCLI-D-15-0232.1, 2016.

Polvani, L.M., L. Wang, V. Aquila, and D.W. Waugh, The impact of ozone depleting substances on tropical upwelling, as revealed by the absence of lower stratospheric cooling since the late 1990s, *J. Clim.*, *30*, 2523–2534, doi:10.1175/JCLI-D-16-0532.1, 2017.

Polvani, L.M., M. Abalos, R. Garcia, D. Kinnison, and W.J. Randel, Significant weakening of Brewer-Dobson circulation trends over the 21st century as a consequence of the Montreal Protocol, *Geophys. Res. Lett.*, *45*, doi:10.1002/2017GL075345, 2018.

Prather, M., P. Midgley, F.S. Rowland, and R. Stolarski, The ozone layer: The road not taken, *Nature*, *381*, 551–554, doi:10.1038/381551a0, 1996.

Previdi, M., and L.M. Polvani, Impact of the Montreal Protocol on Antarctic surface mass balance and implications for global sea level rise, *J. Clim.*, *30* (18), 7247–7253, doi:10.1175/JCLI-D-17-0027.1, 2017.

Purich, A., W. Cai, M.H. England, and T. Cowan, Evidence for link between modelled trends in Antarctic sea ice and underestimated westerly wind changes, *Nat. Commun.*, *7*, (10409), doi:10.1038/ncomms10409, 2016a.

Purich, A., M.H. England, W. Cai, Y. Yoshimitsu, A. Timmermann, F.C. Fyfe, L. Frankcombe, G.A. Meehl, and J.M. Arblaster, Tropical Pacific SST drivers of recent Antarctic sea ice trends, *J. Clim.*, *29*, 8931–8948, doi:10.1175/JCLI-D-16-0440.1, 2016b.

Purich, A., M.H. England, W. Cai, A. Sullivan, and P.J. Durack, Impacts of broad-scale surface freshening of the Southern Ocean in a coupled climate model, *J. Clim.*, *31*, 2613–2632, doi:10.1175/JCLI-D-17-0092.1, 2018.

Quan, X.W., M.P. Hoerling, J. Perlwitz, H.F. Diaz, and T. Xu, How fast are the tropics expanding?, *J. Clim.*, *27* (5), 1999–2013, doi:10.1175/JCLI-D-13-00287.1, 2014.

Randel, W.J., A.K. Smith, F. Wu, C.-Z. Zou, and H. Qian, Stratospheric temperature trends over 1979–2015 derived from combined SSU, MLS and SABER satellite observations, *J. Clim.*, *29*, 4843–4859, doi:10.1175/JCLI-D-15-0629.1, 2016.

Randel, W.J., L. Polvani, F. Wu, D.E. Kinnison, C.-Z. Zou, and C. Mears, Troposphere-stratosphere temperature trends derived from satellite data compared with ensemble simulations from WACCM, *J. Geophys. Res. Atmos.*, *122*, 9651–9667, doi:10.1002/2017JD027158, 2017.

Ray, E.A., F.L. Moore, K.H. Rosenlof, S.M. Davis, H. Boenisch, O. Morgenstern, D. Smale, E. Rozanov, M. Hegglin, G. Pitari, E. Mancini, P. Braesicke, N. Butchart, S. Hardiman, F. Li, K. Shibata, and D.A. Plummer, Evidence for changes in stratospheric transport and mixing over the past three decades based on multiple data sets and tropical leaky pipe analysis, *J. Geophys. Res.*, *115*, D21304, doi:10.1029/2010JD014206, 2010.

Ray, E.A., F.L. Moore, K.H. Rosenlof, S.M. Davis, C. Sweeney, P. Tans, T. Wang, J.W. Elkins, H. Bonisch, A. Engel, S. Sugawara, T. Nakazawa, and S. Aoki, Improving stratospheric transport trend analysis based on SF_6 and CO_2 measurements, *J. Geophys. Res. Atmos.*, *119*, 14,110–14,128, doi:10.1002/2014JD021802, 2014.

Ray, E.A., F.L. Moore, K.H. Rosenlof, D.A. Plummer, F. Kolonjari, and K.A. Walker, An idealized stratospheric model useful for understanding differences between long-lived trace gas measurements and global chemistry-climate model output, *J. Geophys. Res. Atmos.*, *121*, doi:10.1002/2015JD024447, 2016.

Rea, G., A. Riccio, F. Fierli, F. Cairo, and C. Cagnazzo, Stratosphere-resolving CMIP5 models simulate different changes in the Southern Hemisphere, *Clim. Dyn.*, *50*, (5/6), 2239–2255, doi:10.1007/s00382-017-3746-2, 2018.

Revell, L.E., F. Tummon, A. Stenke, T. Sukhodolov, A. Coulon, E. Rozanov, H. Garny, V. Grewe, and T.

Peter, Drivers of the tropospheric ozone budget throughout the 21st century under the medium-high climate scenario RCP 6.0, *Atmos. Chem. Phys.*, *15*, 5887–5902, doi:10.5194/acp-15-5887-2015, 2015.

Revell, L.E., A. Stenke, E. Rozanov, W. Ball, S. Lossow, and T. Peter, The role of methane in projections of 21st century stratospheric water vapour, *Atmos. Chem. Phys.*, *16*, 13,067–13,080, doi:10.5194/acp-16-13067-2016, 2016.

Rieder, H.E., L.M. Polvani, and S. Solomon, Distinguishing the impacts of ozone-depleting substances and well-mixed greenhouse gases on Arctic stratospheric ozone and temperature trends, *Geophys. Res. Lett.*, *41* (7), 2652–2660, doi:10.1002/2014GL059367, 2014.

Ritter, R., P. Landschützer, N. Gruber, A.R. Fay, Y. Iida, S. Jones, S. Nakaoka, G.-H. Park, P. Peylin, C. Rödenbeck, K.B. Rodgers, J.D. Shutler, and J. Zeng, Observation-based trends of the Southern Ocean carbon sink, *Geophys. Res. Lett.*, *44*, 12,339–12,348, doi:10.1002/2017GL074837, 2017.

Rosenblum, E., and I. Eisenman, Sea ice trends in climate models only accurate in runs with biased global warming, *J. Clim.*, *30*, 6265–6278, doi:10.1175/JCLI-D-16-0455.1, 2017.

Rosenlof, K.H., S.J. Oltmans, D. Kley, J.M. Russell III, E.-W. Chiou, W.P. Chu, D.G. Johnson, K.K. Kelly, H.A. Michelsen, G.E. Nedoluha, E.E. Remsberg, G.C. Toon, and M.P. McCormick, Stratospheric water vapor increases over the past half century, *Geophys. Res. Lett.*, *28*,1195–1199, doi:10.1029/2000GL012502, 2001.

Rosenlof, K.H., and G.C. Reid, Trends in the temperature and water vapor content of the tropical lower stratosphere: Sea surface connection, *J. Geophys. Res.*, *113*, D06107, doi:10.1029/2007JD009109, 2008.

Saunois, M., P. Bousquet, B. Poulter, A. Peregon, P. Ciais, J.G. Canadell, E.J. Dlugokencky, G. Etiope, D. Bastviken, S. Houweling, G. Janssens-Maenhout, F.N. Tubiello, S. Castaldi, R.B. Jackson, M. Alexe, V.K. Arora, D.J. Beerling, P. Bergamaschi, D.R. Blake, G. Brailsford, V. Brovkin, L. Bruhwiler, C. Crevoisier, P. Crill, C. Curry, C. Frankenberg, N. Gedney, L. Höglund-Isaksson, M. Ishizawa, A. Ito, F. Joos, H.-S. Kim, T. Kleinen, P. Krummel J.-F. Lamarque, R. Langenfelds, R. Locatelli, T. Machida, S. Maksyutov, K.C. McDonald, J. Marshall, J.R. Melton, I. Morino, S. O'Doherty, F.-J.W. Parmentier, P.K. Patra, C. Peng, S. Peng, G.P. Peters, I. Pison, C. Prigent, R. Prinn, M. Ramonet, W.J. Riley, M. Saito, R. Schroeder, I.J. Simpson, R. Spahni, P. Steele, A. Takizawa, B.F. Thornton, H. Tian, Y. Tohjima, N. Viovy, A. Voulgarakis, M. van Weele, G. van der Werf, R. Weiss, C. Wiedinmyer, D.J. Wilton, A. Wiltshire, D. Worthy, D.B. Wunsch, X. Xu, Y. Yoshida, B. Zhang, Z. Zhang, and Q. Zhu, The global methane budget 2000–2012, *Earth Syst. Sci. Data*, *8*, 697–751, doi:10.5194/essd-8-697-2016, 2016.

Schirber, S., E. Manzini, T. Krismer, and M. Giorgetta, The quasi-biennial oscillation in a warmer climate: Sensitivity to different gravity wave parameterizations, *Clim. Dyn., 45,* 825–836, doi:10.1007/s00382-014-2314-2, 2014, 2015.

Schneider, D., C. Deser, and T. Fan, Comparing the impacts of tropical SST variability and polar tratospheric ozone loss on the Southern Ocean westerly winds, *J. Clim.*, *28*, 9350–9372, doi:10.1175/JCLI-D-15-0090.1, 2015.

Schneider, D.P., and C. Deser, Tropically driven and externally forced patterns of Antarctic sea ice change: Reconciling observed and modeled trends, *Clim. Dyn., 50*, (11/12), 4599–4618, doi:10.1007/s00382-017-3893-5, 2018.

Schwartz, M.J., W.G. Read, M.L. Santee, N.J. Livesey, L. Froidevaux, A. Lambert, and G.L. Manney, Convectively injected water vapor in the North American summer lowermost stratosphere, *Geophys. Res. Lett.*, *40*, 2316–2321, doi:10.1002/grl.50421, 2013.

Seidel, D.J., J. Li, C. Mears, I. Moradi, J. Nash, W.J. Randel, R. Saunders, D.W.J. Thompson, and C.-Z. Zou, Stratospheric temperature changes during the satellite era, *J. Geophys. Res. Atmos.*, *121*, (2), 664–681, doi:10.1002/2015JD024039, 2016.

Sekiya, T., and K. Sudo, Roles of transport and chemistry processes in global ozone change on interannual and multidecadal time scales, *J. Geophys. Res.*, *119*, 4903–4921, doi:10.1002/2013JD020838, 2014.

Seviour, W.J., A. Gnanadesikan, and D.W. Waugh, The transient response of the Southern Ocean to stratospheric ozone depletion, *J. Clim.*, *29* (20), 7383–7396, doi:10.1175/JCLI-D-16-0198.1, 2016.

Seviour, W.J.M., Weakening and shift of the Arctic stratospheric polar vortex: Internal variability or forced response?, *Geophys. Res. Lett.*, *44*, doi:10.1002/2017GL073071, 2017.

Seviour, W.J.M., D.W. Waugh, L.M. Polvani, G.J.P. Correa, and C.I. Garfinkel, Robustness of the simulated tropospheric response to ozone depletion, *J. Clim.*, *30*, 2577–2585, doi:10.1175/JCLI-D-16-0817.1, 2017a.

Seviour, W.J.M., A. Gnanadesikan, D.W. Waugh, and M.-A. Pradal, Transient response of the Southern Ocean to changing ozone: Regional responses and physical mechanisms, *J. Clim.*, *30,* 2463–2480, doi:10.1175/JCLI-D-16-0474.1, 2017b.

Shepherd, T.G., Transport in the Middle Atmosphere, *J. Meteorol. Soc. Japan, 85B*, 165–191, doi:102151/jmsj.85B.165, 2007.

Sherwood, S.C., and N. Nishant, Atmospheric changes through 2012 as shown by iteratively homogenized radiosonde temperature and wind data (IUKv2), *Environ. Res. Lett., 10* (5), doi:10.1088/1748-9326/10/5/054007, 2015.

Sheshadri, A., R.A. Plumb, and D.I.V. Domeisen, Can the delay in Antarctic polar vortex breakup explain recent trends in surface westerlies?, *J. Atmos. Sci.*, *71* (2), 566– 573, doi:10.1175/JAS-D-12-0343.1, 2014.

Sheshadri, A., and R.A. Plumb, Sensitivity of the surface responses of an idealized AGCM to the timing of imposed ozone depletion-like polar stratospheric cooling, *Geophys. Res. Lett.*, *43*, 2330–2336, doi:10.1002/2016GL067964, 2016.

Sigmond, M., J.C. Fyfe, and J.F. Scinocca, Does the ocean impact the atmospheric response to stratospheric ozone depletion?, *Geophys. Res. Lett*., *37*, L12706, doi:10.1029/2010GL043773, 2010.

Sigmond, M., and J.C. Fyfe, The Antarctic sea ice response to the ozone hole in climate models, *J. Clim.*, *27* (3), 1336–1342, doi:10.1175/JCLI-D-13-00590.1, 2014.

Sigmond, M., and T.G. Shepherd, Compensation between resolved wave driving and parameterized orographic gravity wave driving of the Brewer–Dobson circulation and its response to climate change, *J. Clim.*, *27*, 5601–5610, doi:10.1175/JCLI-D-13-00644.1, 2014.

Simmons, A.J., P. Poli, D.P. Dee, P. Berrisford, H. Hersbach, S. Kobayashi, and C. Peubey, Estimating low-frequency variability and trends in atmospheric temperature using ERA-Interim, *Q. J. R. Meteorol. Soc.*, *140*, 329–353, doi:10.1002/qj.2317, 2014.

Simpson, I.R., and L.M. Polvani, Revisiting the relationship between jet position, forced response, and annular mode variability in the southern midlatitudes, *Geophys. Res. Lett.*, *43*, 2896–2903, doi:10.1002/2016GL067989, 2016.

Simpson, I.R., P. Hitchcock, R. Seager, Y. Wu, and P. Callaghan, The downward influence of uncertainty in the Northern Hemisphere stratospheric polar vortex response to climate change, *J. Clim.*, *31*, 6371–639, doi:10.1175/JCLI-D-18-0041.1, 2018.

Škerlak, B., M. Sprenger, and H. Wernli, A global climatology of stratosphere-troposphere exchange using the ERA-Interim data set from 1979 to 2011, *Atmos. Chem. Phys.*, *14*, 913–937, doi:10.5194/acp-14-913-2014, 2014.

Smalley, K.M., A.E. Dessler, S. Bekki, M. Deushi, M. Marchand, O. Morgenstern, D.A. Plummer, K. Shibata, Y. Yamashita, and G. Zeng, Contribution of different processes to changes in tropical lower-stratospheric water vapor in chemistry–climate models, *Atmos. Chem. Phys*., *17*, 8031–8044, doi:10.5194/acp-17-8031-2017, 2017.

Smith, K.L., and L.M. Polvani, The surface impacts of Arctic stratospheric ozone anomalies, *Environ. Res. Lett.*, *9*, (7), doi:10.1088/1748-9326/9/7/074015, 2014.

Smith, K.L., and R.K. Scott, The role of planetary waves in the tropospheric jet response to stratospheric cooling, *Geophys. Res. Lett.*, *43*, 2904–2911, doi:10.1002/2016GL067849, 2016.

Smith, K.L., and L.M. Polvani, Spatial patterns of recent Antarctic surface temperature trends and the importance of natural variability: Lessons from multiple reconstructions and the CMIP5 models, *Clim. Dyn.*, 48 (7/8), 2653–2670, doi:10.1007/s00382-016-3230-4, 2017.

Solman, S.A., and I. Orlanski, Climate change over the extratropical Southern Hemisphere: The tale from an ensemble of reanalysis datasets, *J. Clim.*, *29*, 1673–1687, doi:10.1175/JCLI-D-15-0588.1, 2016.

Solomon, A., A.M. Polvani, K.L. Smith, and R.P. Abernathey, The impact of ozone depleting substances on the circulation, temperature, and salinity of the Southern Ocean: An attribution study with CESM1 (WACCM), *Geophys. Res. Lett.*, *42*, (13), 5547–5555, doi:10.1002/2015GL064744, 2015.

Solomon, A., L.M. Polvani, D.W. Waugh, and S.M. Davis, Contrasting upper and lower atmospheric metrics of tropical expansion in the Southern Hemisphere, *Geophys. Res. Lett., 43* (19), doi:10.1002/2016GL070917, 2016.

Solomon, A., and L.M. Polvani, Highly significant responses to anthropogenic forcings of the midlatitude jet in the Southern Hemisphere, *J. Clim.*, *29* (9), 3463–3470, doi: 0.1175/JCLI-D-16-0034.1, 2016.

Solomon, S., S. Borrmann, R.R. Garcia, R. Portmann, L. Thomason, L.R. Poole, D. Winker, and M.P. McCormick, Heterogeneous chlorine chemistry in the tropopause region, *J. Geophys. Res.*, *102*, 21,411–21,429, doi:10.1029/97JD01525, 1997.

Solomon, S., D.J. Ivy, D. Kinnison, M.J. Mills, R.R. Neely, III, and A. Schmidt, Emergence of healing in the Antarctic ozone layer, *Science, 353* (6296), 269–274, doi:10.1126/science.aae0061, 2016.

Solomon, S., D. Ivy, M. Gupta, J. Bandoro, B. Santer, Q. Fu, P. Lin, R.R. Garcia, D. Kinnison, and M. Mills, Mirrored changes in Antarctic ozone and stratospheric temperature in the late 20th versus early 21st centuries, *J. Geophys. Res. Atmos.*, *122*, 8940–8950, doi:10.1002/2017JD026719, 2017.

Son, S.-W., E.P. Gerber, J. Perlwitz, L.M. Polvani, N.P. Gillett, K.-H. Seo, V. Eyring, T.G. Shepherd, D. Waugh, H. Akiyoshi, J. Austin, A. Baumgaertner, S. Bekki, P. Braesicke, C. Brühl, N. Butchart, M.P. Chipperfield, D. Cugnet, M. Dameris, S. Dhomse, S. Frith, H. Garny, R. Garcia, S.C. Hardiman, P. Jöckel, J.F. Lamarque, E. Mancini, M. Marchand, M. Michou, T. Nakamura, O. Morgenstern, G. Pitari, D.A. Plummer, J. Pyle, E. Rozanov, J.F. Scinocca, K. Shibata, D. Smale, H. Teyssèdre, W. Tian, and Y. Yamashita, Impact of stratospheric ozone on Southern Hemisphere circulation change: A multimodel assessment, *J. Geophys. Res.*, *115*, D00M07, doi:10.1029/2010JD014271, 2010.

Son, S.-W., A. Purich, H.H. Hendon, B.-M. Kim, and L.M. Polvani, Improved seasonal forecast using ozone hole variability?, *Geophys. Res. Lett.*, *40*, 6231–6235, doi: 10.1002/2013GL057731, 2013.

Son, S.-W., B-R Han, C.I. Garfinkel, S.-Y. Kim, P. Rokjin, N.L. Abraham, H. Akiyoshi, A.T. Archibald, N. Butchart, M.P. Chipperfield, M. Dameris, M. Deushi, S.S. Dhomse, S.C. Hardiman, P. Jöckel, D. Kinnison, M. Michou, O. Morgenstern, F.M. O'Connor, L.D. Oman, D.A. Plummer, A. Pozzer, L.E. Revell, E. Rozanov, A. Stenke, K. Stone, S. Tilmes, Y. Yamashita, and G. Zeng, Tropospheric jet response to Antarctic ozone depletion: An update with Chemistry-Climate Model Initiative (CCMI) models, *Environ. Res. Lett.*, *13*, (5), doi:10.1088/1748-9326/aabf21, 2018.

SPARC CCMVal (Stratosphere-troposphere Processes And their Role in Climate) *SPARC Report on the Evaluation of Chemistry-Climate Models*, edited by V. Eyring, T.G. Shepherd, and D.W. Waugh, *SPARC Report No. 5*, WCRP-132, WMO/td-No.1526, available at: http://www.atmosp.physics.utoronto.ca/SPARC/ccmval_final/index.php, 2010.

Staten, P.W., J.J. Rutz, T. Reichler, and J. Lu, Breaking down the tropospheric circulation response by forcing, *Clim. Dyn.*, *39* (9/10), 2361–2375, doi:10.1007/s00382-011-1267-y 2012.

Staten, P.W., and T. Reichler, On the ratio between shifts in the eddy-driven jet and the Hadley-cell edge, *Clim. Dyn.*, *42* (5/6), 1229–1242, doi:10.1007/s00382-013-1905-7, 2014.

Steptoe, H., L.J. Wilcox, and E.J. Highwood, Is there a robust effect of anthropogenic aerosols on the Southern Annular Mode?, *J. Geophys. Res. Atmos.*, *121* (17), doi:10.1002/2015JD024218, 2016.

Stiller, G.P., T. von Clarmann, F. Haenel, B. Funke, N. Glatthor, U. Grabowski, S. Kellmann, M. Kiefer, A. Linden, S. Lossow, and M. López-Puertas, Observed temporal evolution of global mean age of stratospheric air for the 2002 to 2010 period, *Atmos. Chem. Phys.*, *12*, 3311–3331, doi:10.5194/acp-12-3311-2012, 2012.

Stiller, G.P., F. Fierli, F. Ploeger, C. Cagnazzo, B. Funke, F.J. Haenel, T. Reddmann, M. Riese, and T. von Clarmann, Shift of subtropical transport barriers explains observed hemispheric asymmetry of decadal trends of age of air, *Atmos. Chem. Phys.*, *17*, 11,177–11,192, doi:10.5194/acp-17-11177-2017, 2017.

Stohl, A., P. Bonasoni, P. Cristofanelli, W. Collins, J. Feichter, A. Frank, C. Forster, E. Gerasopoulos, H. Gäggeler, P. James, T. Kentarchos, H. Kromp-Kolb, B. Krüger, C. Land, J. Meloen, A. Papayannis, A. Priller, P. Seibert, M. Sprenger, G.J. Roelofs, H.E. Scheel, C. Schnabel, P. Siegmund, L. Tobler, T. Trickl, H. Wernli, V. Wirth, P. Zanis, and C. Zerefos, Stratosphere-troposphere exchange: A review, and what we have learned from STACCATO, *J. Geophys. Res.*, *108* (D12), doi:10.1029/2002JD002490, 2003.

Stolarski, R.S., A.R. Douglass, P.A. Newman, S. Pawson, and M.R. Schoeberl, Relative contribution of greenhouse gases and ozone-depleting substances to temperature trends in the stratosphere:

A chemistry-climate model study, *J. Clim.*, *23*, 28–42, doi:10.1175/2009JCLI2955.1, 2010.

Stone, K.A., O. Morgenstern, D.J. Karoly, A.R. Klekociuk, W.J. French, N.L. Abraham, and R. Schofield, Evaluation of the ACCESS-chemistry-climate model for the Southern Hemisphere, *Atmos. Chem. Phys.*, *16* (4), 2401–2415, doi:10.5194/acp-16-2401-2016, 2016.

Stuecker, M.F., C.M. Bitz, and K.C. Armour, Conditions leading to the unprecedented low Antarctic sea ice extent during the 2016 austral spring season, *Geophys. Res. Lett.*, *44*, doi:10.1002/2017GL074691, 2017.

Sun, L., G. Chen, and W.A. Robinson, The role of stratospheric polar vortex breakdown in Southern Hemisphere climate trends, *J. Atmos. Sci.*, *71* (7), 2335–2353, doi:10.1175/JAS-D-13-0290.1, 2104.

Swart, N.C., and J.C. Fyfe, Observed and simulated changes in the Southern Hemisphere surface westerly wind-stress, *Geophys. Res. Lett.*, *39*, doi:10.1029/2012GL052810, 2012.

Swart, N.C., J.C. Fyfe, O.A. Saenko, and M. Eby, Wind-driven changes in the ocean carbon sink, *Biogeosci., 11*, 6107–6117, doi:10.5194/bg-11-6107-2014, 2014.

Swart, N.C., J.C. Fyfe, N. Gillett, and G.J. Marshall, Comparing trends in the southern annular mode and surface westerly jet, *J. Clim.*, *28*, 8840–8859, doi:10.1175/JCLI-D-15-0334.1, 2015.

Tao, L., Y. Hu, and J. Liu, Anthropogenic forcing on the Hadley circulation in CMIP5 simulations, *Clim. Dyn., 46*, 3337–3350, doi:10.1007/s00382-015-2772-1, 2016.

Thomas, J.L., D.W. Waugh, and A. Gnanadesikan, Southern Hemisphere extratropical circulation: Recent trends and natural variability, *Geophys. Res. Lett., 42*, 13, 5508–5515, doi:10.1002/2015GL064521, 2015.

Thompson, D.W.J., J.C. Furtado, and T.G. Shepherd, On the tropospheric response to anomalous stratospheric wave drag and radiative heating, *J. Atmos. Sci.*, *63* (10), 2616–2629, doi:10.1175/JAS3771.1, 2006.

Thompson, D.W.J., D.J. Seidel, W.J. Randel, C.-Z. Zou, A.H. Butler, R. Lin, C. Long, C. Mears, and A. Osso, The mystery of recent stratospheric temperature trends, *Nature*, *491*, 692–697, doi:10.1038/nature11579, 2012.

Thorne, P.W., D.E. Parker, S.F.B. Tett, P.D. Jones, M. McCarthy, H. Coleman, and P. Brohan, Revisiting radiosonde upper-air temperatures from 1958 to 2002, *J. Geophys. Res.*, *110*, doi:10.1029/2004JD005753, 2005.

Turner, J., J.S. Hosking, G.J. Marshall, T. Phillips, and T.J. Bracegirdle, Antarctic sea ice increase consistent with intrinsic variability of the Amundsen Sea Low, *Clim. Dyn.*, *46*, 2391–2402, doi:10.1007/s00382-015-2708-9, 2015.

Turner, J., H. Lu, I. White, J.C. King, T. Phillips, J.S. Hosking, T.J. Bracegirdle, G.J. Marshall, R. Mulvaney, and P. Deb, Absence of 21st century warming on Antarctic Peninsula consistent with natural variability, *Nature*, *535*, 411–415, doi:10.1038/nature18645, 2016.

Turner, J., T. Phillips, G.J. Marshall, J.S. Hosking, J.O. Pope, T.J. Bracegirdle, and P. Deb, Unprecedented springtime retreat of Antarctic sea ice in 2016, *Geophys. Res. Lett.*, *44*, 6868–6875, doi:10.1002/2017GL073656, 2017.

Ueyama, R., E.J. Jensen, L. Pfister, G.S. Diskin, T.P. Bui, and J.M. Dean-Day, Dehydration in the tropical tropopause layer: A case study for model evaluation using aircraft observations, *J. Geophys. Res. Atmos.*, *119*, 5299–5316, doi:10.1002/2013JD021381, 2014.

Ummenhofer, C.C., P.C. McIntosh, M.J. Pook, J.S. Risbey, Impact of surface forcing on Southern Hemisphere atmospheric blocking in the Australia-New Zealand sector, *J. Clim.*, *26* (21), 8476–8494, doi:10.1175/JCLI-D-12-00860.1, 2013.

USGCRP, *Climate Science Special Report: Fourth National Climate Assessment, Volume I*, edited by D.J. Wuebbles, D.W. Fahey, K.A. Hibbard, D.J. Dokken, B.C. Stewart, and T.K. Maycock, U.S. Global Change Research Program, Washington, D.C., USA, 470 pp., doi:10.7930/J0J964J6, 2017.

Velders, G.J.M., S.O. Andersen, J.S. Daniel, D.W. Fahey, and M. McFarland, The Importance of the Montreal Protocol in protecting climate, *Proc. Natl. Acad. Sci.*, *104* (12), 4814–4819, doi:10.1073/pnas.0610328104, 2007.

Vera, C.S., and L. Díaz, Anthropogenic influence on summer precipitation trends over South America in CMIP5 models, *Int. J. Climatol.*, *35* (10), 3172–3177, doi:10.1002/joc.4153/full, 2015.

Vernier, J.-P., L.W. Thomason, and J. Kar, CALIPSO detection of an Asian tropo-

pause aerosol layer, *Geophys. Res. Lett.*, *38*, doi:10.1029/2010GL046614, 2011.

Vernier, J.-P., T.D. Fairlie, M. Natarajan, F.G. Wienhold, J., Bian, B.G. Martinsson, S. Crumeyrolle, L.W. Thomason, and K. M. Bedka, Increase in upper tropospheric and lower stratospheric aerosol levels and its potential connection with Asian pollution, *J. Geophys. Res. Atmos.*, *120*, 1608–1619. doi:10.1002/2014JD022372, 2015.

Villalba, R.A. Lara, M. Masiokas, R. Urrutia, E.R. Cook, D. Christie, I.A. Mundo, J. Boninsegna, P. Fenwick, R. Neukom, K. Allen, M. Morales, D.C. Araneo, G. Marshall, A. Srur, J.C. Aravena, and J. Palmer, Unusual Southern Hemisphere tree growth patterns induced by changes in the southern annular mode, *Nat. Geosci.*, *5*, 793–798, doi:10.1038/NGEO1613, 2012.

Wang, G., W. Cai, and A. Purich, Trends in Southern Hemisphere wind-driven circulation in CMIP5 models over the 21st century: Ozone recovery versus greenhouse forcing, *J. Geophys. Res. Ocean*, *119,* 2974–2984, doi:10.1002/2013JC009589, 2014.

Wang, L., C.-Z. Zou, and H. Qian, Construction of stratospheric temperature data records from Stratospheric Sounding Units, *J. Clim.*, *25*, 2931–2946, doi:10.1175/JCLI-D-11-00350.1, 2012.

Waugh, D.W., and T.M. Hall, Age of stratospheric air: Theory, observations, and models, *Rev. Geophys.*, *40* (4), doi:10.1029/2000RG000101, 2002.

Waugh D.W., Age of stratospheric air, *Nat. Geosci.*, *2*, (1), 14–16, doi:10.1038/ngeo397, 2009.

Waugh, D.W., L. Oman, P.A. Newman, R.S. Stolarski, S. Pawson, J.E. Nielsen, and J. Perlwitz, Effect of zonal asymmetries in stratospheric ozone on simulated Southern Hemisphere climate trends, *Geophys. Res. Lett.*, *36* (18), doi:10.1029/2009GL040419, 2009.

Waugh, D.W., C.I. Garfinkel, and L.M. Polvani, Drivers of the recent tropical expansion in the Southern Hemisphere: Changing SSTs or ozone depletion?, *J. Clim.*, *28*, 6581–6586, doi:10.1175/JCLI-D-15-0138.1, 2015.

Watanabe, S., K. Hamilton, S. Osprey, Y. Kawatani, and E. Nishimoto, First successful hindcasts of the 2016 Disruption of the stratospheric quasibiennial oscillation, *Geophys. Res. Lett.,44*, doi:10.1002/2017GL076406, 2017.

Wenzel, S., V. Eyring, E.P. Gerber, and A.Yu., Karpechko, Constraining future summer austral jet stream positions in the CMIP5 ensemble by process-oriented multiple diagnostic regression, *J. Clim.*, *29,* 673–687, doi:10.1175/JCLI-D-15-0412.1, 2016.

Wilcox, L.J., A.J. Charlton-Perez, and L.J. Gray, Trends in austral jet position in ensembles of high- and low-top CMIP5 models, *J. Geophys. Res.*, *117*, doi:10.1029/2012JD017597, 2012.

Wilcox, L.J., and A.J. Charlton-Perez, Final warming of the Southern Hemisphere polar vortex in high-and low-top CMIP5 models, *J. Geophys. Res. Atmos.*, *118* (6), 2535–2546, doi:10.1002/jgrd.50254, 2013.

Wu, Y., and L.M. Polvani, Recent trends in extreme precipitation and temperature over southeastern South America: The dominant role of stratospheric ozone depletion, *J. Clim.*, *30*, 6433–6441, doi:10.1175/JCLI-D-17-0124.1, 2017.

Xie, F., J. Li, W. Tian, Q. Fu, F.F. Jin, Y. Hu, J. Zhang, W. Wang, C. Sun, J. Feng, and Y. Yang, A connection from Arctic stratospheric ozone to El Niño-Southern oscillation, *Environ. Res. Lett.*, *11* (12), doi:10.1088/1748-9326/11/12/124026, 2016.

Yang, H., L. Sun, and G. Chen, Separating the mechanisms of transient responses to stratospheric ozone depletion–like cooling in an idealized atmospheric model, *J. Atmospheric Sci.*, *72* (2), 763–773, doi:10.1175/JAS-D-13-0353.1, 2015.

Yang, H., G. Chen, Q. Tang, and P. Hess, Quantifying isentropic stratosphere-troposphere exchange of ozone, *J. Geophys. Res. Atmos.*, *121*, 3372–3387, doi:10.1002/2015JD024180, 2016.

Young, P., K.H. Rosenlof, S. Solomon, S.C. Sherwood, Q. Fu, and J.-F Lamarque, Changes in stratospheric temperatures and their implications for changes in the Brewer–Dobson circulation, 1979–2005, *J. Clim.*, *25*, 1759–1772, doi:10.1175/2011JCLI4048.1, 2012.

Young, P.J., A.T. Archibald, K.W. Bowman, J.-F. Lamarque, V. Naik, D.S. Stevenson, S. Tilmes, A. Voulgarakis, O. Wild, D. Bergmann, P. Cameron-Smith, I. Cionni, W.J. Collins, S.B. Dalsøren, R.M. Doherty, V. Eyring, G. Faluvegi, L.W. Horowitz, B. Josse, Y.H. Lee, I.A. MacKenzie, T. Nagashima, D.A. Plummer, M. Righi, S.T. Rumbold, R.B. Skeie, D.T. Shindell, S.A. Strode, K. Sudo, S. Szopa, and G. Zeng, Pre-industrial to end 21st century projections of tropospheric ozone from the Atmospheric Chemistry and Climate Model Intercomparison Project (ACCMIP), *Atmos. Chem. Phys.*, *13*, 2063–2090, doi:10.5194/

acp-13-2063-2013, 2013.

Young, P.J., S.M. Davis, B. Hassler, S. Solomon, and K.H. Rosenlof, Modeling the climate impact of Southern Hemisphere ozone depletion: The importance of the ozone data set, *Geophys. Res. Lett.*, *41* (24), 9033–9039, doi:10.1002/2014GL061738, 2014.

Young, P.J., V. Naik, A.M. Fiore, A. Gaudel, J. Guo, M.Y. Lin, J.L. Neu, D.D. Parrish, H.E. Rieder, J.L. Schnell, S. Tilmes, O. Wild, L. Zhang, J. Ziemke, J. Brandt, A. Delcloo, R.M. Doherty, C. Geels, M.I. Hegglin, L. Hu, U. Im, R. Kumar, A. Luhar, L. Murray, D. Plummer, J. Rodriguez, A. Saiz-Lopez, M.G. Schultz, M.T. Woodhouse, and G. Zeng, Tropospheric Ozone Assessment Report: Assessment of global-scale model performance for global and regional ozone distributions, variability, and trends, *Elementa-Sci. Anthrop.*, *6*, (10), doi:10.1525/elementa.265, 2018.

Yu, P., D.M. Murphy, R.W. Portmann, O.B. Toon, K.D. Froyd, A.W. Rollins, R.-S. Gao, and K.H. Rosenlof, Radiative forcing from anthropogenic sulfur and organic emissions reaching the stratosphere, Geophys. *Res. Lett., 43*, 9361–9367, doi:10.1002/2016GL070153, 2016.

Yu, P., K.H. Rosenlof, S. Liu, H. Telg, T.D. Thornberry, A.W. Rollins, R.W. Portmann, Z. Bai, E.A. Ray, Y. Duan, L.L. Pan, O.B. Toon, J. Bian, and R.-S. Gao, Efficient transport of tropospheric aerosol into the stratosphere via the Asian summer monsoon anticyclone, *Proc. Natl. Acad. Sci.*, *114* (27), 6972–6977, doi:10.1073/pnas.1701170114, 2017.

Zappa, G., and T.G. Shepherd, Storylines of atmospheric circulation change for European regional climate impact assessment, *J. Clim.*, *30* (16), 6561–6577, doi:10.1175/JCLI-D-16-0807.1, 2017.

Zeng, G., and J.A. Pyle, Influence of El Ninõ Southern Oscillation on stratosphere/troposphere exchange and the global tropospheric ozone budget, *Geophys. Res. Lett.*, *32*, doi:10.1029/2004GL021353, 2005.

Zhang, H., T.L. Delworth, F. Zeng, G. Vecchi, K. Paffendorf, and L. Jia, Detection, Attribution, and Projection of Regional Rainfall Changes on (Multi-) Decadal Time Scales: A Focus on Southeastern South America, *J. Clim.*, *29* (23) 8515–8534, doi: 10.1175/JCLI-D-16-0287.1, 2016.

Zhang, J., W. Tian, M.P. Chipperfield, F. Xie, and J. Huang, Persistent shift of the Arctic polar vortex towards the Eurasian continent in recent decades, *Nat. Clim. Change*, *6*, 1094–1099, doi:10.1038/nclimate3136, 2016.

Zhang, L., T.L. Delworth, and L. Jia, Diagnosis of Decadal Predictability of Southern Ocean Sea Surface Temperature in the GFDL CM2.1 Model, *J. Clim.*, *30*, 6309–6328, doi:10.1175/JCLI-D-16-0537.1, 2017.

Zickfeld, K., S. Solomon, and D.M. Gilford, Centuries of thermal sea-level rise due to anthropogenic emissions of short-lived greenhouse gases, *Proc. Natl. Acad. Sci.*, *114* (4), 657–662, doi:10.1073/pnas.1612066114, 2017.

Zou, C.-Z., M. Goldberg, Z. Cheng, N. Grody, J. Sullivan, C. Cao, and D. Tarpley, Recalibration of microwave sounding unit for climate studies using simultaneous nadir overpasses, *J. Geophys. Res. Atmos.*, *111*, doi:10.1029/2005JD006798, 2006.

Zou, C.-Z., H. Qian, W. Wang, L. Wang, and C. Long, Recalibration and merging of SSU observations for stratospheric temperature trend studies, *J. Geophys. Res. Atmos.*, *119*, 13,180–13,205, doi:10.1002/2014JD021603, 2014.

Zou, C.-Z., and H. Qian, Stratospheric temperature climate data record from merged SSU and AMSU-A observations, *J. Atmos. Oceanic Technol.*, *33* (9), 1967–1984, doi:10.1175/JTECH-D-16-0018.1, 2016.